AD-A084 135 TRINITY COLL DUBLIN (IRELAND) SCHOOL OF ENGINEERING F/G 13/2
ENVIRONMENTAL AND OTHER CRITERIA AND METHODS FOR PAVEMENT DESIG--ETC(U)
FEB 79 R W KIRWAN, E R FARRELL, M L MAHER DA-ERO-76-G-065
UNCLASSIFIED NL

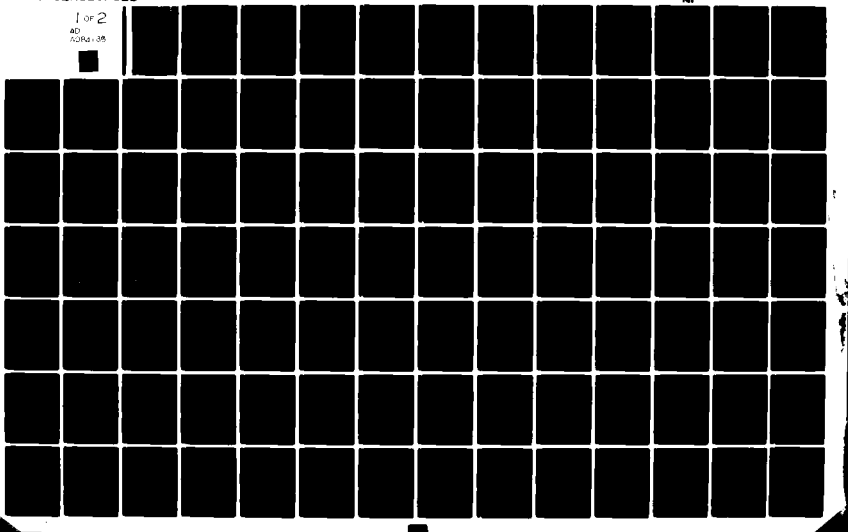

ENVIRONMENTAL AND OTHER CRITERIA AND METHODS FOR PAVEMENT DESIGN

by

R. W. Kirwan *(Principal Investigator)*
E. R. Farrell *(Research Graduate)*
M. L. Maher *(Research Graduate)*

GRANTEE: University of Dublin,
Engineering School,
Trinity College,
Dublin.

EUROPEAN RESEARCH OFFICE
United States Army

GRANT NO: DA-ERO-76-G-065

FINAL TECHNICAL REPORT
October 1976 - December 1978

SECURITY CLASSIFICATION OF THIS PAGE (When Data Entered)

REPORT DOCUMENTATION PAGE	READ INSTRUCTIONS BEFORE COMPLETING FORM
1. REPORT NUMBER	2. GOVT ACCESSION NO. AD-A084 735 (9)
4. TITLE (and Subtitle) (6) Environmental and Other Criteria and Methods for Pavement Design	5. TYPE OF REPORT & PERIOD COVERED Final Technical Report OCT 76 — DEC 78
	6. PERFORMING ORG. REPORT NUMBER
7. AUTHOR(s) (10) R. W. Kirwan, E. R. Farrell, M. L. Maher	8. CONTRACT OR GRANT NUMBER(s) (15) DAERO-76-G-065
9. PERFORMING ORGANIZATION NAME AND ADDRESS Engineering School Univeristy of Dublin Trinity College, Dublin 117975	10. PROGRAM ELEMENT, PROJECT, TASK AREA & WORK UNIT NUMBERS (12) 142
11. CONTROLLING OFFICE NAME AND ADDRESS U. S. Army Research & Standardization Group (EUR) P. O. Box 65 FPO New York, New York 09510	12. REPORT DATE (11) Feb 79
	13. NUMBER OF PAGES 153
14. MONITORING AGENCY NAME & ADDRESS (if different from Controlling Office)	15. SECURITY CLASS. (of this report) Unclassified
	15a. DECLASSIFICATION/DOWNGRADING SCHEDULE
16. DISTRIBUTION STATEMENT (of this Report) Unrestricted	APPROVED FOR PUBLIC RELEASE; Distribution Unlimited
17. DISTRIBUTION STATEMENT (of the abstract entered in Block 20, if different from Report)	
18. SUPPLEMENTARY NOTES	
19. KEY WORDS (Continue on reverse side if necessary and identify by block number) Flexible pavement, pavement design, soil mechanics, environmnetal factors, pavement simulation, rational design, cyclic loading, pavement deflection, subgrade characterization, loading test apparatus, pore pressures, stress dependence, resilent modulus.	
20. ABSTRACT (Continue on reverse side if necessary and identify by block number) Results of an extensive series of repeated load triaxial test on Dublin Brown glacial till are reported. Charts are presented relating the relevant parameters of the till to dry density and moisture content. The effect of stress history is studied. The results indicate that modifications are required to the Kirwan-Snaith nomograph and suggest that the subgrade strain design criterion should vary with the stiffness of the soil. A recently developed low cost pneumatic repeated loading test apparatus is described. Skempton's A and B pore parameters have been used to interpret the response of samples under repeated loading.	

DD FORM 1 JAN 73 1473 EDITION OF 1 NOV 65 IS OBSOLETE

Unclassified

SECURITY CLASSIFICATION OF THIS PAGE (When Data Entered)

117975

A method of determining a stress-dependent resilient modulus by prepared charts from in situ tests on a subgrade is described. Results of laboratory pavement simulator tests on subgrade are compared with those obtained on undisturbed samples and with these results of the repeated loading, testing program. Modifications to DEFPAV which are required in order to include horizontally layered anisotropy are described. Initial results from a testing program to investigate the properties effecting the behaviour of natural gravels in road pavements are presented. Two computer subroutines for optimisation of road pavement design are described.

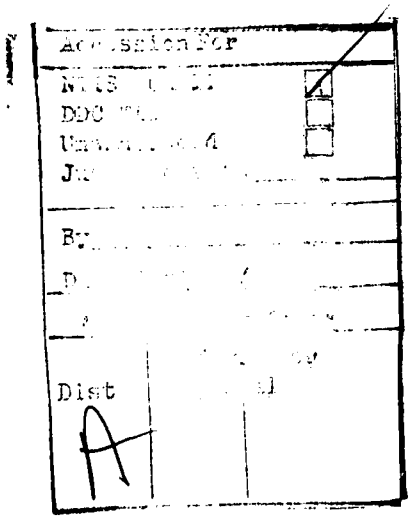

ENVIRONMENTAL AND OTHER CRITERIA AND METHODS FOR PAVEMENT DESIGN

by

R. W. Kirwan (Principal Investigator)
E. R. Farrell (Research Graduate)
M. L. Maher (Research Graduate)

GRANTEE: University of Dublin,
Engineering School,
Trinity College,
Dublin.

EUROPEAN RESEARCH OFFICE

United States Army

GRANT NO: DA-ERO-76-G-065

FINAL TECHNICAL REPORT

October 1976 - December 1978

The research reported in this document has been made possible through the support and sponsorship of the United States Army through its European Research Office. This Report is intended only for the internal management use of the Contractor and the United States Army.

February 1979

ABSTRACT

Results of an extensive series of repeated load triaxial tests on Dublin Brown Glacial Till are reported. Charts are presented relating the relevant parameters of the till to dry density and moisture content. The effect of stress history is studied. The results indicate that the Kirwan Snaith nomograph should be modified and suggest that the subgrade strain design criterion should vary with the stiffness of the soil.

A recently developed low cost pneumatic repeated loading test apparatus is described.

Skempton's A and B pore pressure parameters have been used to interpret the response of samples under repeated loading.

A method of determining a stress dependent resilient modulus using charts prepared from insitu tests on a subgrade is described.

Results of Laboratory Pavement Simulator tests on a subgrade material are compared with those obtained from undisturbed samples tested under repeated loading conditions, and also with those obtained from a nomograph prepared from the triaxial testing program.

The modifications that were made to the computer program DEFPAV to include horizontally layered anisotropy are described.

Initial results from a testing programme to investigate the properties affecting the behaviour of natural gravels in road pavements are presented.

Two computer subroutines for optimisation of road pavement design are described.

TABLE OF CONTENTS

CHAPTER 1

INTRODUCTION

This Final Technical Report for the two-year grant (Grant No. DAERO-76-6-065) covers the research carried out during the period September 1976 to December 1978.

This is a continuation of the work carried out by the Pavement Research Group at Trinity College, Dublin, Ireland during the past twelve years. It has previously been funded by E.R.O., with five separate annual contracts, followed by one three year Grant (No. DA-ERO-591-73-60017). Three Annual Reports were provided for the latter grant, the last being dated April 1976.

The object of the recent research has been to work towards a simple and rational method of design for flexible pavements by means of a better understanding of the behaviour of the constituent materials, with possible verification in the field.

An extensive series of triaxial tests was carried out on Dublin glacial till in order to study its behaviour under repeated loading, with particular emphasis on the variation of the relevant properties with dry density and moisture content. The effect of stress history was also studied. The results of this work indicate that the nomograph proposed in the Report of April 1975 requires certain modification.

It is also suggested that the resilient subgrade strain criterion, which is frequently used to limit permanent deformation in the subgrade, be varied with the stiffness of the soil. Limited test results indicate that the permanent deformation behaviour of a soil depends on the degree of strain of the samples.

In order to carry out this program of triaxial tests a simple low cost pneumatic repeated loading test apparatus has been developed, along with a ram load cell and lateral strain indicator.

Skempton's A and B pore pressure parameters have been used to interpret the resilient vertical and lateral response of a sample under repeated loading.

A method of determining the variation of resilient modulus with stress level from an insitu test on a subgrade using prepared charts is given.

Good comparison was obtained between the stress dependent resilient modulus determined from the back analysis of tests on a glacial till subgrade in the Laboratory Pavement Simulator with that recorded in triaxial tests on undisturbed samples and also with that interpolated from the chart prepared from the triaxial testing programme.

The T.C.D. Finite Element Program has been modified to include horizontally layered anisotropy.

The initial results of a series of repeated loading tests on gravel pavements in the Laboratory Pavement Simulator are reported.

The computer subroutines, SELPAV and OPTPAV, are presented for optimisation in road pavement design. The former is incorporated into the proposed design system DEFPAV and is a modification of that described in our previous report. The latter is an independent package which considers the cost implications of a wide range of design alternatives, including stage construction.

Attempts made to verify our design methods by monitoring the performance of a section of the Stillorgan Dual Carriageway outside Dublin were frustrated by vandalism, construction difficulties and unsuitable equipment for the field use. It

is considered impracticable to get successful field verification of our work with the present resources of the Pavement Research Group. A proposal for funds for this work has been sent to the European Economic Community but no reply has been received to date.

CHAPTER 2

REPEATED LOADING APPARATUS

2.1 Introduction

The initial series of repeated loading triaxial tests were carried out on the mechanically operated rig described by Glynn (1) but with the method of applying cell pressure altered to the pneumatic/hydraulic system shown in Fig. 2.1. This alteration allowed a cyclic cell pressure to be superimposed on a constant initial confining pressure. The system was designed to allow a back pressure in a sample, if required. The mechanical section of the apparatus has been in use in Trinity College since 1967 and was beginning to show its age. Considerable skill was required by the operator to get the correct axial load and the permanent deformation compensator required regular inspection. Furthermore, the maximum axial stress which could be applied to a 100mm diameter sample was limited to approximately 120kN/m^2. It was therefore decided to develop and construct a new twin cell repeated loading rig for the series of tests required for our material characterisation program. Barksdale (2) and others have shown that a passing wheel applied an approximately sinusoidal or triangular type load pulse to a subgrade element under a road pavement of duration of the order of 0.2 - 0.4 secs. Apart from the rotation of the axis of the principal stresses which occurs under a passing wheel, the insitu stresses on a soil element can be modelled in a triaxial cell by an axial stress pulse and a confining cell pressure pulse of similar waveform and duration superimposed on a static confining pressure which represents the insitu overburden pressure. The load in a triaxial cell must be applied without impact and completely removed between load applications to allow the sample recover for simulated rest periods.

A servo-controlled electro-hydraulic system would give the required loading but was ruled out because of its cost. Pneumatic or pneumatic/hydraulic systems are considerably

cheaper and easier to construct. Several such apparatii which have been reported in the technical literature, were tried out but were eventually discarded either because they did not meet our specific requirements or because they included equipment not readily available in Ireland or the British Isles.

2.2. New Repeated Loading Testing Rig

A pneumatic loading rig was therefore designed and built at Trinity College, Dublin, to meet our specific requirements. Details of this rig are given on Fig. 2.2 the particular features of which are the following:-

(1) Air supply with normal working pressures of 700 kN/m^2.

(2) Axial load applied through a 70mm dia piston capable of applying 300 kN/m^2 to a 102mm dia sample with an air pressure of 700 kN/m^2.

(3) Inlet air supply to piston taken from an air reservoir, pressure of which is adjusted by an air regulator, through an on/off solenoid which is controlled by a timer unit, and through a needle valve which controls the air supply.

(4) Exhaust air supply from piston taken through an on/off solenoid which is controlled by a timer and interval delay relay, and through a needle valve.

(5) Low pressure air supply taken through a non return valve to the loading piston to bring loading ram in contact with the sample before each load pulse.

(6) Water reservoir located above test rig. This gives a hydrostatic cell pressure of 14 kN/m^2 when the reservoir is open to the atmosphere.

(7) Inlet air supply to reservoir taken through a timer controlled solenoid and the exhaust also through a timer controlled solenoid and through a pressure relief valve if it is required to increase the constant cell pressure above that mentioned in (6) above.

(8) Timing relay (T1) Electromatic asymmetrical recycler with time range of 0.15-3 secs on both on and off time.

(9) Interval timer (T2) which is reset by a relay working from the "on time" of the times relay (T1). Friction in the water time delays the cell pressure pulse in the triaxial cell and consequently the load pulse must be delayed to get both waveforms in phase.

(10) Delay on operation of timing relay (T3) worked from (T2) to control the duration of the axial load pulse.

(11) Interval times (T4) to delay closing the exhaust solenoid of the loading piston. The circuit of this unit which was designed and constructed at T.C.D. is shown in Fig. 2.3.

The sequence of operation is as follows:

(a) Timer relay T1 closes solenoid A and opens B to pulse the air pressure in the water reservoir for the desired pulse duration which is set by Dial X. The start of this load pulse also closes the relay which in turn resets the interval times T2. At the end of the desired period the solenoid A is opened and B closed, thus relieving the air pressure.

(b) After the time interval set on timer T2, the circuit to the delay timer T3 is opened which in turn closes solenoid C and opens solenoid D, also triggering the interval timer T4, which pulses the axial load for the length of time set on T3.

(c) After the desired time set on T4, solenoid C, which opens to relieve the axial load, is closed thus allowing the low cell pressure supply to bring the ram into contact with the sample.

(d) The sequence is repeated after the period of time set on dial Y of the timer unit.

The initial calculation and the development tests indicated that the pneumatic system could be easily controlled to

give a triangular or approximately sinusoidal loading but gave an unsatisfactory approximation of a reversed sine waveform on the unloading phase which resulted in a sawtooth waveform. An automatic system was designed to overcome this and hopefully give an approximately sinusoidal unloading phase. This has not been constructed to date as the response of the system when the sample is included appears to give a satisfactory waveform on both phases. Typical axial and cell pressure loading pulses are shown in Fig. 2.4

2.3 Load and Deflection Measurements

The methods for deflection and load measurements on the old mechanically operated loading rig were as described by Glynn (1), with the exception that the axial load was measured on a load cell incorporated in the triaxial loading ram inside the cell. Initially it was intended to measure the load using strain gauges on the inside of a hollowed out portion of the ram. This proved difficult to construct and lacked sensitivity. The sensitivity was increased and the construction simplified by using the module sensor as shown in Fig. 2.5. This load cell generally gave satisfactory performance but the following points were noted:

(a) Sealing off the cell pressure from the sensor sometimes gave problems, particularly at high pressure. The sensor was insensitive to the normal range cyclic cell pressure.

(b) The increase in sensitivity of the load cell was not as great as was expected. This may have been caused by elasticity in the system and could probably be eliminated by careful design and construction.

Load measurements in the new R.L.T. rig were measured on a Proving Ring outside the cell which incorporated an

LVDT and also on a strain gauged miniature proving ring constructed from the loading ram inside the cell. The latter type of load cell was noted during a visit to Nottingham University but in order to enable it to be used under water the strain gauges and leads were waterproofed. In Nottingham, it is used in a non-conductive oil environment.

The resilient and permanent deflections of the sample were measured by a twin LVDT located on top of the cell as shown in Fig. 2.6. Permanent deflection was recorded by the LVDT and checked by readings to the top of nut A by micrometers.

2.4 Lateral Deflection Measurements

The initial series of triaxial tests carried out in the old mechanical rig did not allow the lateral deflection of samples to be measured.

Problems were encountered in developing a simple reliable system for the measuring to small lateral deflections of samples surrounded by water. The strain band as described by El-Ruwayih(3) when constructed at T.C.D. was not sufficiently sensitive and was affected by the cycled cell pressure. No miniature LVDT was readily available for use under water.

Satisfactory results have recently been achieved with the lateral strain indicator (LSI) shown in Fig. 2.7. This apparatus is sensitive, appears to be unaffected by cell pressure and to date has been reliable. The pressure exerted by this L.S.I. is of the order of $0.04 kN/m^2$ per 0.01mm deflection. This means that for lateral deflection of 0.2mm which would correspond to vertical strains of the order of 0.004 mm/mm the pressure on the side of a sample at the supports would be approximately $0.8 kN/m^2$. This is not therefore considered an important factor.

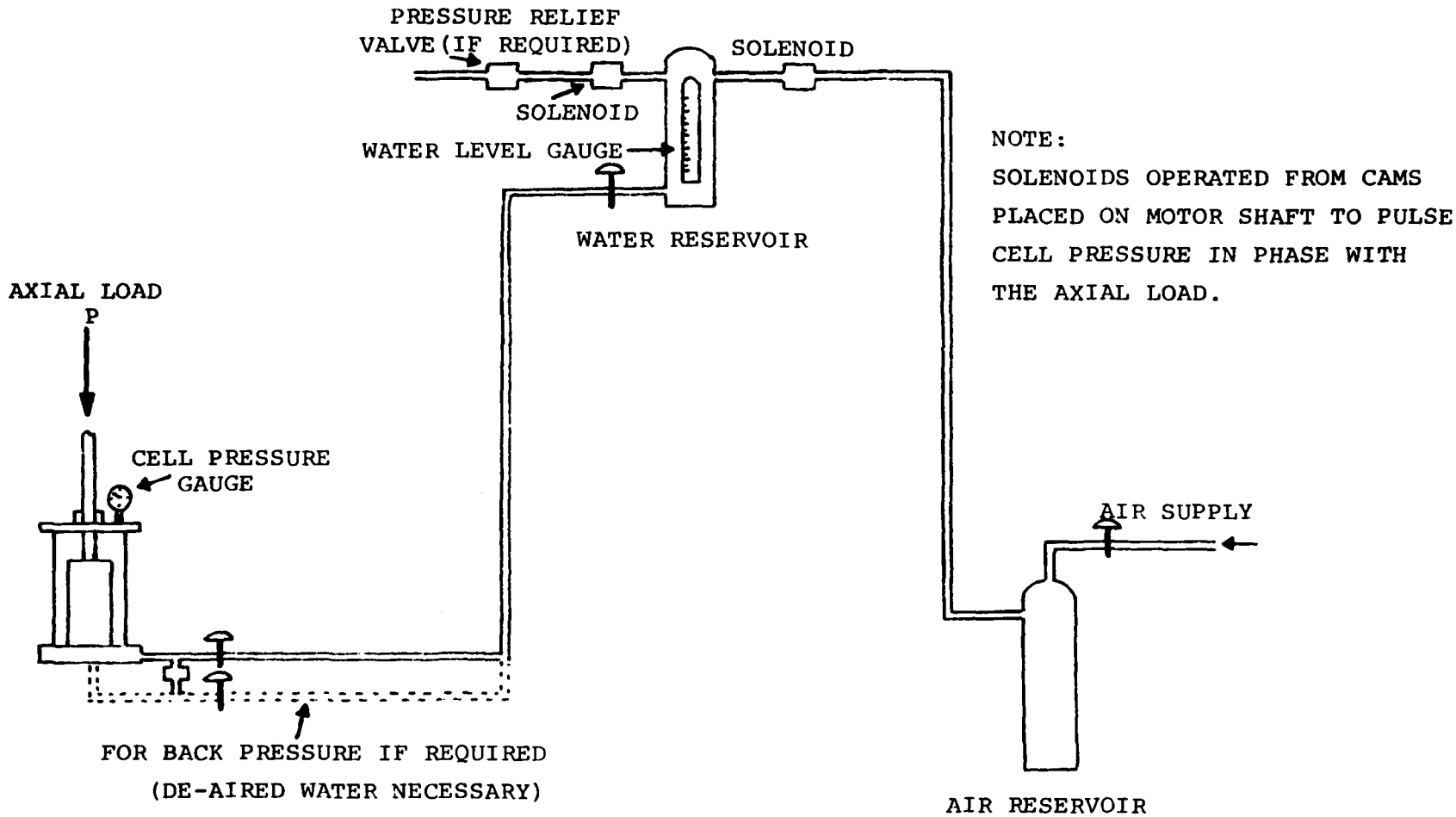

MODIFIED CELL PRESSURE SYSTEM TO OLD TRIAXIAL RIG

Fig. 2.1

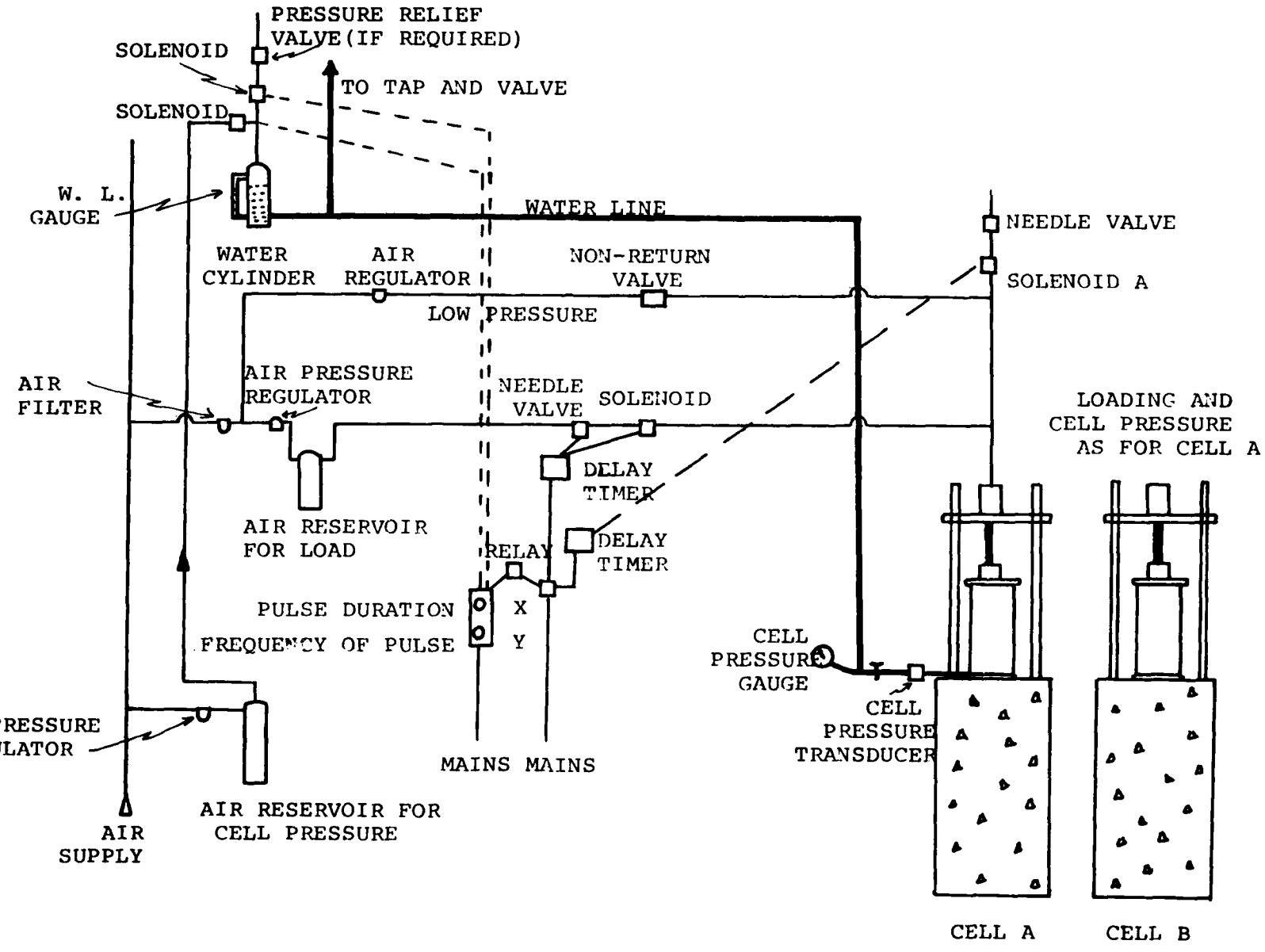

Fig. 2.2

PNEUMATIC REPEATED LOADING APPARATUS

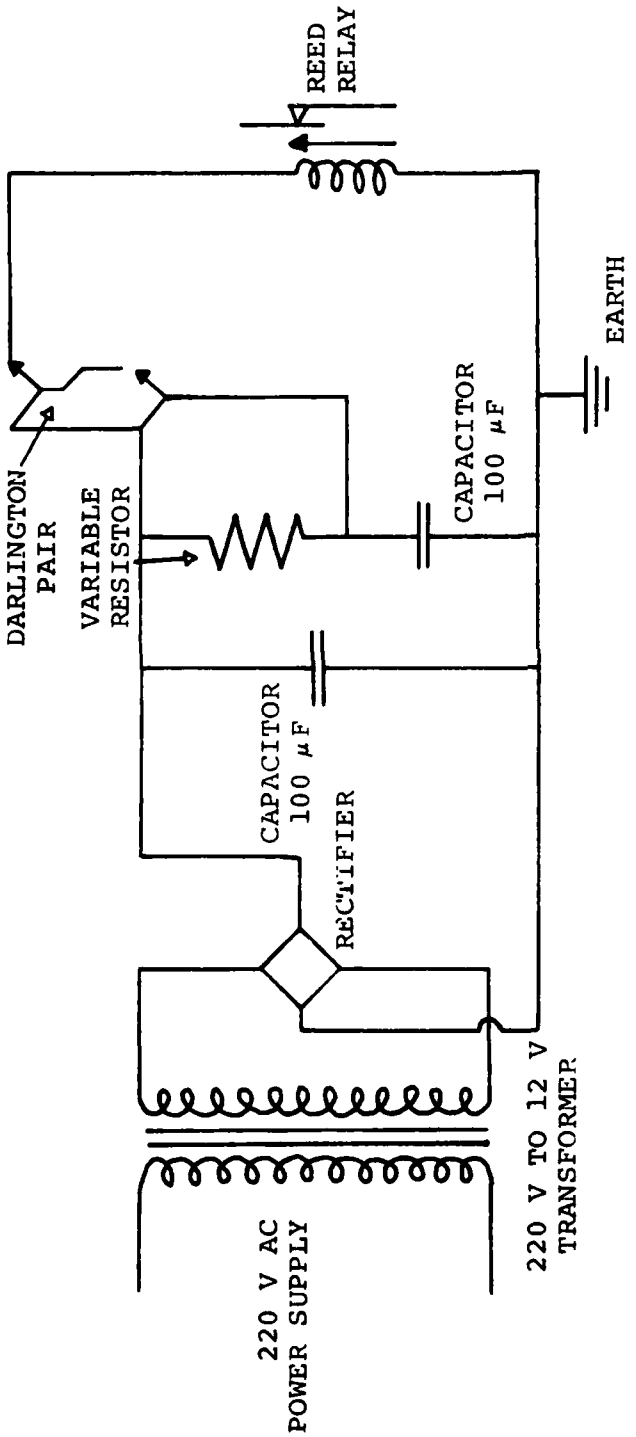

CIRCUIT DIAGRAM FOR TIMER DELAY UNIT

Fig. 2.3

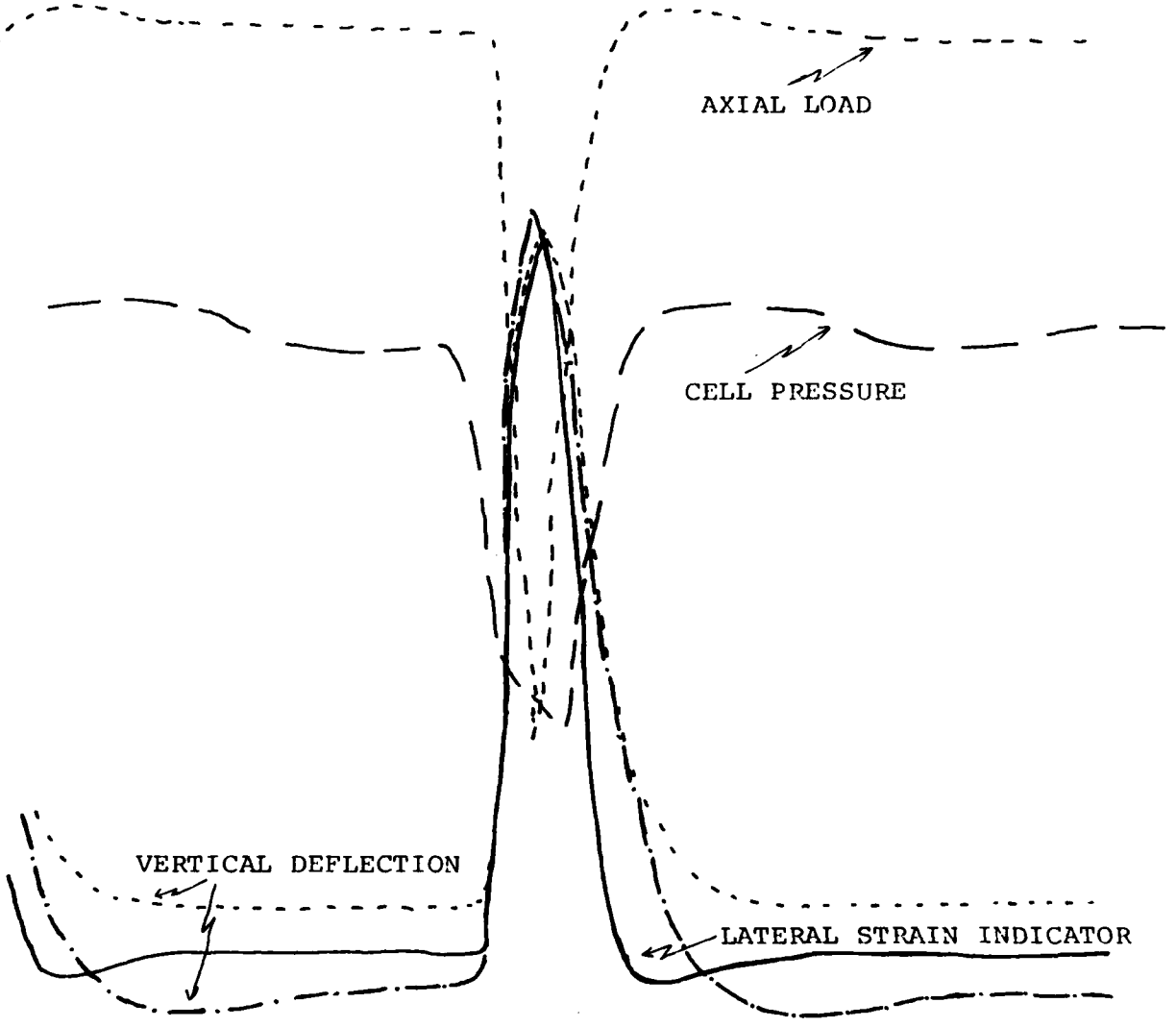

Fig. 2.4 TYPICAL TRANSDUCER PULSES FROM TRIAXIAL TESTING

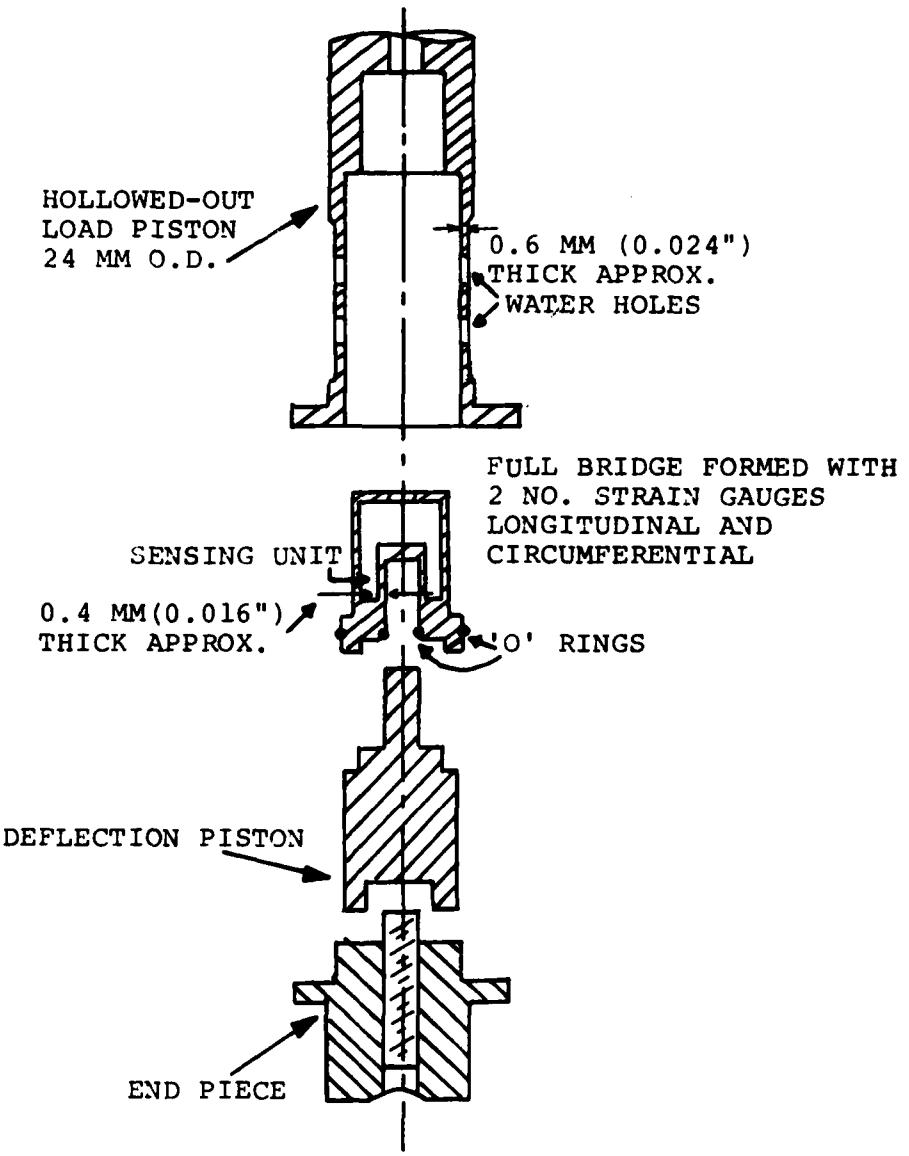

NEW TCD LOAD CELL FOR LARGE TRIAXIAL CELLS

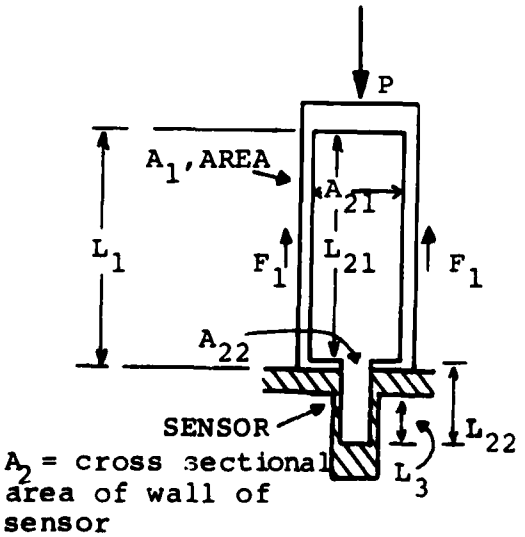

A_2 = cross sectional area of wall of sensor

STRAIN IN SENSOR, ε_3

$$= \frac{P}{E\left\{\frac{A_1}{L_1}\left(L_3 + \frac{A_3 L_2^*}{A_2} + A_3\right)\right\}}$$

$$L_2^* = A_{22}\left\{\frac{L_{21}}{A_{21}} + \frac{L_{22}}{A_{22}}\right\}$$

PRINCIPLE OF LOAD CELL OPERATION

Fig. 2.5

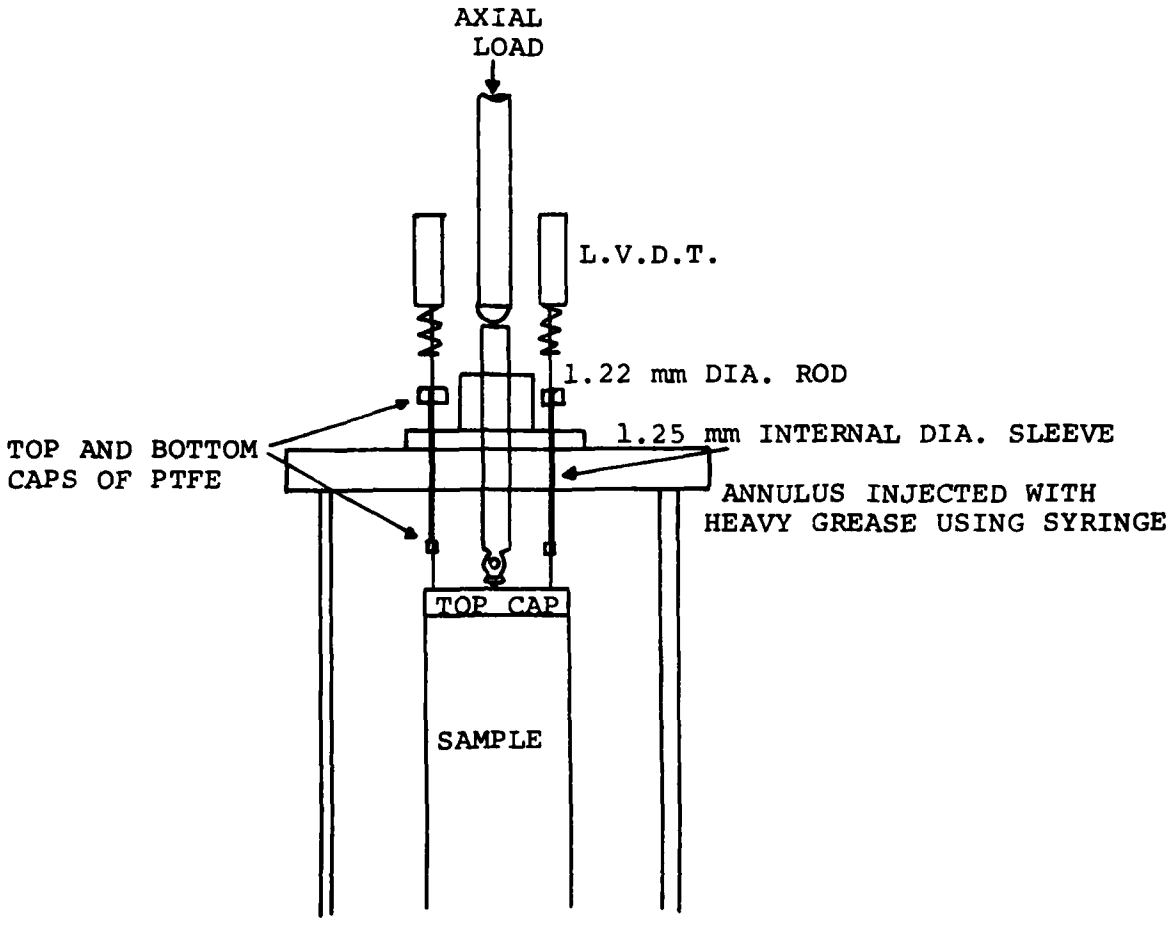

METHOD OF RESILIENT DEFLECTION MEASUREMENTS

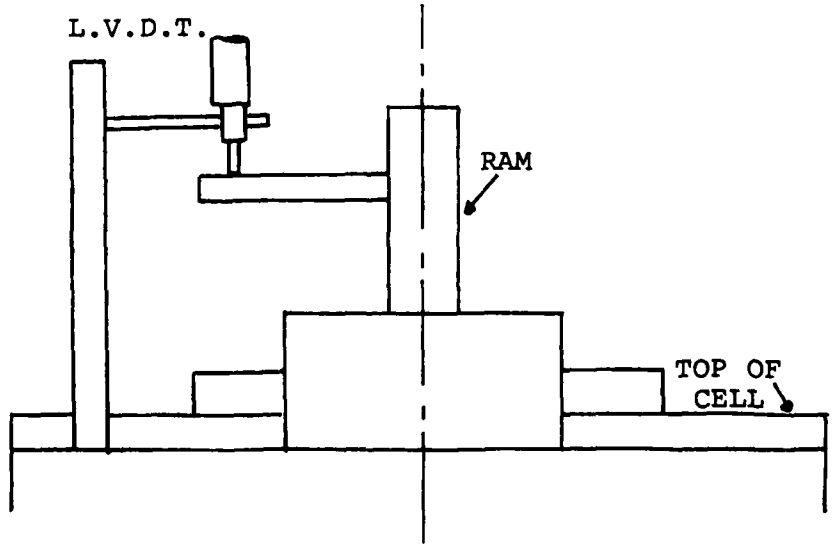

METHOD OF PERMANENT DEFLECTION MEASUREMENTS

Fig. 2.6

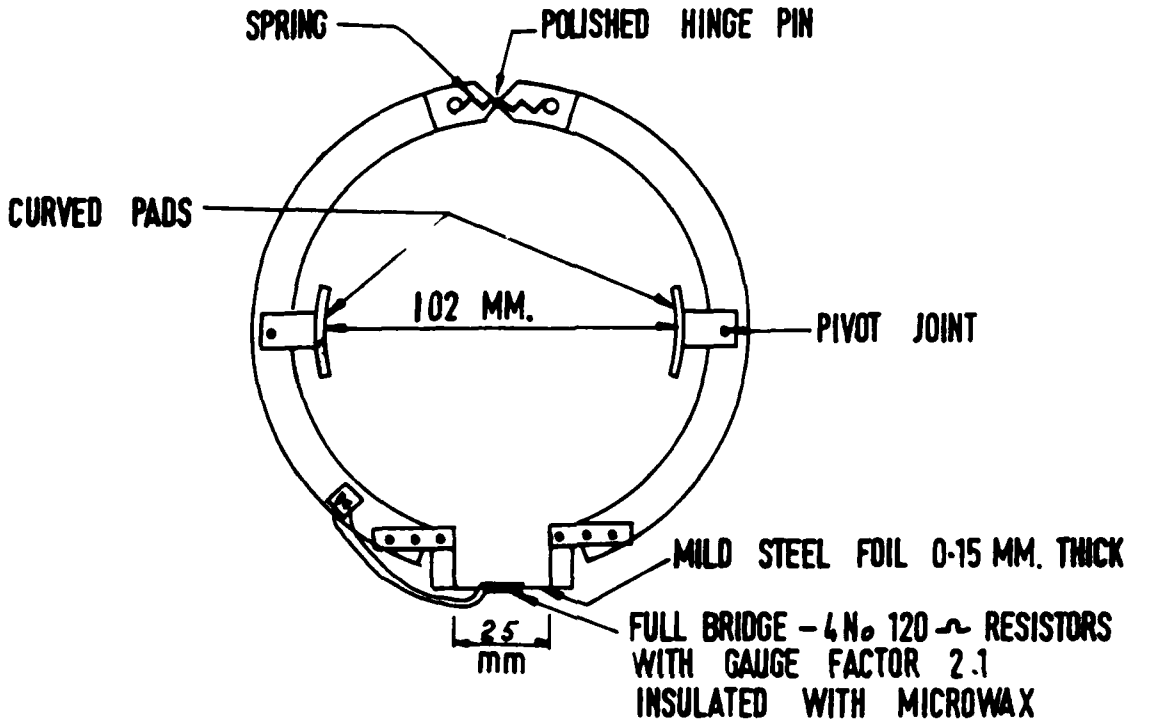

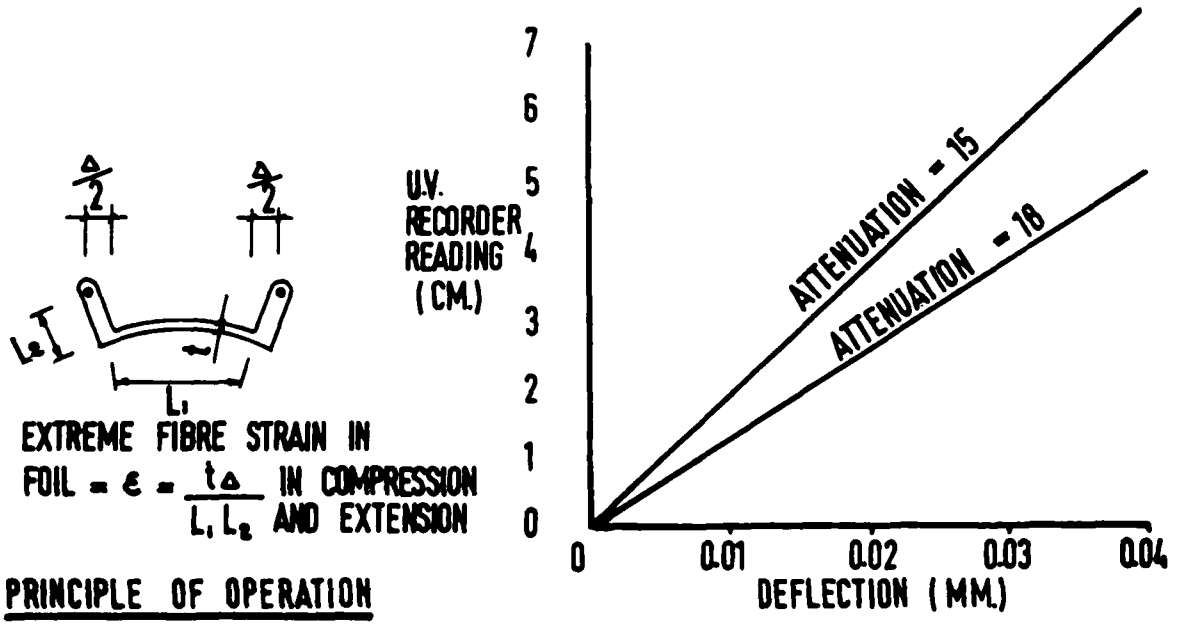

PRINCIPLE OF OPERATION

T.C.D. LATERAL STRAIN INDICATOR FIG. 2.7

CHAPTER 3

REPEATED LOAD TRIAXIAL TESTS ON A GLACIAL TILL

3.1 Introduction

The subgrade forms a major element in a road structure, yet comparatively little research has been carried out on the behaviour of subgrade materials. It is generally agreed that methods for analysing road pavements have reached a satisfactory level of development and that further work should concentrate on the choice of suitable input parameters and on verification by monitoring insitu performance. It is therefore of prime importance to develop a better understanding of the factors affecting the behaviour of subgrade materials under repeated loading and under various stress histories. Hopefully from the knowledge obtained, parameters necessary for input into the design systems can then be related to simple laboratory or insitu tests.

Kirwan and Snaith (4) suggested that the resilient modulus (M_r) of a soil could be related to its Relative Compaction (R_c) and to its Relative Moisture Content (R_w), by means of a nomograph where

$$\text{Relative Compaction} = \frac{\text{Insitu dry density}}{\text{Modified AASHO maximum dry density}}$$

$$\text{Relative Moisture content} = \frac{\text{Insitu moisture content}}{\text{Modified AASHO optimum moisture content}}$$

The nomograph that was produced to relate these parameters was based on the limited results that were available to them at the time. It was decided to initiate a program of repeated load triaxial testing of soils at a wide range of dry densities and moisture contents in order to investigate further the Kirwan Snaith nomograph, to study the effect of

stress history on these parameters and to see if the R_c and R_w concept could be extended to the creep behaviour.

3.2 Testing Procedures

A glacial till, commonly called Dublin Brown Boulder Clay, was used throughout the testing program. This forms the predominant subgrade in Ireland. A large quantity of the soil was sieved through a 5mm sieve, thoroughly mixed and stored in bins for testing at a later date. The properties of this soil are given in Fig 3.1. Similar soil but sometimes with different maximum stone size was used by Snaith (5), Glynn (1) and Casey (6).

The old twin-cell repeated load triaxial test rig as described by Glynn (1) with the modifications mentioned in Chapter 2 of this report was used for the series of tests carried out to date on the material characterisation program. The new rig is now operational and the testing program has been moved over to that equipment.

The soil was compacted by the method recommended by Snaith (5). Electro-osmosis was sometimes used to bring the samples close to saturation. The initial confining stress (σ_{3c}) was held constant throughout the tests at 14 kN/m^2 with the cycled cell pressure ($\Delta\sigma_3$) in phase with the axial load at ½ ($\Delta\sigma_1 - \Delta\sigma_3$) unless specific tests were made to study the effect of cycled cell pressure. The sequence of loading was varied to study the effects of various stress histories.

Every effort was made to duplicate each test. Nevertheless, more often than not the inevitable small differences in the dry density γ_d and moisture content were sufficient to significantly affect the results. An example of the effect of a small variation of moisture content on the permanent strain is shown in Fig. 3.2. Where samples were more or less the same, the results from each were consistent, as shown in Fig. 3.3. The test results from the different cells were also consistent.

3.3 Modulus of Resilience Versus Dry Density and Moisture Content

The variation of the modulus of resilience (M_r) with and m/c for an applied axial stress of 20kN/m^2 is shown in Fig. 3.4. These results form a consistent trend and as can be seen, agree well with those recorded by Snaith (5) which are also plotted for comparison.

One noticeable feature is the absence of any local peak value for M_r near mod ASSHO optimum density and moisture content which would be predicted from the Kirwan and Snaith nomograph. Contours of equal M_r interpreted from the present tests are shown. Replotting the results of Seed et al (7) in a similar form (Fig. 3.5) gives the same type of contour diagram. It is therefore suggested that part of the Kirwan Snaith nomograph requires modification. Contours of equal M_r plotted against R_c and R_w for the brown glacial till are shown in Fig. 3.6. The curves for Mod AASHO and Proctor Compaction are superimposed on the tentative contour diagram shown in Fig. 3.4. The maximum resilient modulus was not at the optimum moisture and maximum dry density for these compactive efforts. A similar finding can be interpreted from the results of Seed et al (7). The resilient modulus plotted against moisture content for given compactive efforts for the T.C.D. and Seed et al tests shown in Fig 3.7 illustrate the point. This result is contrary to the findings of Majedzadeh and Guirguis (8), who reported that for a given compactive effort, the maximum resilient modulus occurred at optimum conditions of dry density and moisture content.

3.4 Effect of Incremental and Decremental Loading on the Modulus of Resilience.

The change in the resilient modulus with increases or decreases in the applied axial load and cell pressure are illustrated by some typical results shown in Fig 3.8. Soft samples showed little change in M_r with increases in deviator stress, medium stiffness samples decreased in

modulus with increasing stress level while the results of the tests on stiff samples showed an initial increase in M_r, followed by a decrease. The initial increase in M_r exhibited by the stiff soils was not expected. It may have been caused by the seating of the top cap. However, further tests are being carried out to investigate this.

The behaviour of the soft and medium strength stiff soils can be explained by considering the resilient deformation as being dependent on the structure of the soil and on the orientation of the particles.

The particles of a soft soil reorientate themselves under low stresses and any decrease in modulus with increase in stress is due solely to the non-linear elasticity of the soil system. An increase in applied stress for a medium strength stiff soil can gradually break down the orientation of particles and possibly lead to an increase in compaction. Therefore the change in M_r reflects the non-linear elasticity of the soil structure as well as the work hardening due to compaction. Subsequent unloading and loading at constant permanent strain would be expected to give lower moduli values should the former process predominate, as the structure would be broken down to some extent. The test results shown in Fig. 3.9. confirm this for the medium stiff soil ($M_r \approx 50$ to 80 MN/m^2). Some investigators have found an increase in modulus of resilience for some soils at high deviator stresses. Under these conditions the work hardening effect would predominate.

Soil compacted at optimum modified AASHO moisture content and dry density would be classified as medium stiffness soils, therefore the stress dependent modulus would be affected by the stress history. It is suggested that the modulus-stress relationship for the loading, unloading curve be used for design on the basis that it is the weaker condition and also the condition which would exist after an initial settling-in period of a subgrade. Expressing the stress depending

dependent resilient modulus in the form:

$$M_r = C\sigma_c^{-\gamma}$$

the test results for the unloading, reloading curves gave an approximate value of γ of 0.14.

The sine function relationship developed previously by Kirwan and Snaith (4) did not fit these curves but most of the present tests were incrementally loaded as opposed to individual samples being tested under different loads.

3.5 Permanent Strain

In order to study the variation of permanent strain (ε_p) with dry density γ_d and moisture content (m/c) it was necessary to model the behaviour of each sample by a creep function to compare parameters. The permanent strain for 9 tests are plotted in Fig. 3.10 against deviator stress for 40,000 cycles. Owing to the lack of adequate information on the creep behaviour of soils, permanent deformation of subgrade materials is generally controlled in road design by ensuring that the maximum resilient subgrade strain does not exceed values which have been determined from the back analyses of existing road structures which have behaved satisfactorily. The relationship suggested by Brown et al (9) for British soils gives a limiting subgrade strain of 1.0×10^{-3} for a design life of 40,000 cycles. Working back from the measured values of the resilient modulus from the test results the resulting permanent strains are shown in Fig. 3.10. Thus the working range is less than 1.0% permanent axial strain. Below this value the permanent strain results can be approximated to a straight line $\varepsilon_p = f^n(N, \sigma_d, m/c) * \sigma_d$, where N = number of cycles. This function $f^n(N, \sigma_d, m/c)$ corresponds to the creep compliance used by Glynn (1) the value of which (at a given number of cycles) can be used to compare the permanent deformation of soils of different

dry densities and moisture contents. Permanent strain is generally expressed in the form $\varepsilon_p = f^n(N)\sigma$ for constant values of moisture content and dry density.

Glynn (1) on his tests on Dublin brown boulder clay (Fig. 3.11) used a value of b = 1 thus (assuming linear variation with stress) but incorporated the concept of a threshold stress. Applying the condition that the applied load must result in strains below those allowed by the subgrade strain criterion, Glynn's test results can be approximated by a straight line if the threshold stress is ignored. Kirwan and Snaith (10) argued that a value of b = 1.75 was more correct but their results are more difficult to interpret as separate samples were used at each stress level with corresponding small differences in γ_d and m/c. Nevertheless the assumption of linear behaviour appears to be reasonable within the normal working range of stress and deformation.

3.6 Creep Compliance vs Dry Density and Moisture Content

The creep compliance at 40,000 load repetitions for the tests to date are shown in Fig 3.12, plotted against dry density and moisture content. The results form a consistent trend and illustrate the dramatic increase in permanent deformation that can occur with an increase in moisture content.

3.7 Subgrade Strain Criterion

The subgrade resilient strain criterion would be expected to give a relatively constant permanent deformation if, as it is generally assumed, it controls the permanent deformation in the subgrade. Most of these empirically derived relationships depend solely on the number of load repetitions and therefore, like that of Brown et al which is plotted on Fig. 3.13, would give much less permanent deformation for the stiff samples (0.2% for $M_r = 75MN/m^2$) than for the softer samples (1% for $M_r = 20MN/m^2$). Barker et al (11) from a back analysis of

airfield runways, suggested that the limiting design subgrade strain be varied with the stiffness of the soil. Their relationship would allow an increase in the resilient strain for stiffer soils, which is in agreement with the test results. The tests to date therefore suggest that the subgrade strain criterion should be varied with the stiffness of the soil.

3.8 Permanent Strain and Stress History

The limited results to date suggest that the permanent strain is strain dependant. This is shown in Fig. 3.14 where two identical samples were incrementally loaded with different initial stress levels. It can be seen that once the samples reached the same permanent strain their behaviour was almost identical. A sample unloaded from a stress level of 80kN/m^2 and subsequently unloaded and reloaded at various lower stress levels suffered no measurable increase in permanent deformation as can be seen in Fig. 3.15.

The test results indicate that when a certain strain is reached as a result of a given number of repetitions of load, at a particular stress, then additional repetitions of load at a lower stress will not result in any further increase in strain provided that the strain attained at the higher stress level exceeds the maximum possible strain at the lower stress level. This behaviour agrees with a "time-hardening model" for permanent strain suggested by Monismith et al (12) but here the term strain dependent is considered more suitable. This point is illustrated in Fig. 3.16. The cumulative permanent deformation of a spectrum of loads cannot therefore be added together to give the total deformation, as the sequence of loading would affect the result. This is a point that is being investigated further at T.C.D.

3.9 Permanent Strain vs Resilient Strains

Barker (11A) found a relationship between the permanent and resilient strains from published results of repeated load

tests from various investigators. The results of the present series of tests plotted in Fig. 3.17 to both a natural and log-log scale tend to confirm this finding. The results of Snaith (5) fall within the same zone.

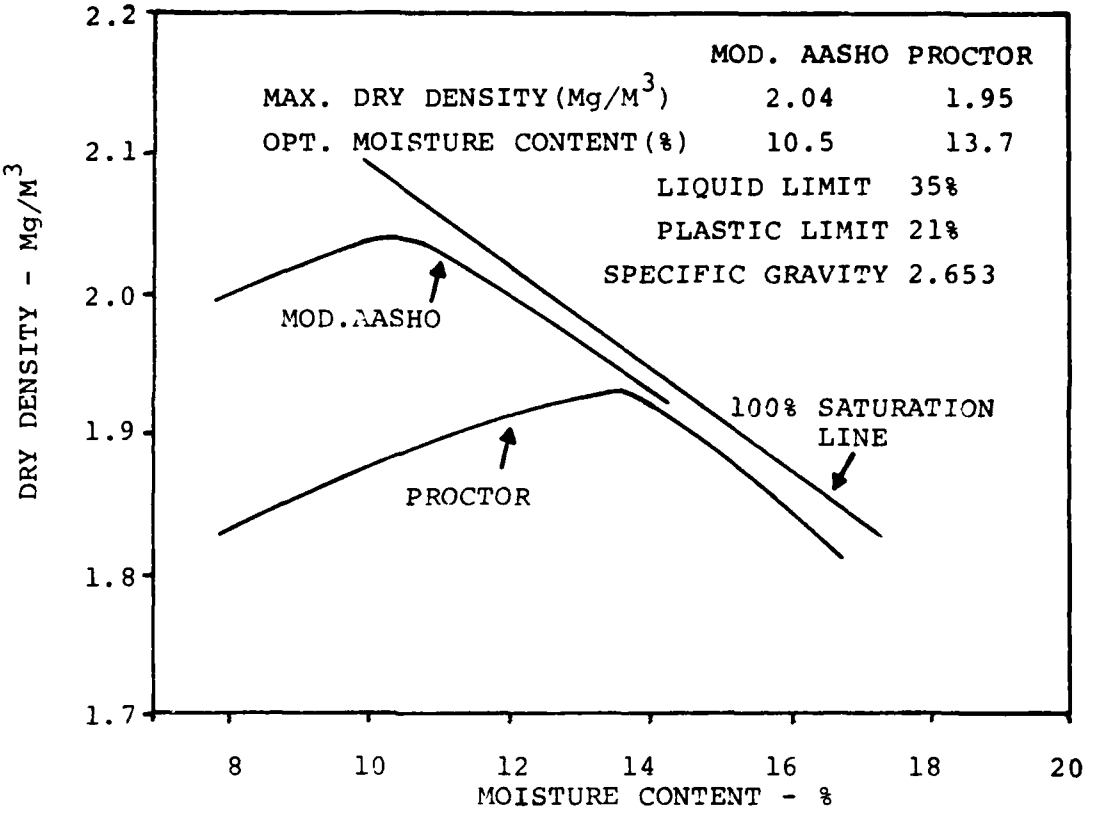

DRY DENSITY Vs MOISTURE CONTENT

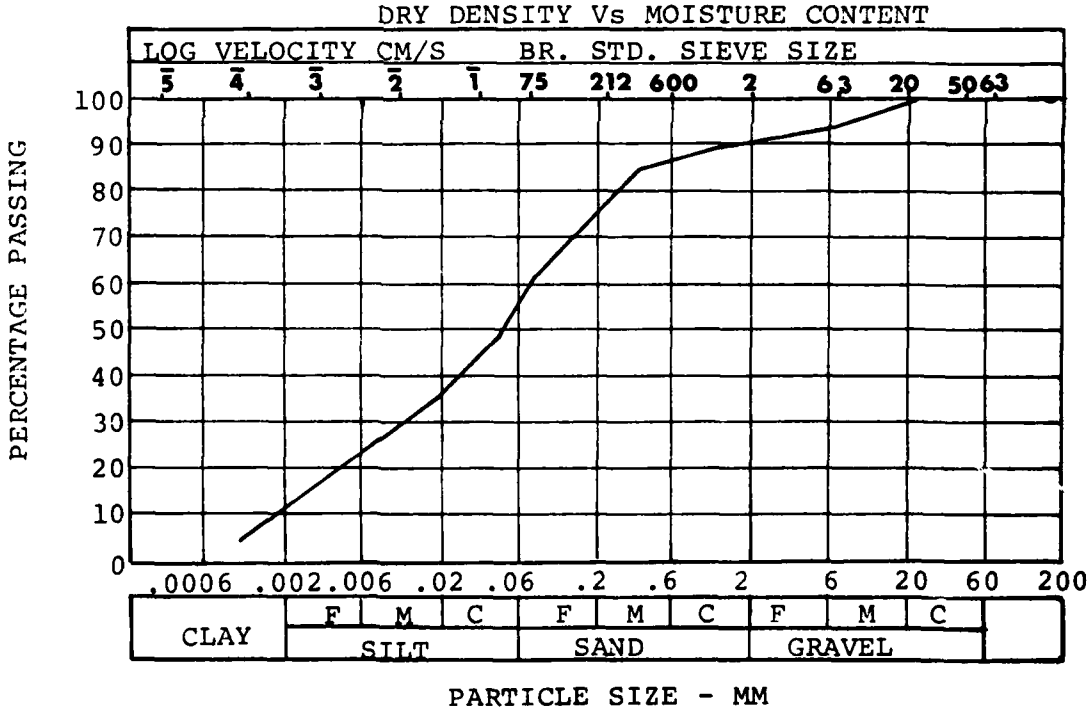

PARTICLE SIZE DISTRIBUTION CURVE

Fig. 3.1

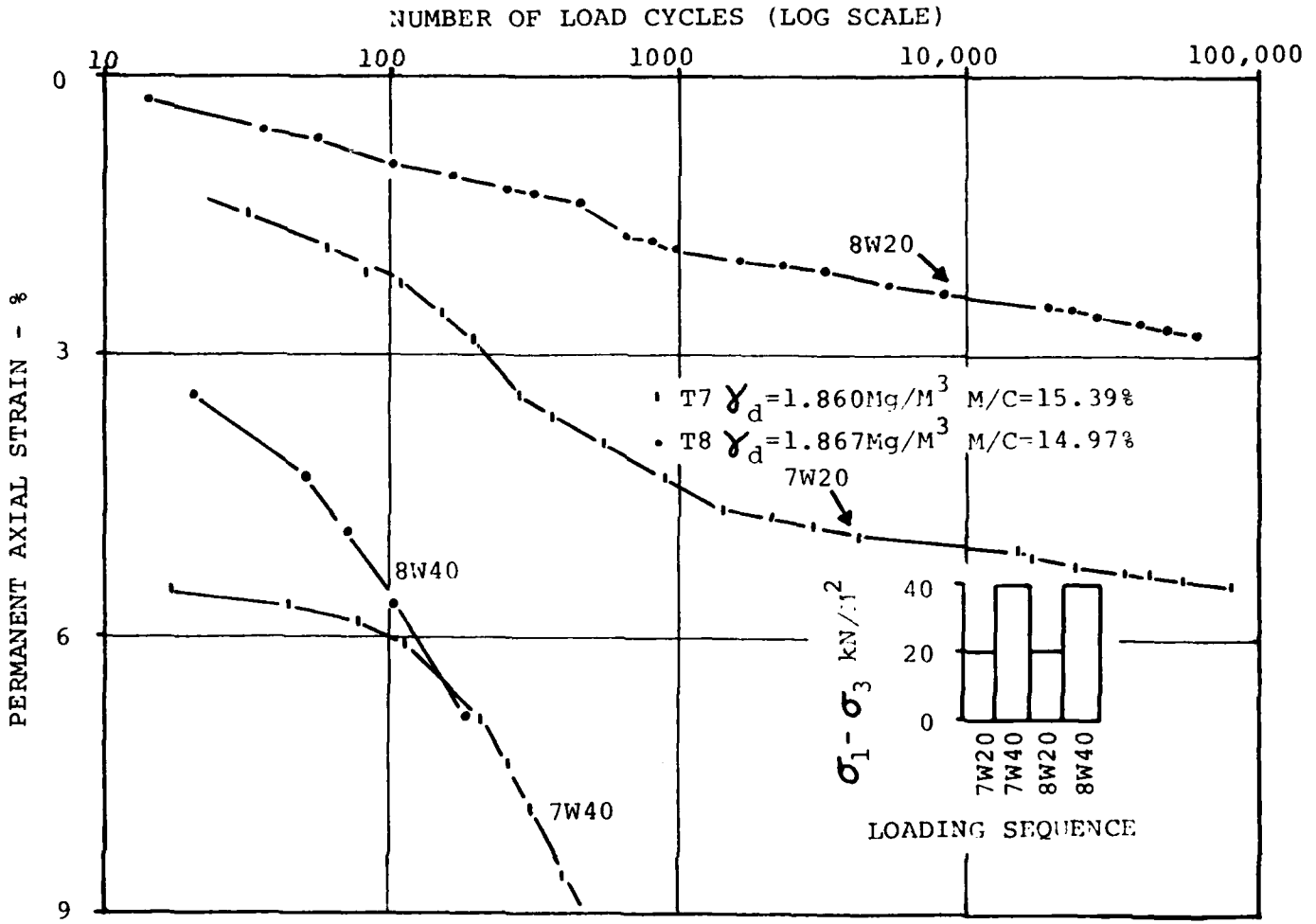

PERMANENT DEFORMATION Vs NO. OF LOAD CYCLES FOR DUBLIN GLACIAL TILL

Fig. 3.2

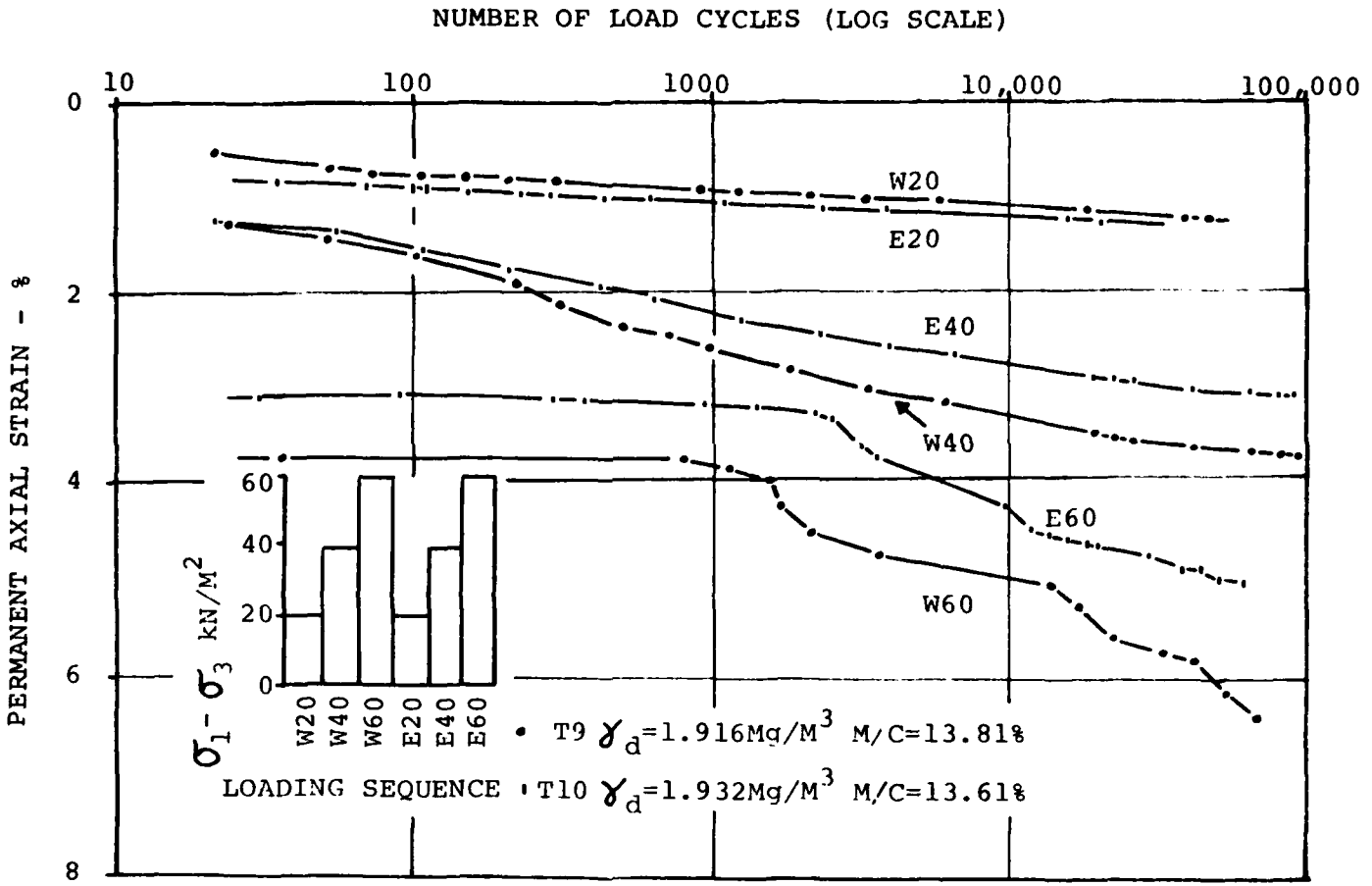

PERMANENT DEFORMATION Vs NO. OF CYCLES FOR DIFFERENT CELLS

Fig. 3.3

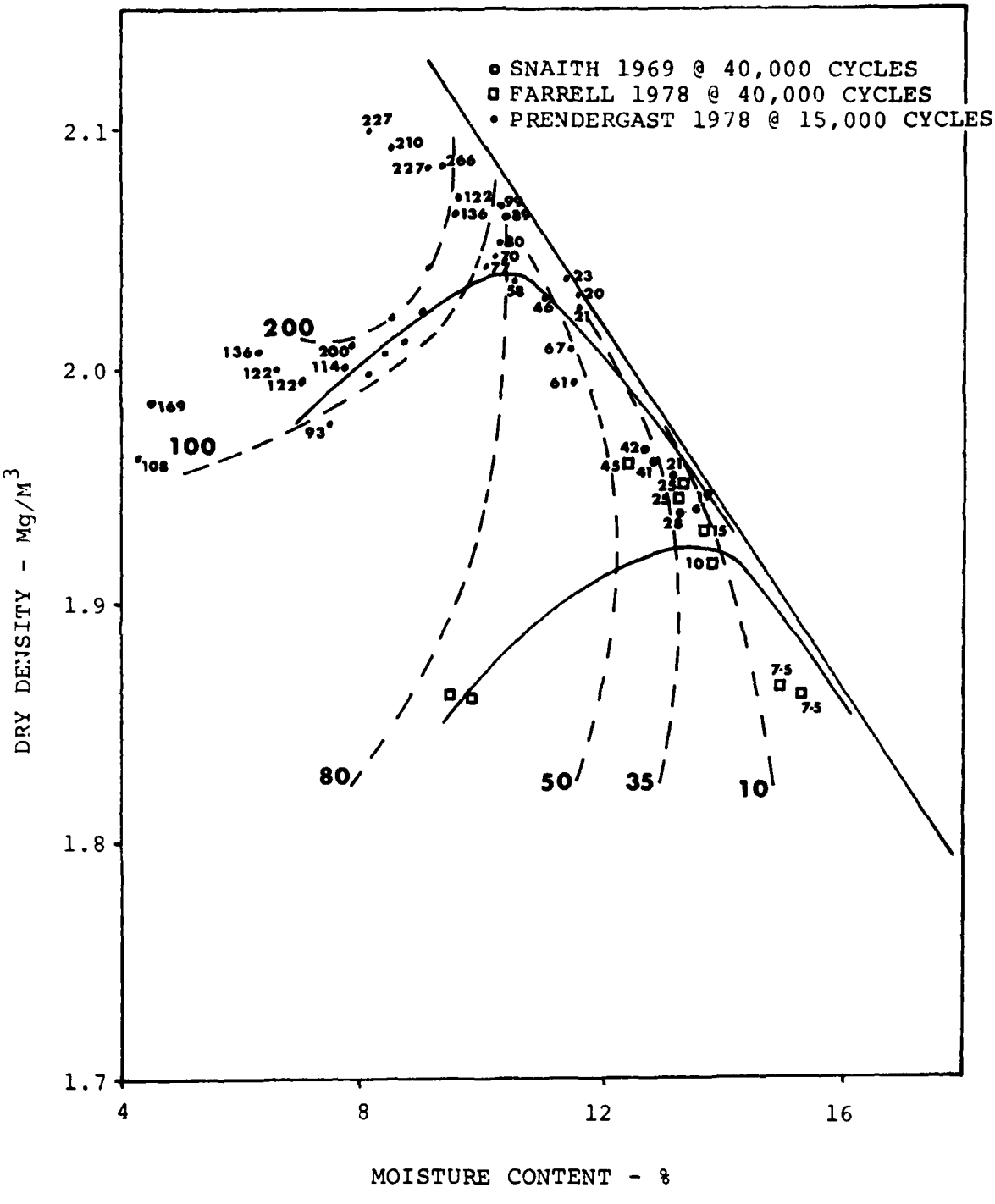

RESILIENT MODULUS Vs DRY DENSITY AND MOISTURE CONTENT FOR DEVIATOR STRESS OF 20 kN/M^2

Fig. 3.4

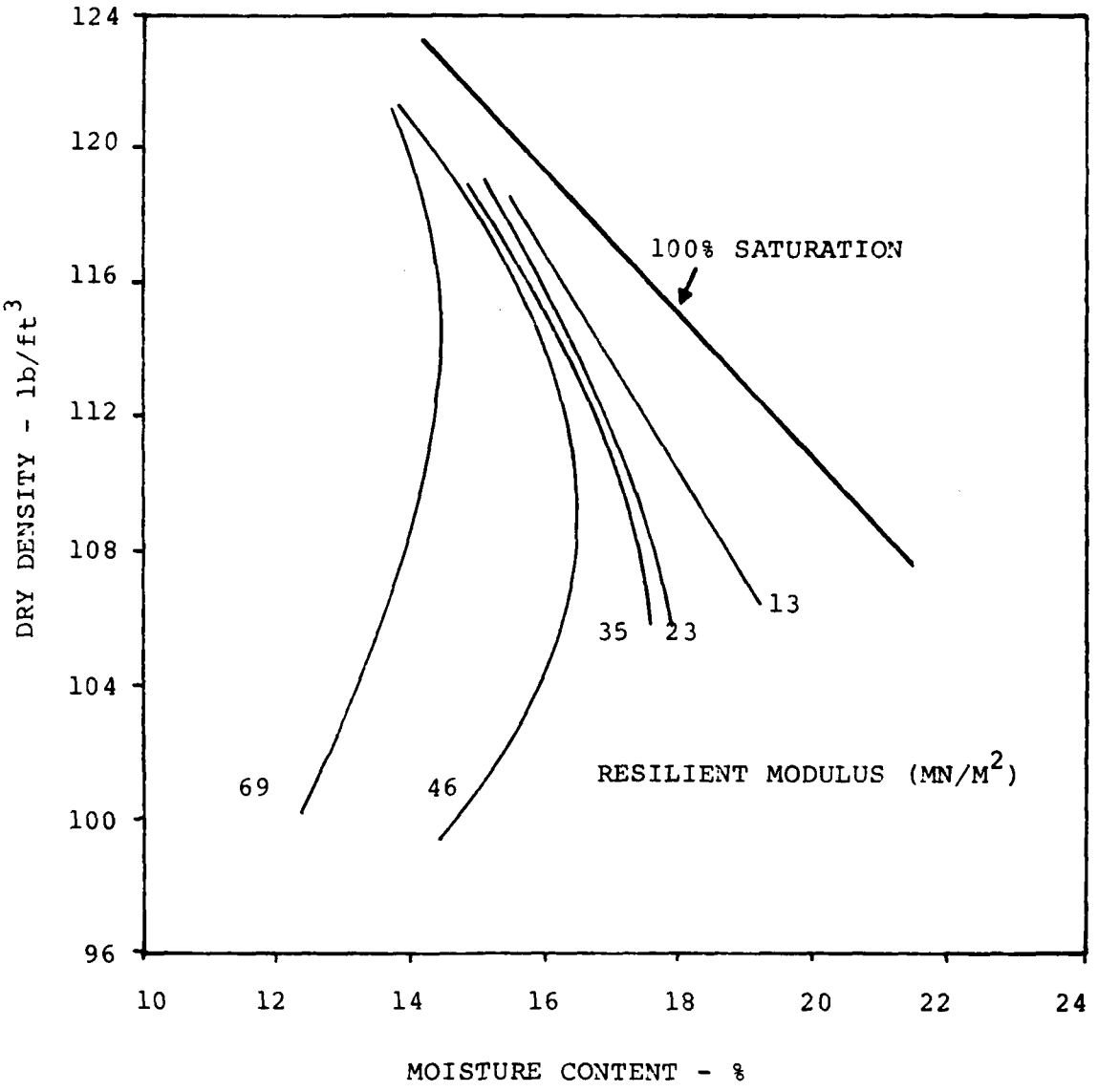

CONTOURS OF EQUAL RESILIENT MODULUS ON γ_d, M/C PLOT {SEED ET AL( )}

Fig. 3.5

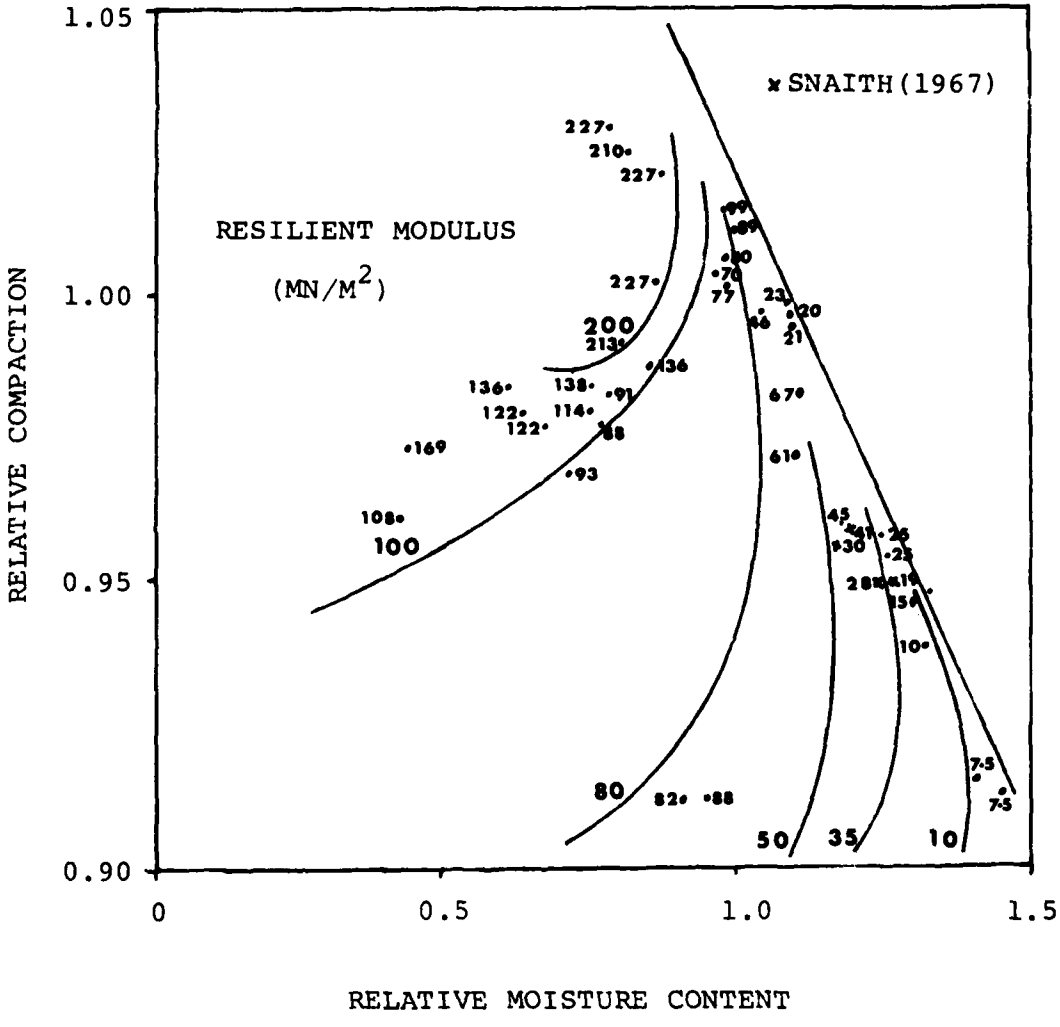

RELATIVE COMPACTION / RELATIVE MOISTURE CONTENT RELATIONSHIP FOR DUBLIN BROWN GLACIAL TILL

Fig. 3.6

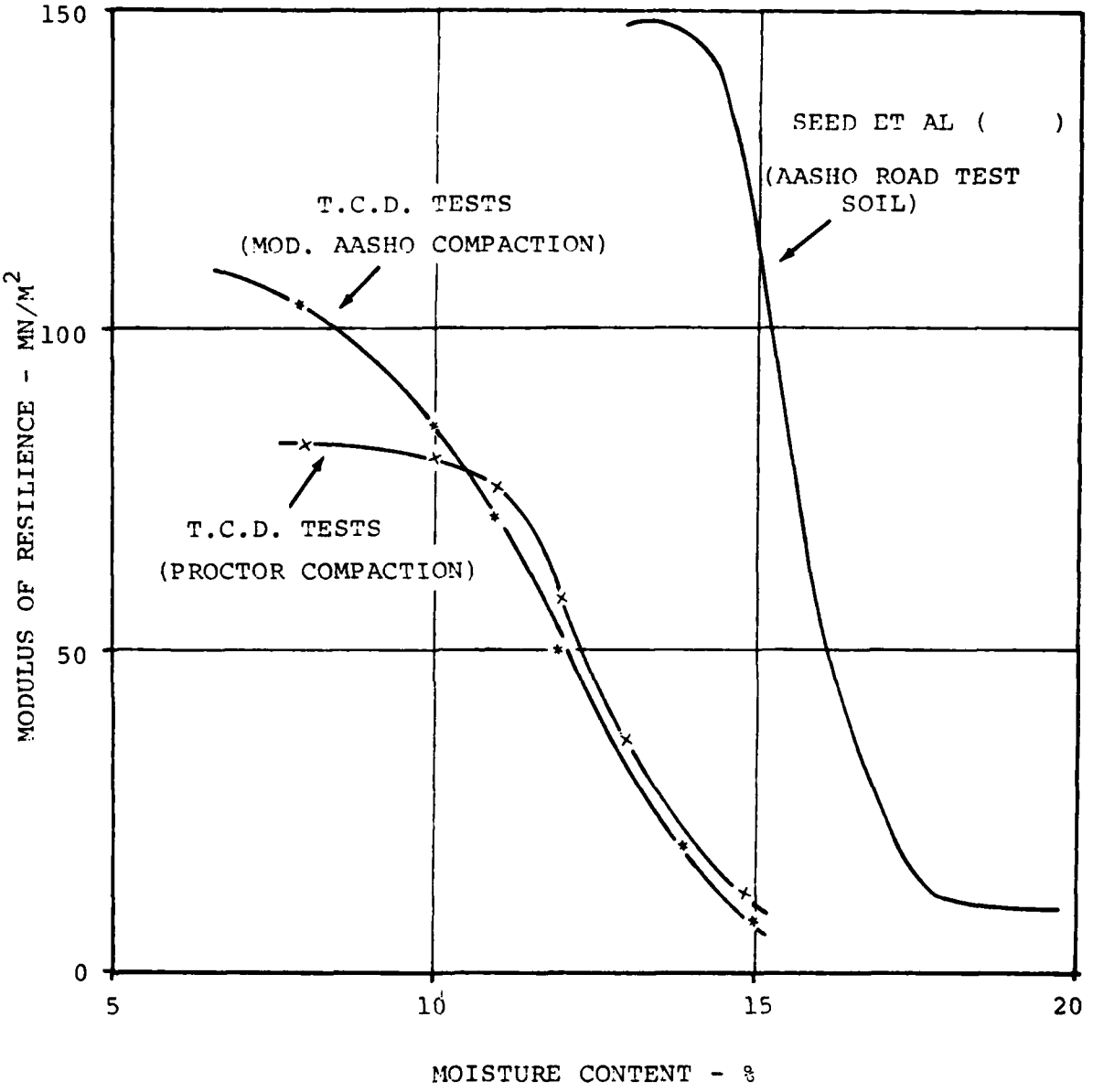

MODULUS OF RESILIENCE AGAINST MOISTURE CONTENT FOR CONSTANT DRY DENSITY

Fig. 3.7

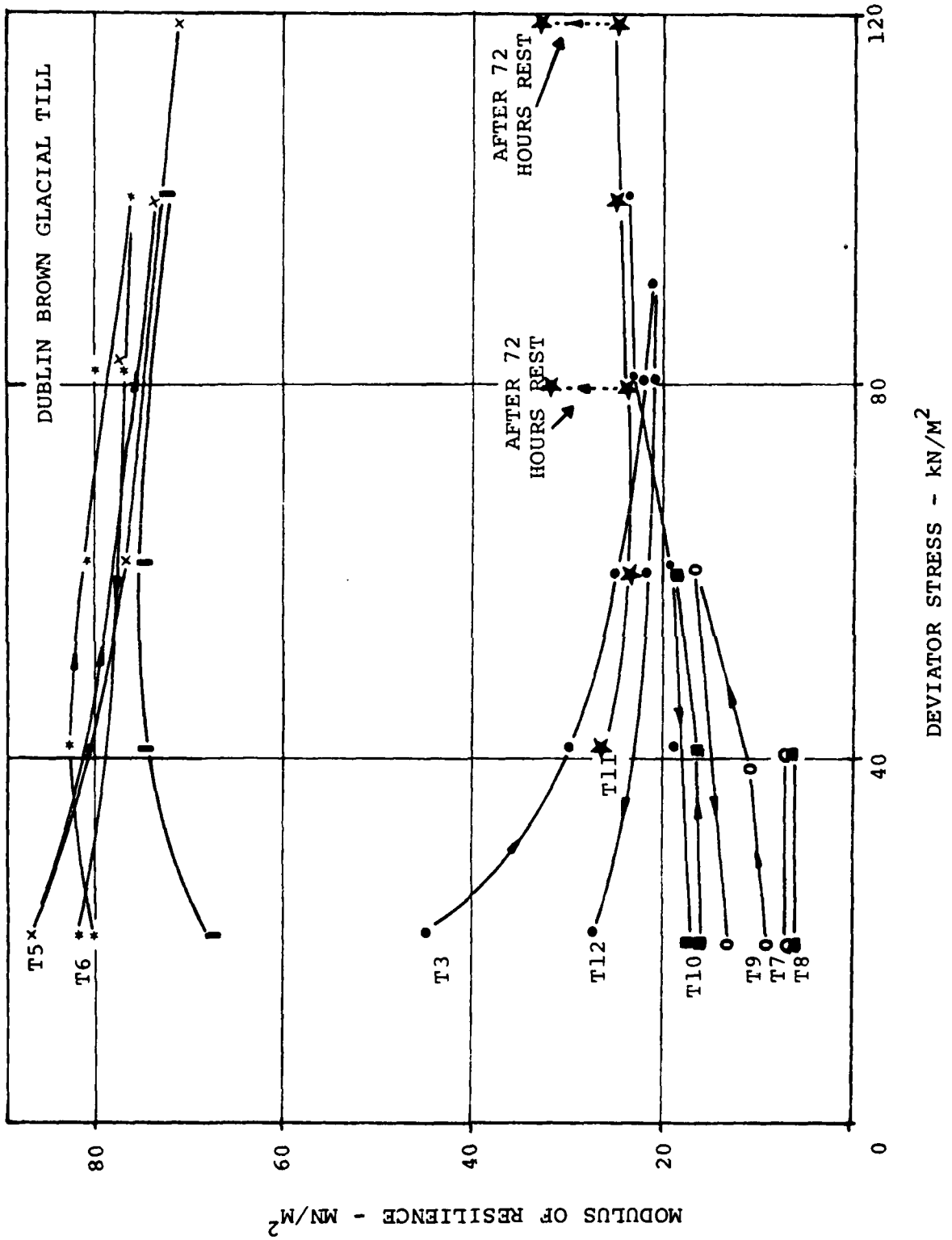
DUBLIN BROWN GLACIAL TILL
AFTER 72 HOURS REST
AFTER 72 HOURS REST
T5
T6
T3
T11
T12
T10
T9
T7
T8
0
20
40
60
80
0
40
80
120
MODULUS OF RESILIENCE - MN/M2
DEVIATOR STRESS - kN/M2

Fig. 3.8

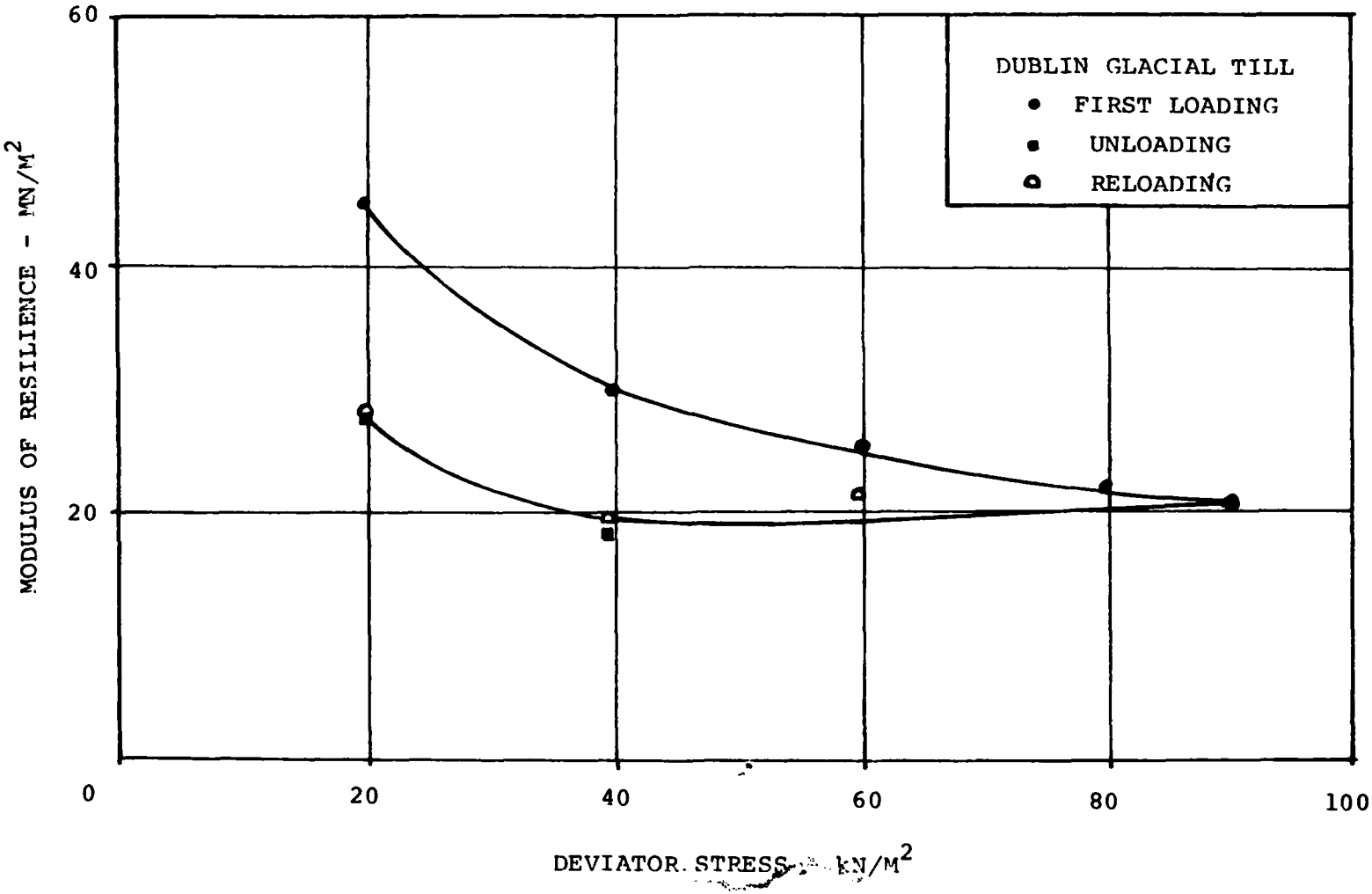

Fig. 3.9 MODULUS OF RESILIENCE AGAINST DEVIATOR STRESS AT 20,000 CYCLES FOR TEST T3

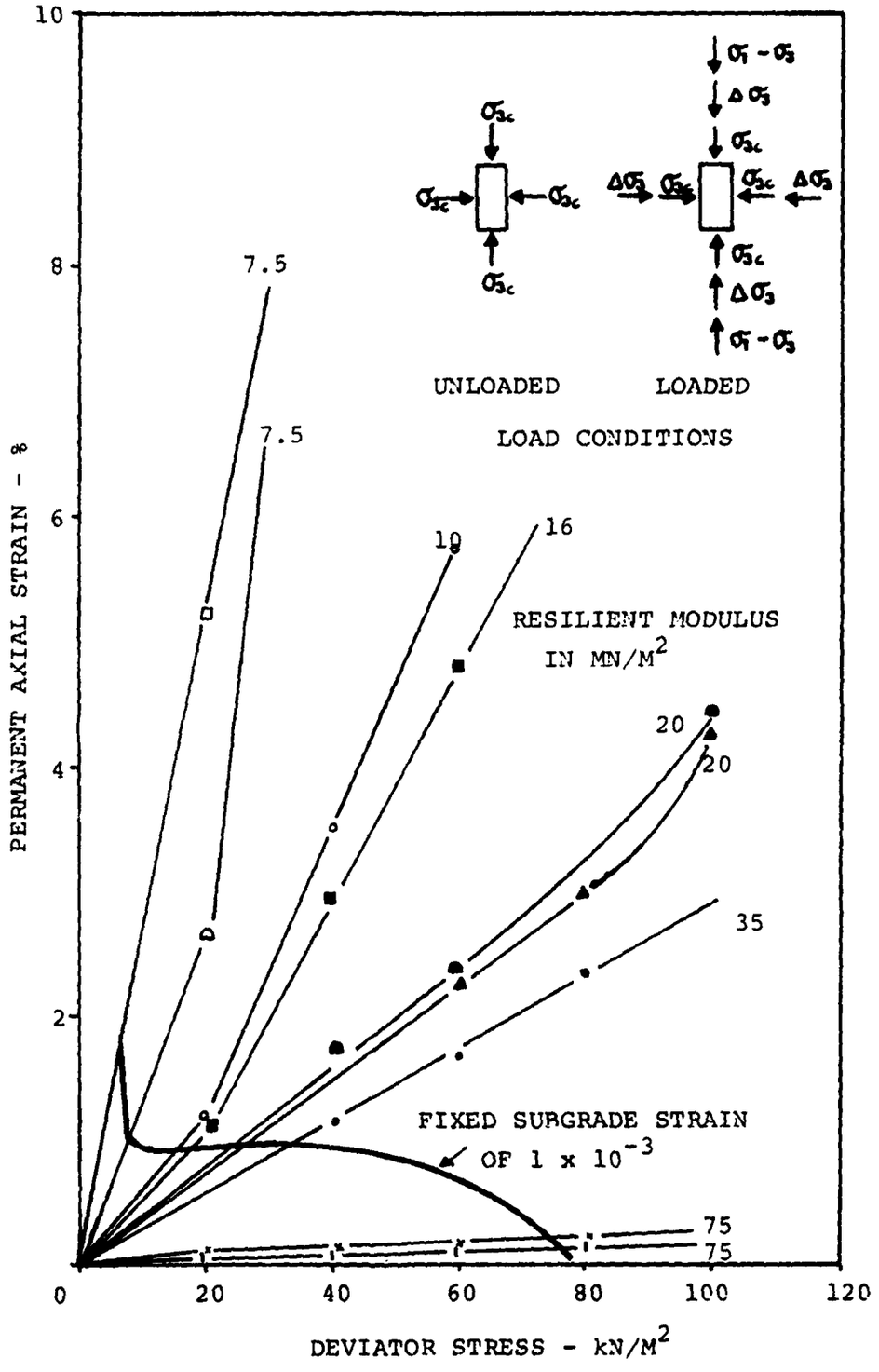

PERMANENT STRAIN AT 40,000 CYCLES Vs DEVIATOR STRESS

Fig. 3.10

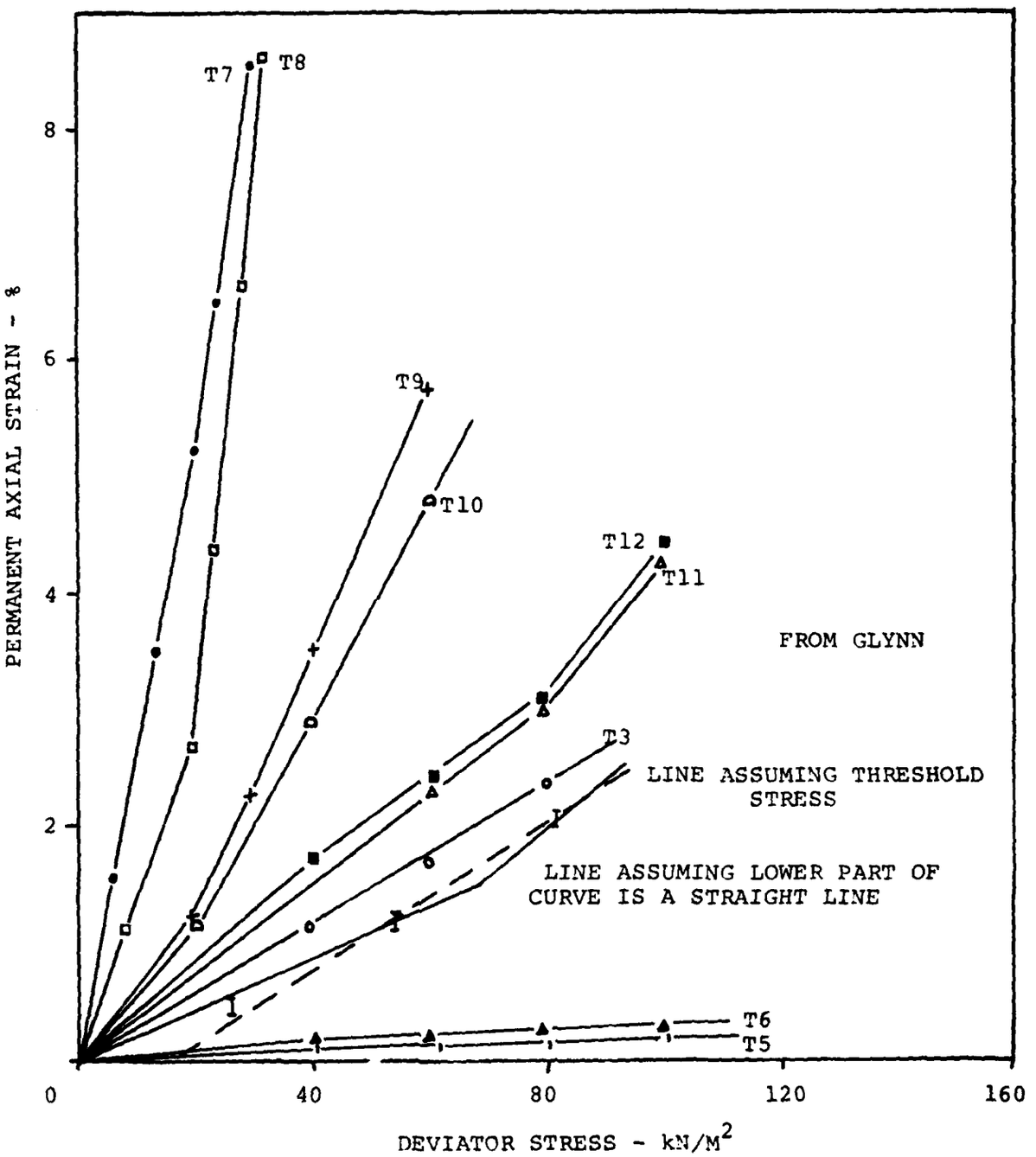

PERMANENT STRAIN Vs DEVIATOR STRESS AT 40,000 CYCLES

Fig. 3.11

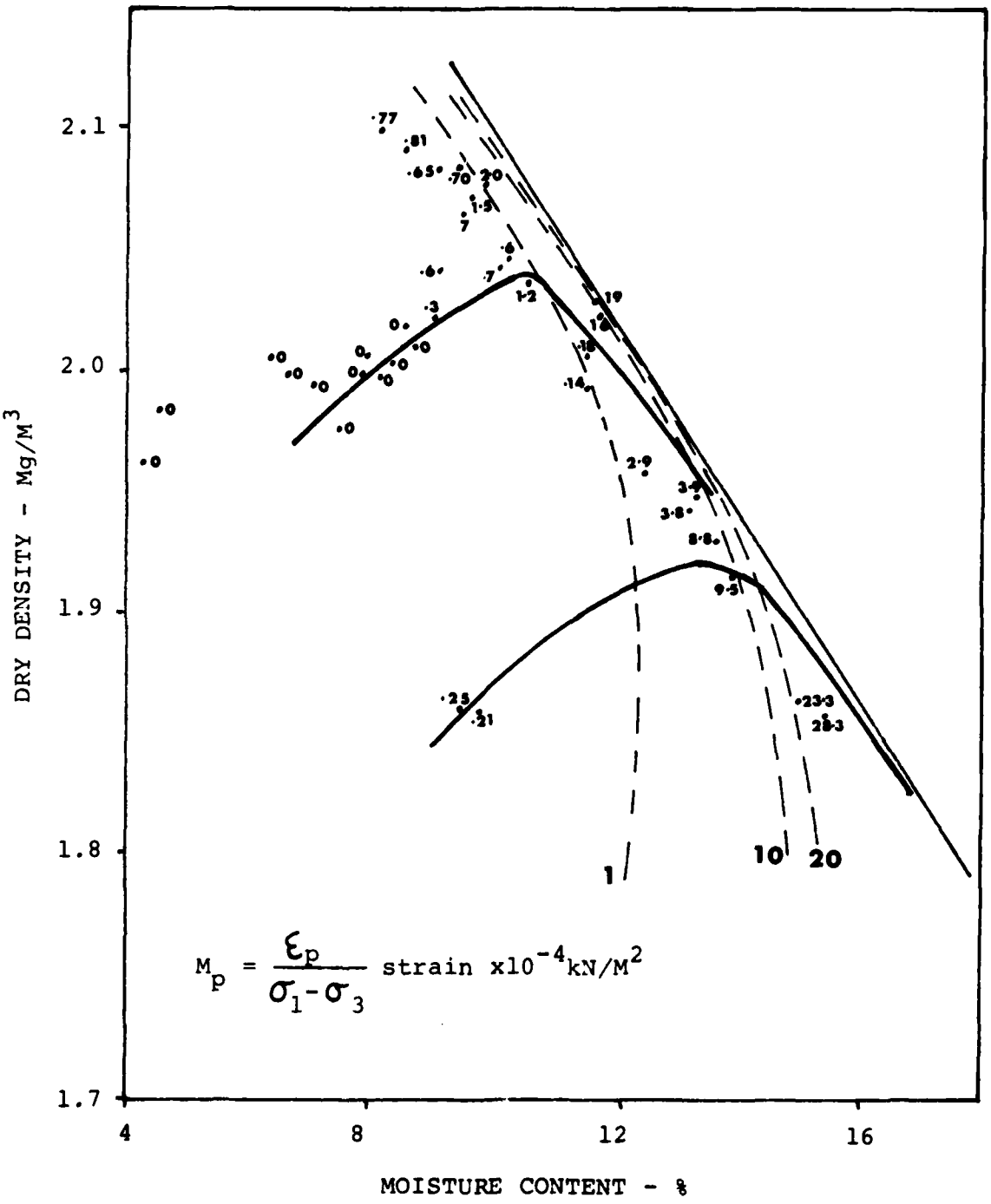

DRY DENSITY - VS - MOISTURE CONTENT SHOWING CREEP COMPLIANCE

Fig. 3.12

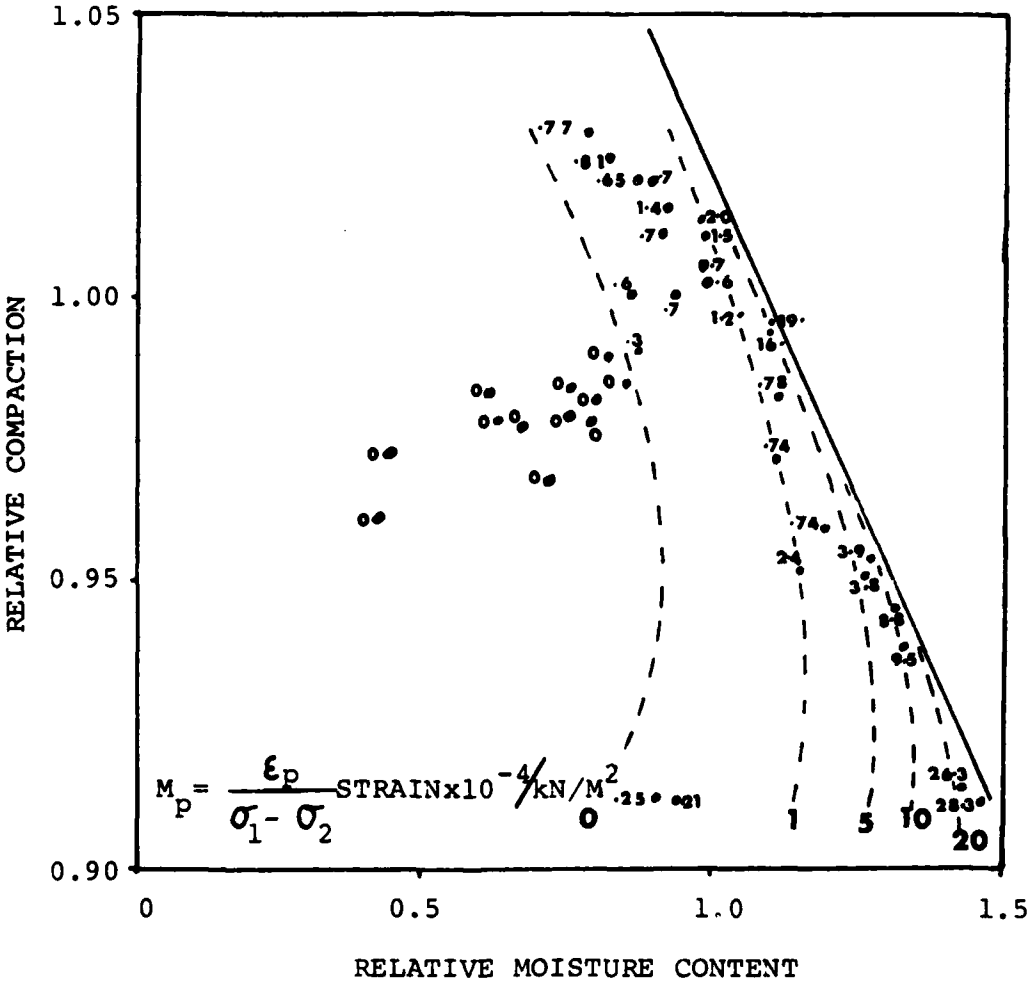

CONTOURS OF EQUAL CREEP COMPLIANCE Vs RELATIVE COMPACTION AND RELATIVE MOISTURE CONTENT

Fig. 3.13

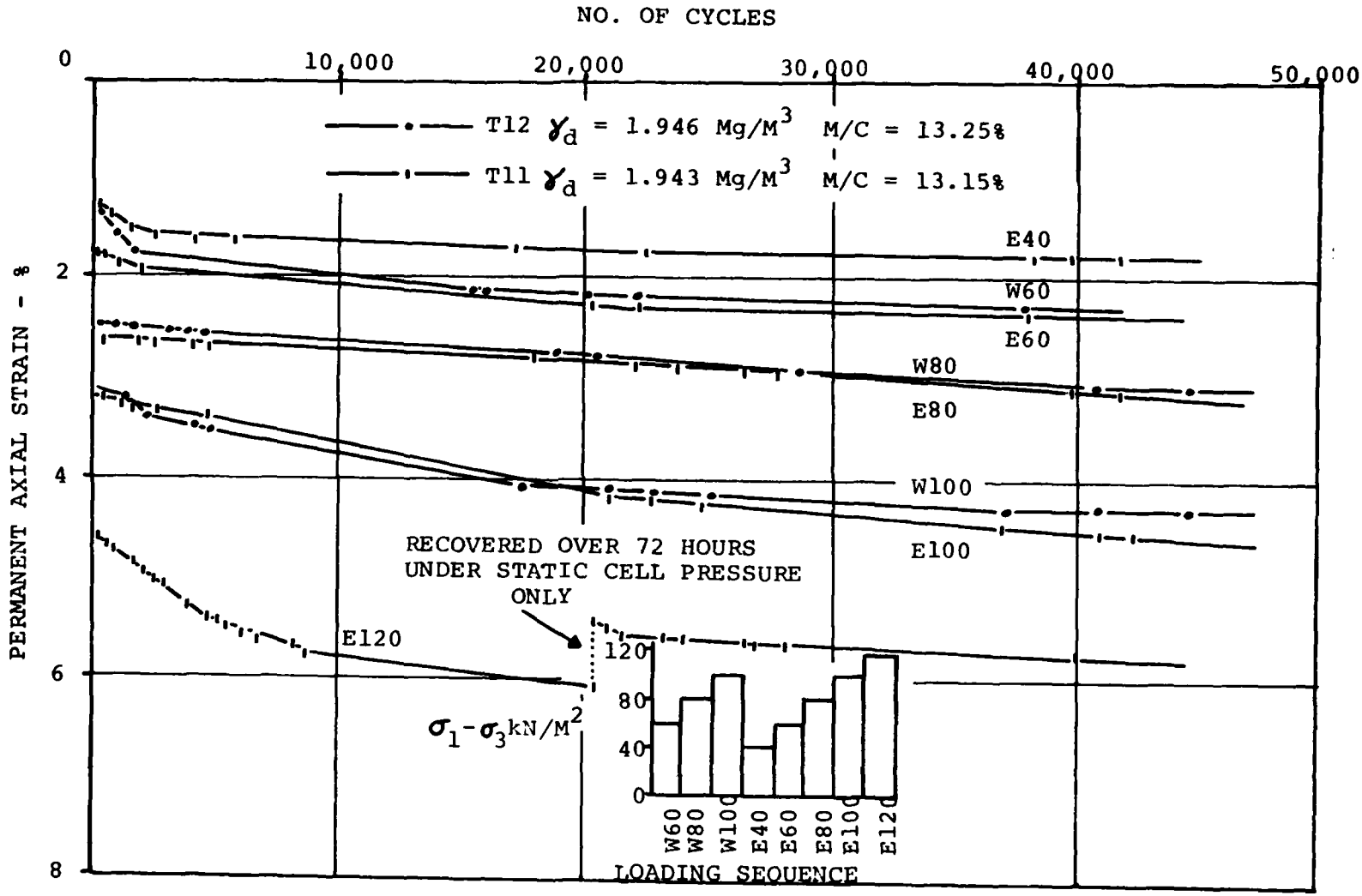

PERMANENT STRAIN Vs NO. OF CYCLES FOR INCREMENTAL LOADING ON TWO SIMILAR SAMPLES

Fig. 3.14

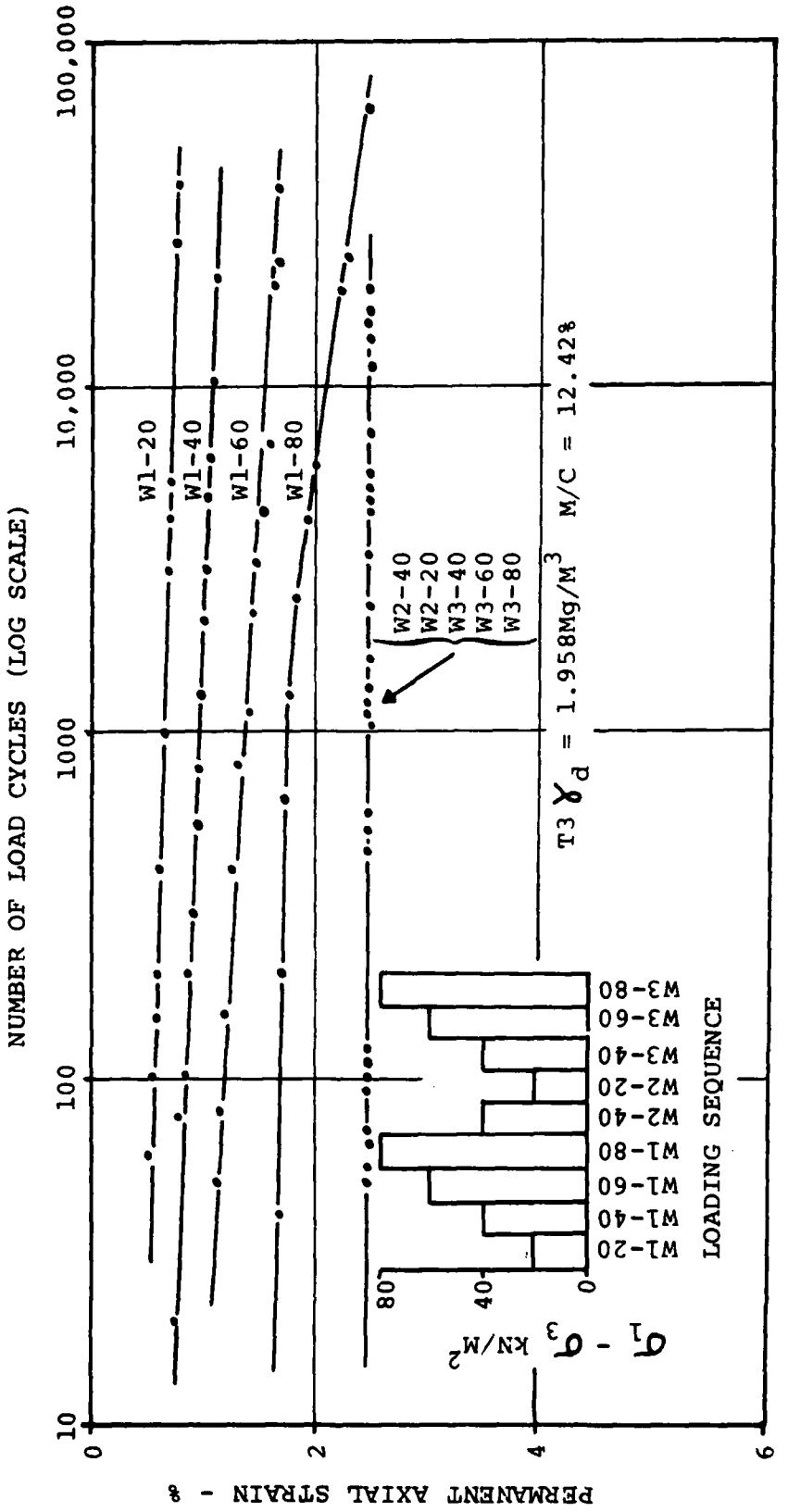

PERMANENT DEFORMATION Vs NO. OF LOAD CYCLES FOR INCREMENTAL & DECREMENTAL LOADING

Fig. 3.15

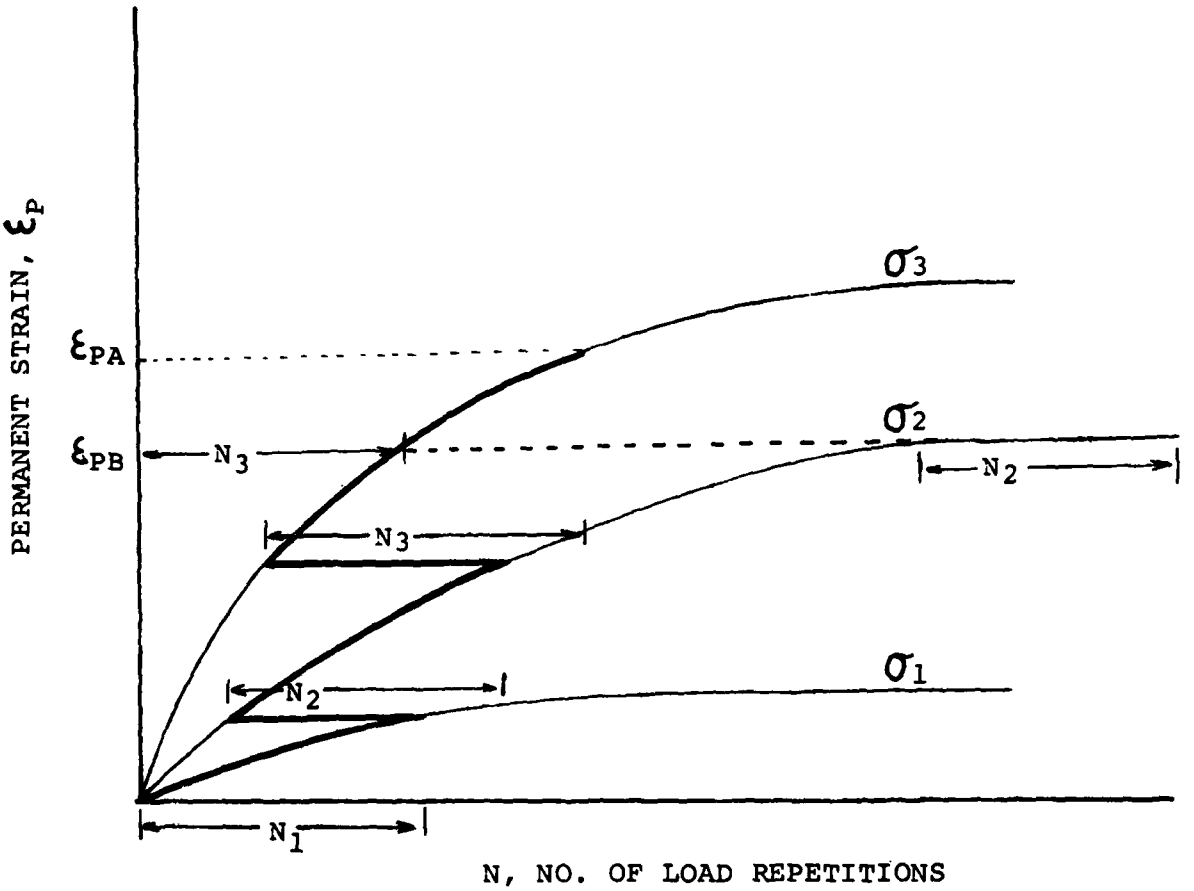

SEQUENCE: A) N_1 of σ_1, N_2 of σ_2, N_3 of σ_3 gives ε_{PA}

B) N_3 of σ_3, N_1 of σ_1, N_2 of σ_2 gives ε_{PB}

NOTE $\varepsilon_{PA} \neq \varepsilon_{PB}$

"TIME - HARDENING" BEHAVIOUR

Fig. 3.16

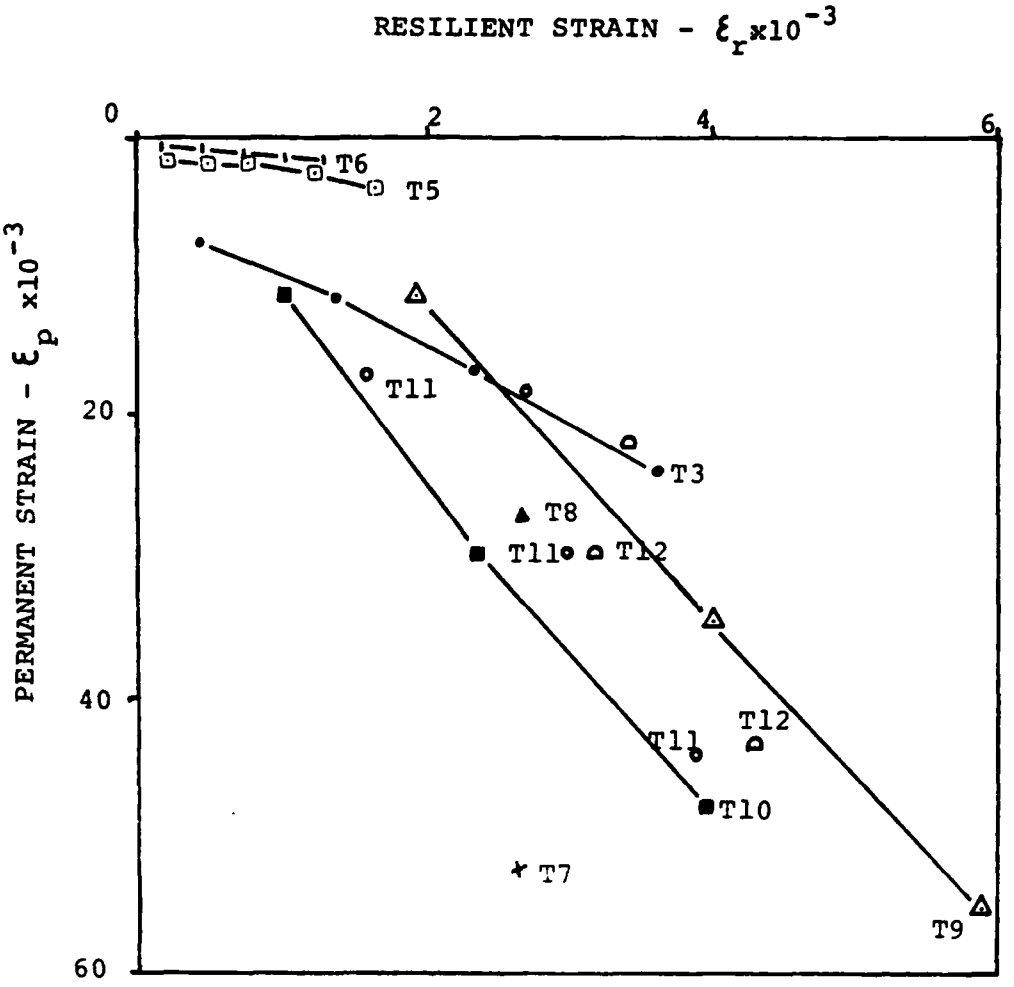

PERMANENT Vs RESILIENT STRAIN AT 40,000 CYCLES

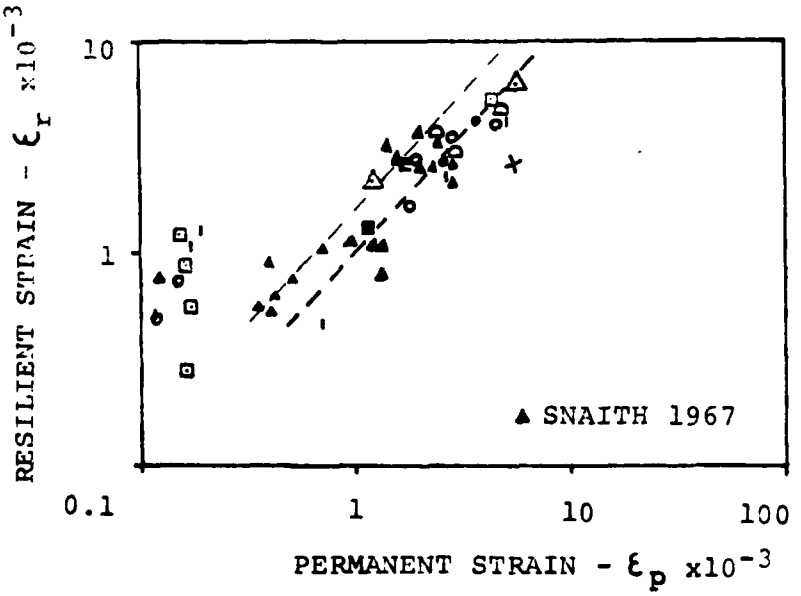

PERMANENT Vs RESILIENT STRAIN AT 40,000 CYCLES (LOG-LOG SCALE)

Fig. 3.17

CHAPTER 4

Study of effect of degree of saturation on Resilient Modulus and Poisson's Ratio.

The lateral deflection of samples under repeated loading in the triaxial apparatus was not measured in the initial series of tests because of the difficulty in developing measuring equipment of sufficient sensitivity. In order to simulate the permanent deformation of the soil insitu, the axial loads and lateral pressure were cycled in phase. The measured vertical deformation was therefore a combination of deformation under axial load and volume compressibility under the cell pressure e.g.

$$\varepsilon_v = \frac{(\Delta\sigma_1 - \Delta\sigma_3)}{M_r} + \frac{\Delta\sigma_3}{3K_r}$$

where ε_v = Vertical Strain
M_r = Resilient Modulus
K_r = Bulk Modulus
ν = Poissons Ratio

or

$$\varepsilon_v = \frac{(\Delta\sigma_1 - 2\nu\Delta\sigma_3)}{M_r}$$

assuming that the material behaved elastically.

Poisson's Ratio can be estimated by closing off the cycled cell pressure for one cycle, measuring the Resilient Modulus, and then substituting back into the equations above. Given that Poisson's ratio varies between 0.1 and 0.5 normally, it is clear that the measured M_r and therefore the M_r computed from tests in which the cell pressure is cycled, can be in error by

$$\text{Measured Modulus} = \frac{\Delta\sigma_1 - \Delta\sigma_3}{\varepsilon_v} = \frac{\Delta\sigma_1 - \Delta\sigma_3}{\frac{\Delta\sigma_1 - 2\nu\Delta\sigma_3}{M_r}}$$

if $\nu = 0.5$ i.e. the material is saturated, the Resilient

Modulus computed from the vertical deflection with the cycled cell pressure would be similar to that computed without the cycled cell pressure. The error between the measured value of M_r and the computed value of M_r is of the order of 25% for $\nu = 0.2$ and a cycled cell pressure of $\frac{1}{2}(\Delta\sigma_1 - \Delta\sigma_3)$

It is of interest to study the expected variation with γ_d and m/c. To do this, use is made of the Skempton's A and B pore pressure parameters (13). The material is assumed to be elastic (a staged approached where the permanent deformation if negligible), linear, isotropic and that the degree of saturation is sufficiently high such that surface tension can be ignored.

With reference to Bishop and Henkel (14), the change in pore pressure due to applied total stresses $\Delta\sigma_1$ and $\Delta\sigma_3$ is

$$\Delta u = B\{\Delta\sigma_3 + A(\Delta\sigma_1 - \Delta\sigma_3)\}$$

for isotropic elastic behaviour A = 1/3

$$\therefore \quad \Delta u = B\{\Delta\sigma_3 + \frac{1}{3}(\Delta\sigma_1 - \Delta\sigma_3)\}$$

The vertical strain is therefore:

$$\varepsilon_v = \frac{\Delta\sigma_1 - \Delta\sigma_3}{E'} + \frac{(1-2\nu')}{E'}\{\Delta\sigma_3 - B(\Delta\sigma_3 + \frac{(\Delta\sigma_1 - \Delta\sigma_3)}{3}\}$$

where E' = Elastic modulus of soil skeleton in effective stresses

ν' = Poisson's ratio of soil skeleton in effective stresses.

Taking $\Delta\sigma_3 = Y(\Delta\sigma_1 - \Delta\sigma_3)$

$$\varepsilon_v = \frac{(\Delta\sigma_1 - \Delta\sigma_3)}{E'}\{1 + (1-2\nu')\ (Y - B(Y + \frac{1}{3})\ )\}$$

The resilient modulus measured in a triaxial sample with no cycled cell pressure is therefore:

$$M_r = \frac{\Delta\sigma_1}{\frac{\Delta\sigma_1}{E'}\{1-\frac{B}{3}(1-2\nu')\}} = \frac{E'}{\{1-\frac{B}{3}(1-2\nu')\}} \quad \ldots\ldots (1)$$

with the cell pressure cycles at ½ $(\Delta\sigma_1 - \Delta\sigma_3)$ as it was for the initial tests. The deviator stress divided by vertical strain is

$$\frac{\Delta\sigma_1 - \Delta\sigma_3}{\varepsilon_v} = \frac{E'}{\{1 + (1-2\nu')(0.5-0.833B)\}}$$

The variation of the ratio, $\frac{\Delta\sigma_1 - \Delta\sigma_3}{\left(\frac{\varepsilon_v}{M_r}\right)}$ is shown in Fig. 4.1. assuming that $\nu' = 0.2$ as got from Calladine (15) for a soil with Plasticity Index of 14.

This again shows that the error in the estimation of Resilient Modulus is negligible at 100% saturation but can be expected to increase at lesser saturation levels. A knowledge of the variation of the B pore pressure parameter with γ_d and m/c would therefore give an indication of the degree of error.

Extending this analysis to study the measured resilient Poisson's Ratio under repeated loading, the lateral strain is

$$\varepsilon_r = \frac{\Delta\sigma_3}{E'} - \frac{\nu'}{E'}(\Delta\sigma_1' + \Delta\sigma_3')$$

$$= \frac{1}{E'}\{\Delta\sigma_3 - \Delta u - \nu'(\Delta\sigma_1 + \Delta\sigma_3 - 2\Delta u)\}$$

neglecting the cycles cell pressure

$$\varepsilon_r = \frac{1}{E'}\{-\Delta u - \nu'(\Delta\sigma_1 - 2\Delta u)\}$$

but $\Delta u = \frac{B}{3} \Delta\sigma_1$

$$\therefore \quad \varepsilon_r = -\frac{\Delta\sigma_1}{E'} \left\{\frac{B}{3} + \nu'\left(1-\frac{2B}{3}\right)\right\}$$

$$\nu_r = \frac{\frac{\Delta\sigma_1}{E'} \left\{\frac{B}{3} + \nu'\left(1-\frac{2B}{3}\right)\right\}}{\frac{\Delta\sigma_1}{E'} \left\{1-\frac{B}{3}\left(1-2\nu'\right)\right\}} = \frac{\frac{B}{3} + \nu'\left(1-\frac{2B}{3}\right)}{1 - \frac{B}{3}\left(1-2\nu'\right)} \quad \ldots\ldots(2)$$

It can be shown that equation (2) is also true if the cell pressure is cycled.

With B = 1 i.e. saturated $\nu_r = 0.5$

as expected, regardless of the Poisson's Ratio of the soil structure.

With B = 0.5 $\nu_r = \dfrac{0.166 + 0.67}{0.834 + 0.332}$

Thus, although the Poisson's Ratio of the structure could be 0.2, the resilient Poisson's Ratio of the partially saturated material could be much higher.

With B = 0 $\nu_r = \nu'$ obviously

With $\nu' = 0.25$, a low value B = 0.5 $\nu_r = 0.364$

The variation in the resilient Poisson's ratio against the B pore pressure parameter is illustrated in Fig. 4.2. Thus the measured Poisson's Ratio in a repeated load triaxial apparatus would be expected to be higher than that of the soil skeleton owing to the build-up of positive pore pressure during loading.

Equation (1) is independent of the cycled cell pressure, thus the Poisson's Ratio measured with a constant confining pressure should be similar to that measured with a cycled confining pressure. Allen and Thompson (15a) recorded noticable

different values for Poisson's Ratio for these two types of tests which suggests that either the soil structure changed, or that there were inaccuracies in the measuring equipment, or possibly anisotropic behaviour of the samples.

Preliminary triaxial tests have confirmed that the resilient vertical deflection is unaffected by cell pressure for saturated sampled but that, for unsaturated samples, the cell pressure had a slightly greater effect than predicted by pore pressure parameter analysis. Previous investigations have found that the effective stress elastic modulus of some soils is dependent on the confining pressure. Work is being carried out to see if this is significant, particularly as high soil suction or negative pore water pressures are involved in partially saturated soils. Considering the modulus of resilience in terms of a constant effective stress modulus (Equation 1) implies that a reduction of the B pore pressure parameter, i.e. drying out of the soil, reduces the resilient modulus. This is not true in practice. Thus, while this form of analysis can usefully study the behaviour of a single sample under varying stress conditions, as yet it cannot be extended to predict the effect of changing moisture content or dry density. Information on soil suction variation may bridge this gap. This is being investigated.

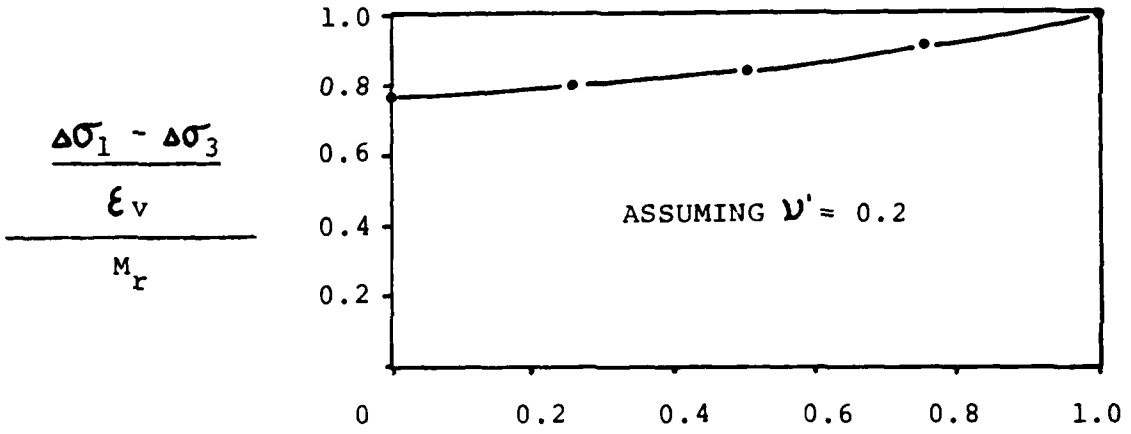

COMPARISON OF VERTICAL RESILIENT MODULUS $\left(\frac{\Delta\sigma_1-\Delta\sigma_3}{\varepsilon_v}\right)$ AGAINST AGAINST RESILIENT MODULUS OF SOIL

Fig. 4.1

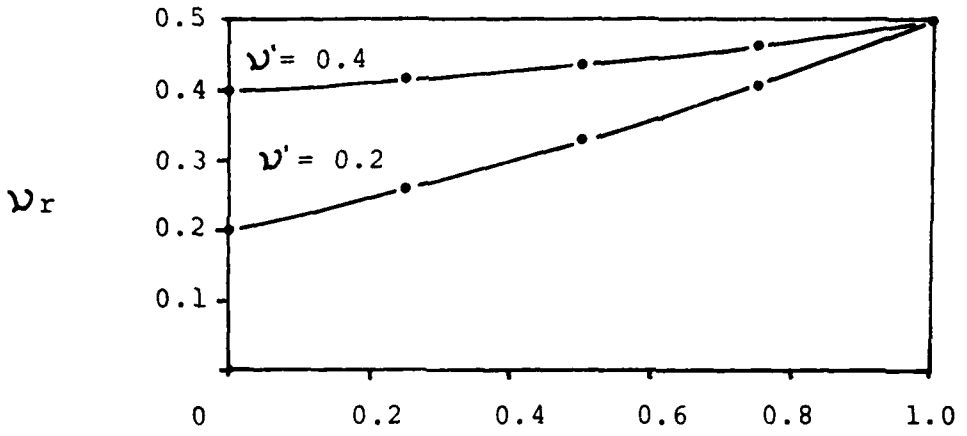

RESILIENT POISSON'S RATIO IN TOTAL STRESS (ν_r) AGAINST POISSON'S RATIO OF SOIL SKELETON IN EFFECTIVE STRESS (ν')

Fig. 4.2

CHAPTER 5

METHOD OF DETERMINING RESILIENT MODULI FROM DEFLECTION MEASUREMENTS

5.1 Introduction

For pavement design procedures based on a computer analysis of stresses, strains and deflections in a multi-layered system, an estimate of the elastic moduli of each constituent material is required as input to program. The most difficult material to characterise in this way is the subgrade, since its modulus depends on moisture content, dry density, stress level, structure and stress history.

Subgrade material can be tested in repeated load triaxial testing machines so as to determine the relative effects of the above mentioned variables on the dynamic response of the soil. While this test is necessary to determine the susceptibility of a soil to creep deformation and to provide an estimate of the variation in modulus with traffic loading and changes in environmental conditions, it has its limitations in yielding a suitable design modulus for a subgrade, since it is impossible to model the true in-situ stresses and in-situ soil structure in a triaxial type machine.

In recent years, the results from many full-scale instrumented test tracks have been used to provide verification of the predictive capabilities of the various theoretical analysis procedures. In general, it has been found that the greatest difficulty has arisen in selecting suitable characteristics for the subgrade material.

A simple method has been devised to interpret the results of an in-situ deflection test on the subgrade to obtain an estimate of its stress dependent modulus. It is based on the

principle that the shape of the deflection bowl is a function of the rate of variation of modulus with stress right through the soil mass.

Other investigators (Leger (16), Grant and Walker (17), among others) have used a radius of curvature as a measure of deflection bowl profile, to obtain information on base and subgrade moduli in roads with thin surfacings. Also, deflection ratios have been used to obtain estimates of moduli in a multi-layered elastic system. Valkering (18), by assuming a subgrade with a constant modulus, overlain by a granular base course having a constant modulus which is a fixed ratio of that of the subgrade (Dormon and Metcalf (19)) has produced a chart relating the modulus of the surface layer to the deflection ratio. This principle has been extended for use in the Shell (Claessen and Ditmarsch (20)) overlay design method.

Ullidtz (21) has also used deflection ratios in his overlay design method and allowed the non-linear effect of the sub-grade to be taken into account in their interpretation. Others have used measured deflections at off-centre points to produce a spreadability index which can be related to material moduli values.

Here the use of deflection ratios is extended to allow the stress dependent modulus of a subgrade to be determined with the aid of a non-linear elastic computer analysis. From this, nomographs have been produced which allow the stress dependent modulus to be estimated without using the program. Also, the method of obtaining the in-situ modulus values of the consituent layers in a multi-layered system is explained.

5.2 Basis of Nomograph

The principle behind the nomograph can best be understood by considering the finite element modelling of a single layer isotropic material with boundary conditions and loading area constant.

$$\{P\} = [K]\ \{U\}$$

where $\{P\}$ = load vector
$[K]$ = stiffness matrix
$\{U\}$ = deflection vector

The stress dependent modulus of resilience can be modelled by a function of the stress in an element e.g. $M_r = Cf^n(\sigma_d)$.....(2)
where C = constant σ_d = deviator stress

The individual terms in the stiffness matrix are multiplied by the modulus of resilience appropriate to the stress condition in the element. For a single layer the constant in equation (2) above can be taken out of the stiffness matrix such that

$$[K] = C\ [K']$$

where $[K']$ is the adjusted stiffness matrix.
Equation (1) therefore becomes

$$\{P\} = C\ [K']\ \{U\}$$
$$\{U\} = \frac{1}{C}\ [K']\ \{P\} \qquad (3)$$

Since each term on the right-hand side of equation (3) is multiplied by 1/C, the relative magnitude of the terms in $\{U\}$ remains independent of C. The stress dependent modulus of resilience of soils is generally represented by an exponential function e.g.

$M_r = C\sigma_d^{-\gamma}$ where C and γ are soil constants.....(4)

σ_d is the deviator stress

The deviator stress is proportional to applied load for a linear elastic system. Maher (22) has shown, using the finite element program DEFPAV, that for a constant value of γ a similar relationship exists. Thus

$$\frac{\sigma_{d_1}}{\sigma_0} \propto \frac{P_1}{P_0}$$

For an increase in applied load from P_o to P_1, each modulus of resilience in the stiffness matrix is increased by $(P_1/P_o)^{-\gamma}$ from equation (4) above. This has no effect on the ratio of

deflections but decreases each term by $1/(P_1/P_o)$.

Therefore (a) the relative magnitude of terms in the deflection vector $\{U\}$ is determined solely by the value of γ

(b) the magnitude of the deflection is proportional to $\frac{P}{C(P)^{-\gamma}}$

The nomograph is drawn up for C = 100 and P = 100.
Given two soils with modulus relationships.

$$M_{r1} = C_1\sigma_d^{-\gamma} \quad \text{and} \quad M_{r2} = C_2\sigma_d^{-\gamma}$$

under loads $\{P_1\}$ and $\{P_2\}$ respectively, the ratio of the central deflections are from equation (5):

$$\frac{u_1}{u_2} = \frac{\frac{P_1}{C_1 P_1^{-\gamma}}}{\frac{P_2}{C_2 P_2^{-\gamma}}} = \frac{C_2}{C_1}\frac{(\frac{P_1}{P_2})}{(\frac{P_1}{P_2})^{-\gamma}} \quad \therefore \quad C_1 = C_2 \frac{u_2}{u_1}\frac{(\frac{P_1}{P_2})}{(\frac{P_1}{P_2})^{-\gamma}}$$

The nomograph shown in Fig. 5.1 shows the relationship between γ and the deflection for a range of radial distances, computed from DEFPAV.

Also plotted on the nomograph is the central deflection (U_2) computed by DEFPAV, for C_2 = 100 and P_2 = 100, for various values of γ. The value of C_1 for the soil measured can therefore be calculated from

$$C_1 = 100 \times \frac{u_2}{u_m} \times \frac{\frac{P_a}{100}}{(\frac{P_a}{100})^{-\gamma}}$$

where u_m is the measured central deflection and P_a is the applied pressure.

5.3 Boundary Effects and Influence of Poisson's Ratio

Since the interpretation method is based on measured deflections, it is essential that the computer model, from which the nomograph is prepared, is an exact representation of the

measured system.

Particularly in the case of the simulator tank results, boundary discontinuities must be placed in the approximate positions in the computer model. Fig.5.2 shows the effect of promixity of the vertical boundary (nodes free to move vertically but fixed horizontially) on the values of D_r. Beyond 1.5 metres the effect is negligible.

Since the elastic behaviour of a subgrade is dependent on the value of Poisson's Ratio as well as on that of the Resilient Modulus, it is important to determine the effect of this parameter on the values of the deflection ratios.

Fig.5.3 shows the variation in deflection ratios for Poisson's Ratio varying from 0.22 to 0.47. It can be seen not to have a marked effect, thus making the use of a constant value an acceptable simplification.

To illustrate the use of the interpretation methos, suppose a clay subgrade is loaded with a stress of 50kN/m^2 over a circular area of radius 100mm and a deflection of 0.27mm is measured at the centre and 0.08mm at 120mm from the centre. Then

$$D_{120} = \frac{0.08}{0.27} = 0.296$$

Then, from Fig.5.1, for $D_{120} = 0.296$, $\gamma = 0.85$ and $\delta_{o\,std} = 2.7$mm, Maher (22) suggests,

$$c_p = \frac{\delta_{o\,std} \times p}{\delta_{op} \times \frac{(p)}{100}^{-\gamma}}$$

$$= \frac{2.7 \times 50}{0.27 \times \frac{(50)}{100}^{-0.85}}$$

$$= 227.8$$

$$\therefore \quad M_r = 277.8\ \sigma_d^{-0.85} \quad MN/m^2$$

5.4 APPLICATION OF THE METHOD IN THE INTERPRETATION OF SOME PREVIOUSLY PUBLISHED RESEARCH

Tests were performed at the University of Nottingham to measure the stresses and strains occurring in a typical cohesive subgrade when subjected to dynamic loading. The tests were performed in a test pit, 1.52m deep by 2.44m square with the load being applied to the surface over a circular area of radius 152mm using a pneumatic loading system.

A series of tests were carried out (Sparrow & Tory(24)) at varying contact pressures (50-100kN/m^2) and loading times. Surface deflections were plotted in terms of normalised values so that, for the purposes of this investigation, they have been converted to actual deflections corresponding to an applied stress of 69kN/m^2 (Fig.5.4).

Assuming a semi-infinite elastic isotropic soil with a Poisson's Ratio of 0.3 then a modulus of 12.4 MN/m^2 is required to produce a similar centreline deflection to the measured value. However, at off-centre points it can be seen that the deflection bowl departs substantially from that measured.

By producing nomographs in the same form as that in Fig.5.1 but with radius of 152mm and boundaries similar to those in the tests, then a stress dependent modulus can be determined which results in deflections which more closely follow the measured values. Exact coincidence is not obtained due to the fact that, as reported by Sparrow and Tory, the resilient modulus, calculated from in-situ measurements, increased markedly with depth and also the exact influence of the boundaries is unknown.

Approximate linear and exponential M_r/σ_d relationships for the test material are shown in Fig. 5.5.

A further more thorough series of tests were performed by Brown and Pell (25) in the same test pit. The effect of applied stress, loading area and loading frequency on the measured

response of the soil was investigated. It was found that, to satisfactorily predict the subgrade strains and maximum surface deflections, using linear elastic theory, a variety of modulus values was required. It was found that strains and deflections were also very dependant on local values of the Resilient Modulus.

Fig 5.6 shows the measured deflection points for four of the tests. A summary of the test conditions is given in Table 5.1.

Test No.	Normal Contact Pressure (kN/M^2)	Time for load pulse (sec.)	Estimated γ	C_p
S/A	117	2.0	0.38	67.64
S/B	117	0.1	0.44	93.15
S/C	52	0.1	0.435	78.10
S/D	52	2.0	0.33	56.35

Table 5.1 Summary of Nottingham Tests

It can be seen from Fig. 5.6 that fitting the Boussinesq equation to the centre-line deflection causes a large divergence from the measured values with distance from the loading area.(25)

Assuming an exponential M_r/σ_d relationship and obtaining average values for γ and C_p (Table 5.1) which most closely fit the deflection ratio at each of the measured points, M_r/σ_d curves as shown in Fig. 5.7 are obtained. It is seen that these fall very closely together and give a more accurate representation of the measured deflection values (Fig. 5.6) at off-load points. It is also seen that, when a constant value of modulus is chosen, the value required to yield the correct centreline deflection in each case is very dependent on the magnitude of the test conditions.

5.5 INTERPRETATION METHOD FOR MULTI-LAYERED SYSTEMS

Two-Layer Systems

For a two-layer linear elastic system with fixed dimensions and subjected to a constant stress over a fixed circular area, the resilient moduli of the material can be determined from the shape and magnitude of the deflection bowl. The shape of the deflected profile is a function of the ratio of the two moduli and the maximum centre-line deflection depends on the absolute value of these moduli. Thus an interpretation nomograph can be prepared giving the relationship between the deflection ratio, the ratio of the moduli and the magnitude of the centre-line deflection, for predetermined values of layer thickness and the load radius. The applied stress can be accounted for by plotting the deflection in terms of deflection per unit stress or more conveniently as deflection per 100 kN/M^2 of applied stress.

In the case of a two-layer system in which the lower layer is a clay subgrade with a marked non-linear modulus, the deflection bowl shape as measured at the surface will be substantially modified, particularly where the surface layer is thin and of a comparable modulus to that of the subgrade. To allow for this, the value of one of the parameters in the modulus/stress relationship of the subgrade must be assumed. The nomograph can then be prepared in terms of this known parameter and the unknown one estimated from the nomograph using the measured deflections.

Examples of both these nomographs and their use are given in Chapter 8.

The value of the vertical stress at either of the layer interfaces, if known, also provides information on the modular ratios and, in conjunction with the deflection ratio, deflection magnitudes and layer thicknesses would permit determination of the layer moduli.

5.6 SUMMARY

A simple method is derived and explained for back-analysing measured deflection profiles from dynamic tests on a subgrade. This provides the magnitude and non-linearity of the resilient modulus as a function of deviator stress.

The technique is demonstrated for an assumed exponential modulus stress relationship. However, the method is not restricted to this. Nomographs can be constructed in terms of any desired function and for any given loading conditions.

Examples are given which demonstrate the use of the analysis procedure in providing consistent modulus values for a series of test results.

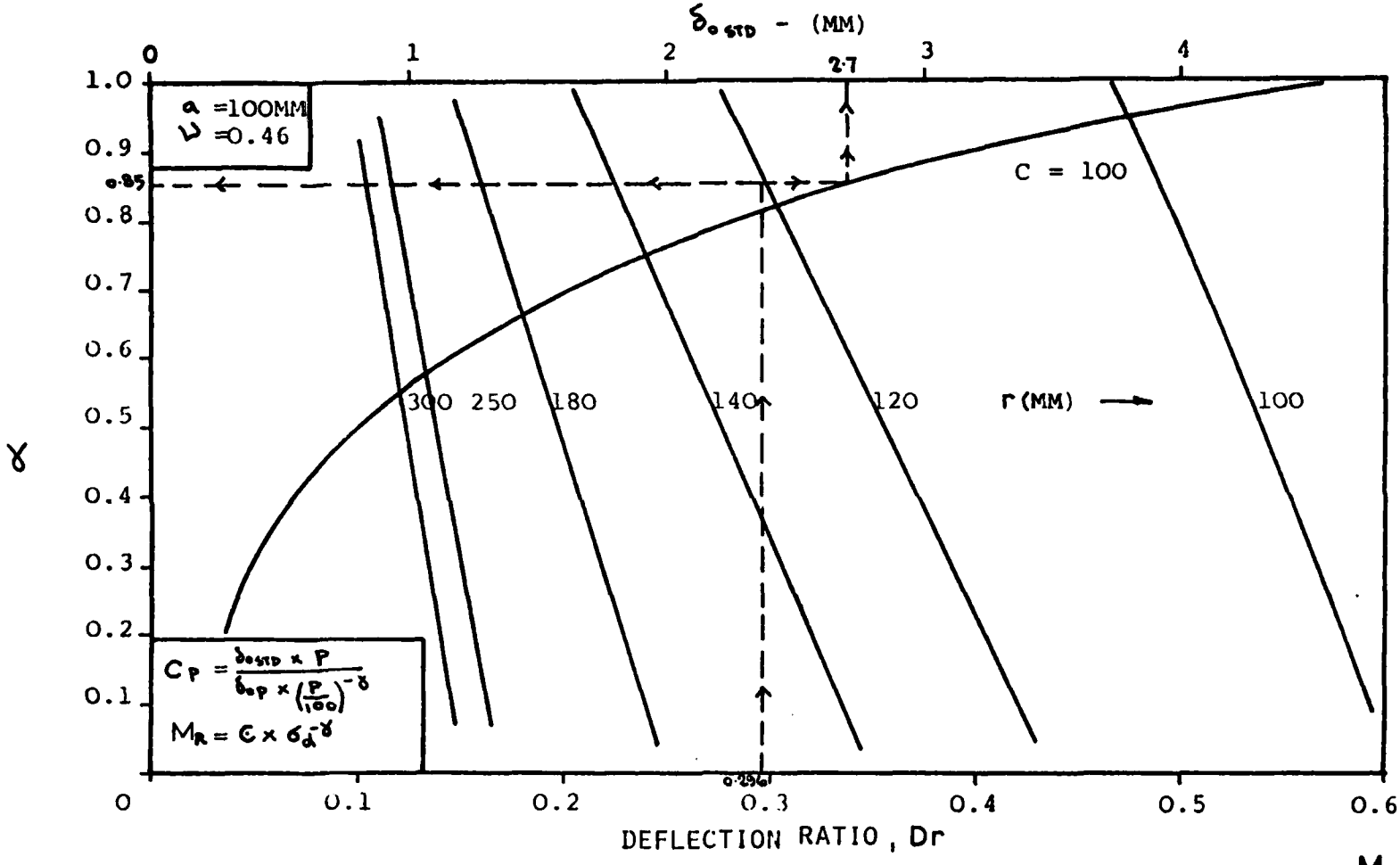

Fig. 5.1 VARIATION OF Dr AND $\delta_{o\,STD.}$ WITH C AND γ FOR EXPONENTIAL M_R/σ_d RELATIONSHIP

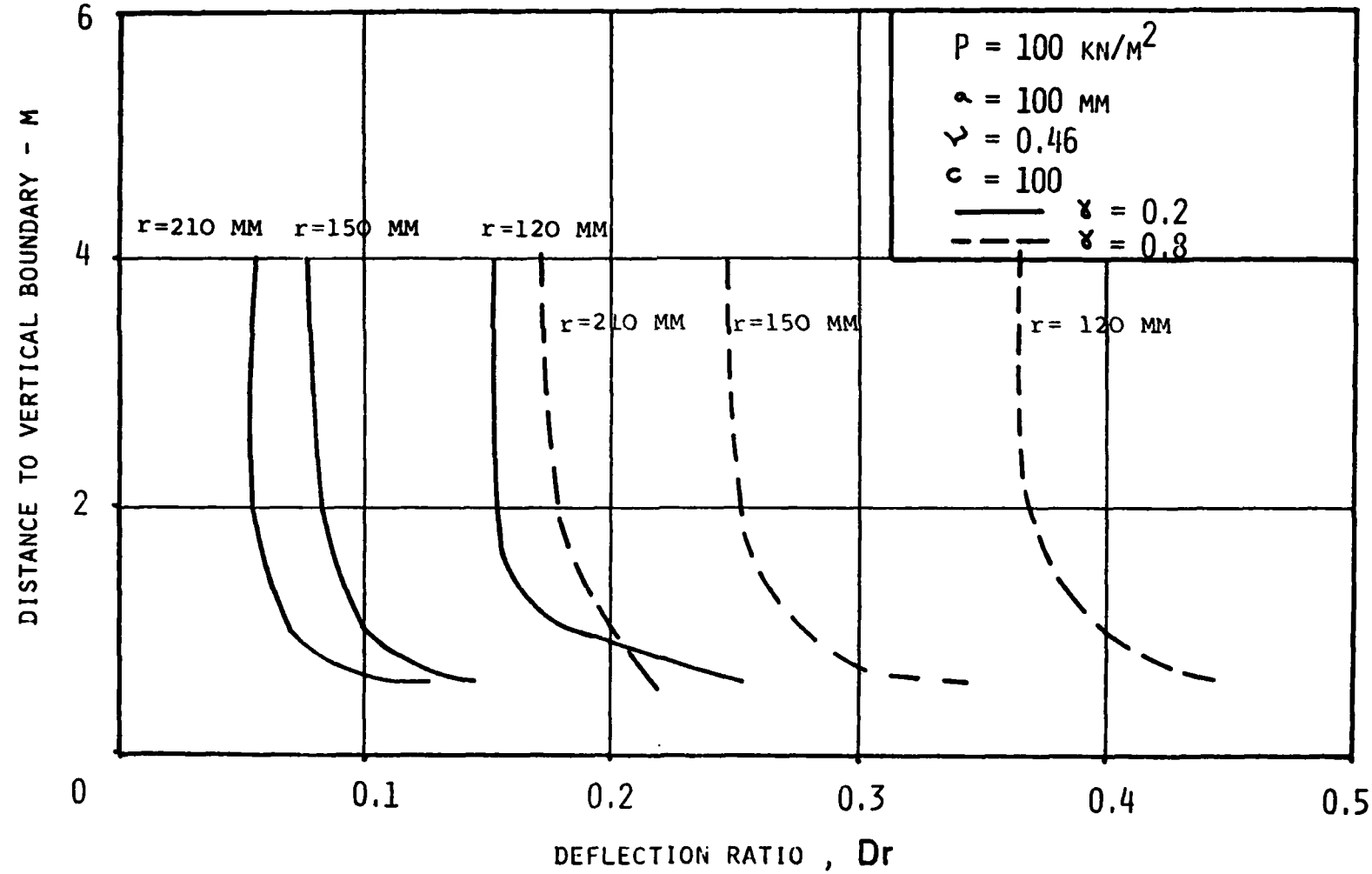

Fig.52

EFFECT OF DISTANCE TO BOUNDARY ON DEFLECTION RATIO

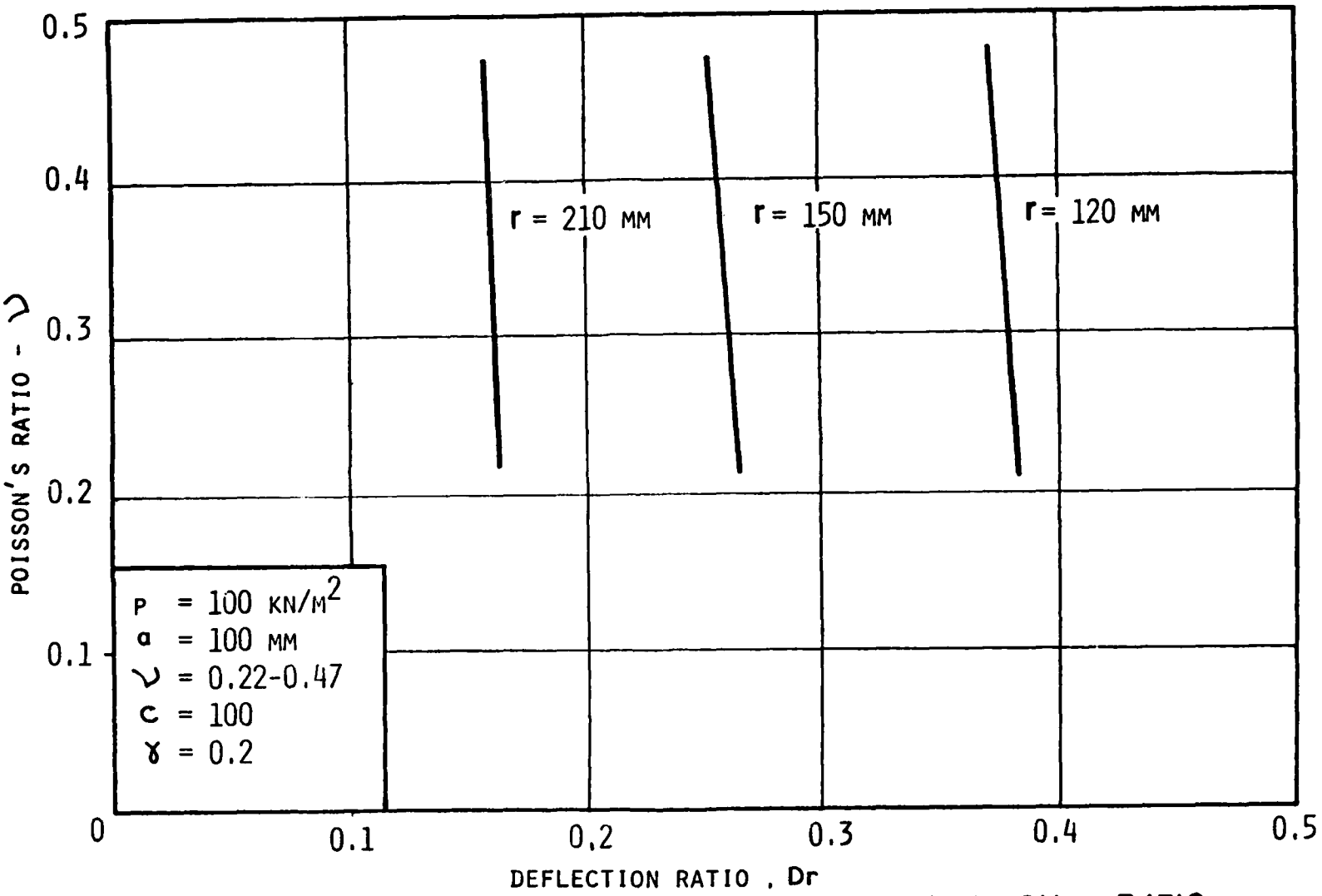

Fig. 5.3 EFFECT OF POISSON'S RATIO ON DEFLECTION RATIO

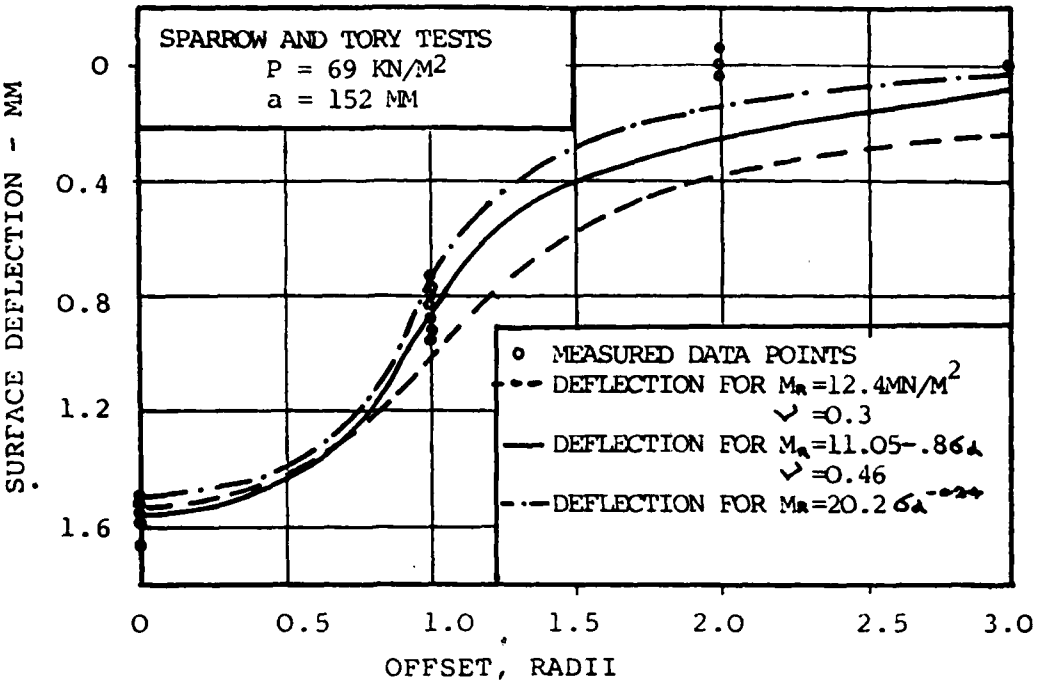

SURFACE DEFLECTION BASINS FOR SPARROW & TORY TESTS

Fig. 5.4

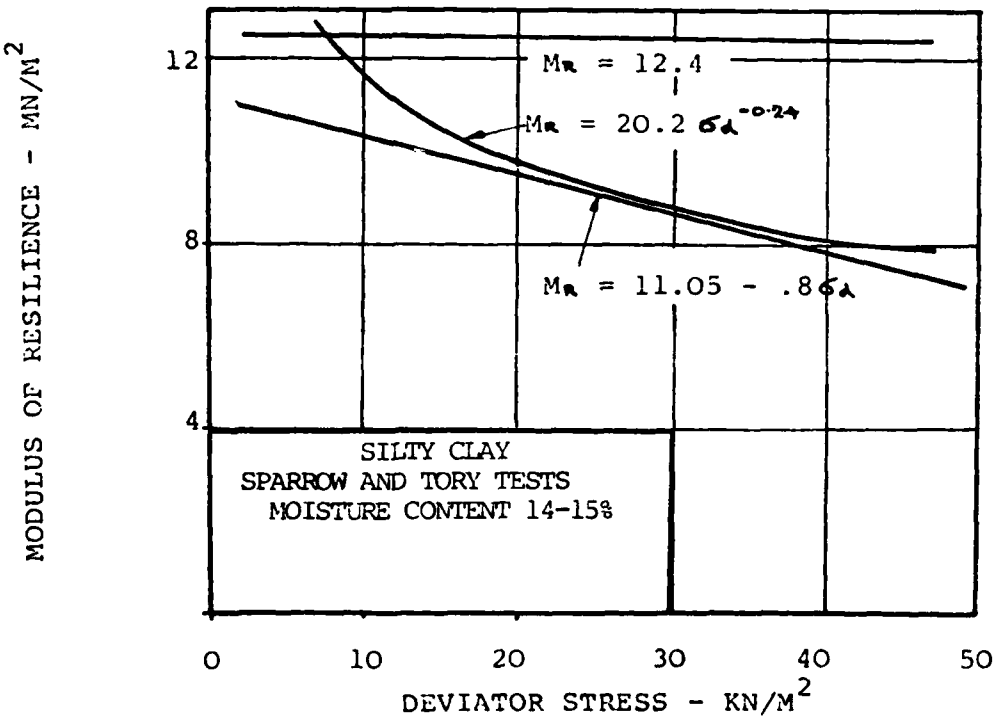

ESTIMATES OF RESILIENT MODULI FOR A SILTY CLAY SUBGRADE

Fig. 5.5

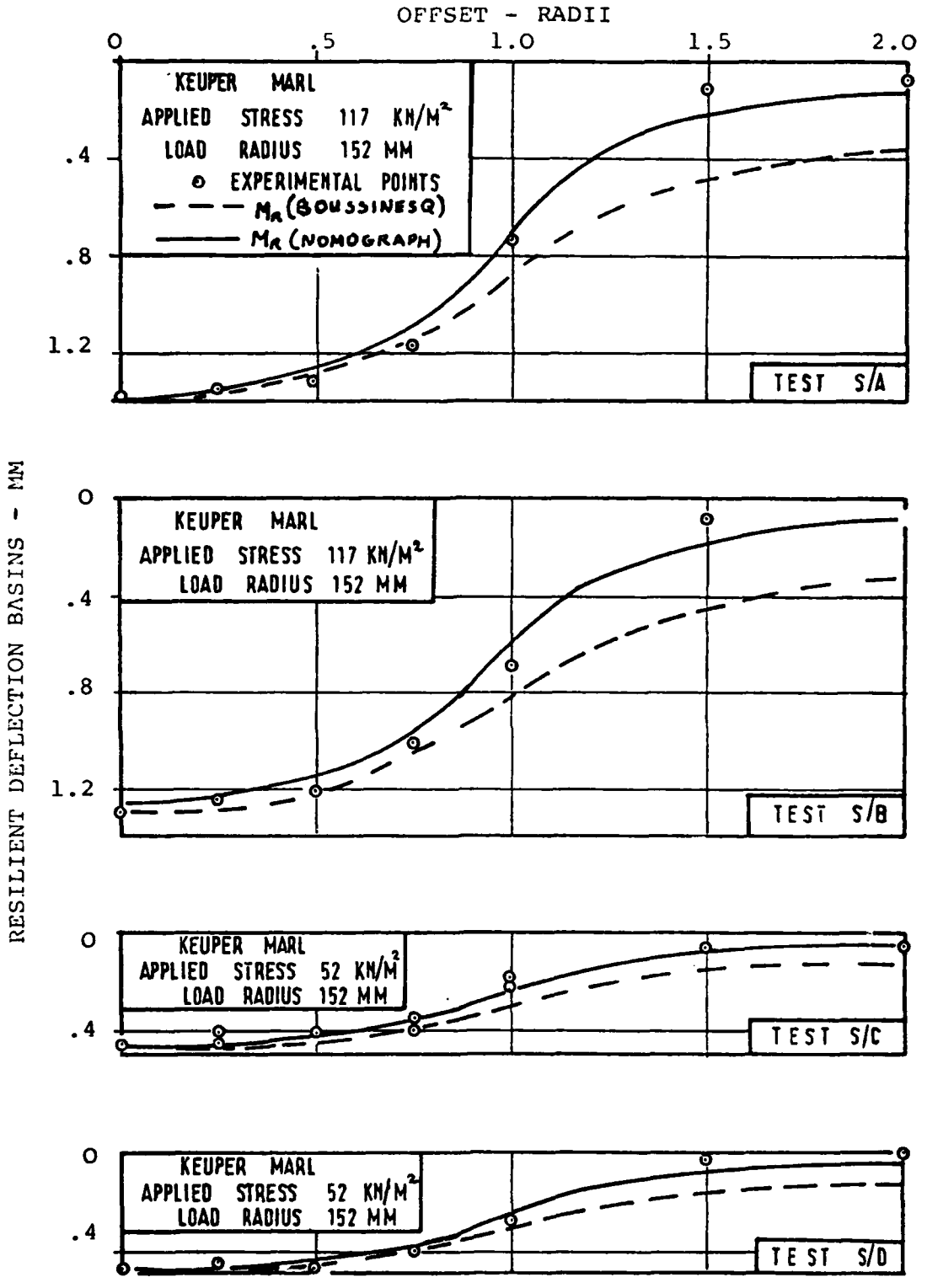

DEFLECTION BASINS FROM NOTTINGHAM TESTS

Fig. 5.6

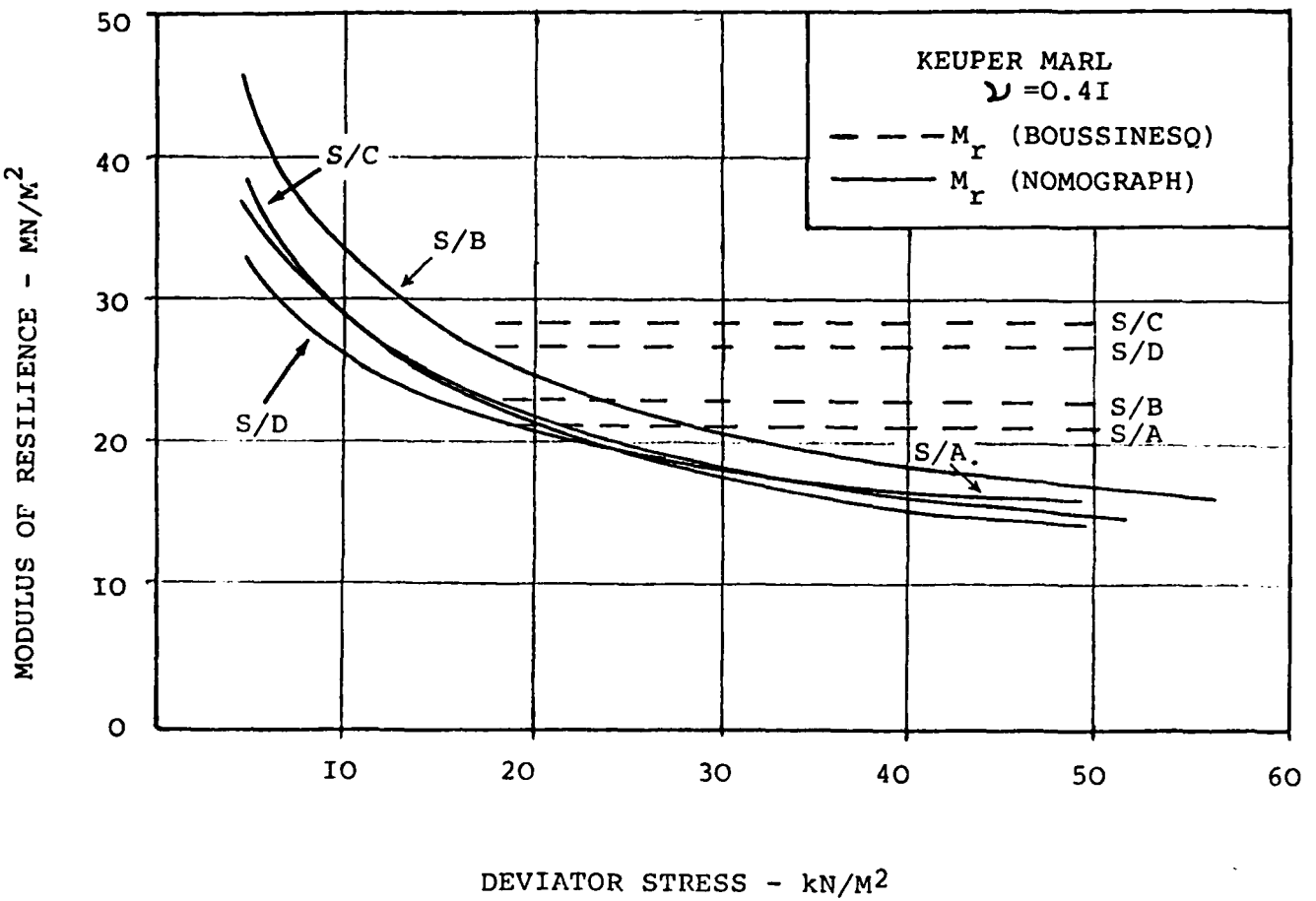

ESTIMATED M_R/σ_d RELATIONSHIPS FROM NOTTINGHAM TESTS (79)

Fig. 5.7

CHAPTER 6

Comparison of Resilient Modulus determined from Pavement Simulaton tests to those from triaxial tests and from the nomograph.

6.1 INTRODUCTION

In order to take the study of the behaviour of glacial till under repeated loading a stage beyond triaxial testing and nearer the insitu conditions, two series of tests were carried out on glacial till subgrades in the Laboratory Pavement Simulator. Undisturbed samples of these subgrades were also recovered and tested in the repeated loading triaxial rig to study the effects of sampling procedures on the relevant parameters.

The Laboratory Pavement Simulator (L.P.S.) has previously been described by Kirwan et al (26). The resilient and permanent deflections were measured at the centreline and at distances of 120mm and 210mm from the centre on an extended diameter.

6.2 TESTING METHODS

The tests were carried out on the glacial till subgrade after removal of the gravel sub-base used in the Gravel Road experiments of the Foras Forbartha which are described in Chapter 8 of this report. The surface was covered with wax immediately after removal of the gravel. The glacial till was taken from a different area of Dublin (Ballybrack) than that used in the triaxial experiments and consequently exhibited slightly different gradings and index properties as can be seen from Fig. 6.1.

The following is a summary of the testing program for the two

series of tests carried out in the L.P.S. to date. In each series, three of four areas of the subgrade surface were loaded vertically under applied uniform pressure which varied from 100kN/m^2 to 300kN/m^2 over a circular area of 204mm diameter. The resilient and permanent deformations were measured at the centre and at distances of 120mm and 210mm from the centre.

L.P.S. Test Series A

Average m/c	11.1%
Average dry density	19.5mg/m^2
Insitu CBR	25 to 29%

Test No.	Applied pressure kN/m^2	No. of stress application
C8	70-320	
C9	73	1,600
	154	1,900
C10	238	10,000
	303	10,000
	181	9,000
C11	70-310	
C12	130	2,000
	205	4,000
C13	40-330	

L.P.S. Test Series B

Average m/c	11.4%
Average dry density	1.98Mg/m^3
CBR	15-18%

Test No.		Applied pressure kN/m^2	No. of stress application
1.	a)	100	6,000
	b)	200	67,000
2.	a)	100	32,000
	b)	200	44,000
	c)	300	29,000
	d)	100-300	Varied
3.	a)	100	30,000
	b)	200	21,450
	c)	100-200	Varied
	d)	300	28.000
	e)	100-300	Varied
4.	a)	200	26,000
	b)	300	78,000
	c)	100-300	Varied

Undisturbed sampled were taken following each test, both adjacent to and from under the test areas. These samples were obtained either by jacking U4 thin walled sample tubes (100mm dia, 450mm in length) into the soil or by cutting blocks of the soil.

6.3 RESILIENT RESPONSE

SERIES A

The results of this test series indicated much higher moduli than anticipated. The recorded readings for Series A must therefore be questioned. No reason can be found for such an error other than that the tests were carried out under supervision as part of a final year project by students who were not completely familiar with the equipment. Further tests are in progress which hopefully will confirm that the Series A results were in error. The report on this test series given below should be read with this in mind.

Centreline deflections only were measured in tests C8 and C9. The material was assumed linear and the modulus of resilience determined by Boussinesq analysis. This gave values of:

C8 M_r = 340MN/m^2 at 100kN/m^2 dropping to 283KN/m^2 at 300kN/m^2

C9 M_r = 628MN/m^2 at 100kN/m^2 dropping to 501MN/m^2 at 300kN/m^2

The resilient moduli for tests C10 and C13 were determined from the deflection bowl measurements using the nomograph given in Fig. 6.2. This assumes a stress dependent modulus of the form: $M_r = C\sigma_d^{-\gamma}$

where C and γ are material parameters and σ_d the deviator stress. The results are shown in Fig. 6.3. Good agreement was generally obtained for individual tests carried out at different loading pressures but it was clear that the subgrades for the latter two tests C12 and C13 were considerably softer than the previous tests.

The resilient modulus of the above test, which comprised the Series A tests, were surprisingly high for brown glacial till at the measured moisture content and dry density. This would also explain the agreement between the empirical relationship, M_r = 10 x CBR MN/m^2 and the reported insitu values.

Repeated load triaxial tests on undisturbed samples gave a Resilient Modulus of 38 to 54MN/m^2 which was almost independent of the deviator stress. The lower modulus values were on samples taken from previously loaded areas. These results are considerably lower than those recorded on the subgrade in the L.P.S. The constand confining pressure in the triaxial tests which was normally 14kN/m^2 to represent typical over-burden pressure, was increased to 70kN/m^2 with no marked effect on the measured resilient response. The samples were remoulded and recompacted to their original moisture content and dry density but again gave similar results. The relative densities were:

Sample Number	Dry Density Mg/m^2	Moisture Content Percentage	Relative Density	Relative Moisture Content
1	1.968	11.1%	0.95	1.11
2	1.918	11.0%	0.93	1.10

The resilient modulus determined from the nomograph given in Fig. 3.6, Chapter 3 using the above γ_d and m/c gave values of approximately 60kN/m^2 for a deviator stress of 20kN/m^2. This compares favourably with the values measured in the triaxial tests but not to those from insitu tests in the L.P.S. The back analysis of the tests on the Gravel Pavements in the L.P.S. (Chapter 8) showed a subgrade modulus of the order of 80-110MN/m^2. Assuming that a stress dependent modulus for the subgrade gave lower values as shown in Fig. 6.4. This agrees favourably with the triaxial results and the nomograph but not with those obtained from tests on the surface of the subgrade or with the empirical relationship relating the resilient modulus to the CBR. It would appear therefore that there were recording errors in the results of those tests taken on the subgrade surface.

SERIES B

The resilient moduli recorded from the second series of tests

on a subgrade, Series B, were considerably lower than those reported for Series A.

The stress dependent moduli (assuming $M_r = C\ \sigma_d^{-\gamma}$) for tests 3 and 4 are shown in Fig. 6.5. Test 2, an area previously loaded in the gravel experiments, gave an almost stress independent modulus of between 163MN/m^2 with an applied pressure of 100kN/m^2, to 94MN/m^2 at an applied pressure of 300kN/m^2.

Tests carried out at different applied pressures but on the same test area of the subgrade surface gave consistent results.

A total of twelve undisturbed samples were taken from the subgrade after the test, three from under the loaded area, six from areas not previously loaded and three taken horizontally to study anisotropy.

Two samples have been tested to date, all in the recently developed Repeated Loading Testing Rig. The results of these two tests, shown in Fig. 6.6, show similar type curves for M_r Vs σ_d as that given by back analysis of the insitu tests.

Furthermore, the results of the two tests are compatible. The triaxial results are slightly lower than the insitu values which is to be expected from sampling disturbance. The dry densities, moisture content, relative density and relative moisture content of the samples were as follows:

Sample	Dry Density Mg/m^3	Moisture Content Percentage	Relative Density	Relative Moisture Content
6	1.974	11.5%	0.954	1.15
A	1.989	11.6%	0.96	1.16

The resilient moduli interpreted from the nomograph (Fig.3.6, Chapter 3) are 55MN/m^2 and 50MN/m^2 for the two samples. These

compare favourably with the measured insitu response. Furthermore, back analysis of the Gravel tests which were carried out on this subgrade gave resilient moduli, approximately 45-64 MN/m^2, which again compares favourably.

6.4 PERMANENT DEFORMATION

The results of the Series A tests were discarded because of possible recording errors which became apparent from the analysis of the resilient response.

The permanent deformation against number of load repetitions for tests 1, 2 and 3 are shown in Fig. 6.7 and for test 4, in Fig. 6.8. The latter tests are shown separately as the applied load reduced from $200kN/m^2$ to zero when run overnight (from 6,000 to 19,000 repetitions). The general shape of the curves is similar to those obtained from the triaxial tests reported in Chapter 3.

The triaxial tests reported in Chapter 3 indicated that , within the normal working subgrade stress range, the permanent deformation could be taken as an approximately linear function of deviator stress for a given number of repetitions. This implies that there is a straight line relationship between the permanent deformation in the L.P.S. tests and the applied pressure. These parameters are plotted on Fig. 6.9. Test 2 did give a straight line plot but this area had been loaded previously in Foras Forbartha gravel experiments. The tests gave an almost linear response for applied pressure of up to $200kN/m^3$ but diverged from a straight line when the applied pressure was increased to $300kN/m^2$. The maximum resilient strain in the subgrade under $300kN/m^2$ pressure was of the order of 3.5×10^{-3}. The curve produced by Brown et al (9) implies that the subgrade under this resilient strain should fail with 512 repetitions. This load is therefore outside the normal level which would be applied to the subgrade.

The permanent deformation vs applied pressure can be approximated to a straight line for the loads less than 200kN/m^2 as shown in Fig. 6.9. The slope of the permanent deformation - deviator stress line obtained from the triaxial tests was called the modulus of compliance (Mp) and was used to compare the performance of different samples. The line shown on Fig.6.9 implies a modulus of compliance of 2 x 10^{-5}/kN/m^2. This compares favourably with that obtained from the triaxial tests for soils of similar stiffness.

The Relative Compaction vs Relative Moisture Content plot shown on Fig.3.6, Chapter 3 indicated an $M_p \simeq 0.00009$ kN/m^2 for the subgrade tested. This is greater than that recorded by a factor of 4.5. The contours of equal M_p change rapidly for a small change in moisture content in the area of the diagram in which the insitu soil tests are plotted. Nevertheless, the reasons for this descrepancy are being investigated.

6.5 SUMMARY

Two series of repeated load tests were carried out on glacial till from Ballybrack, Co. Dublin in the Laboratory Pavement Simulator. Analysis of the resilient response of these tests indicated possible recording errors in the first series of tests. The stress dependent resilient modulus determined by the deflection bowl method described in Chapter 5 on the second series of tests compared favourably with those recorded on triaxial tests on undisturbed samples and with values interpolated from the chart given on Fig.3.6, Chapter 3. The empirical relationship M_r = 10CBR MN/m^2 gave unsatisfactory results.

While the general trends of the permanent deformation complied with the behaviour recorded for the triaxial tests, the actual deflection was approximately 4.5 times less than predicted from the R_c, R_w chart given on Fig.3.13, Chapter 3.

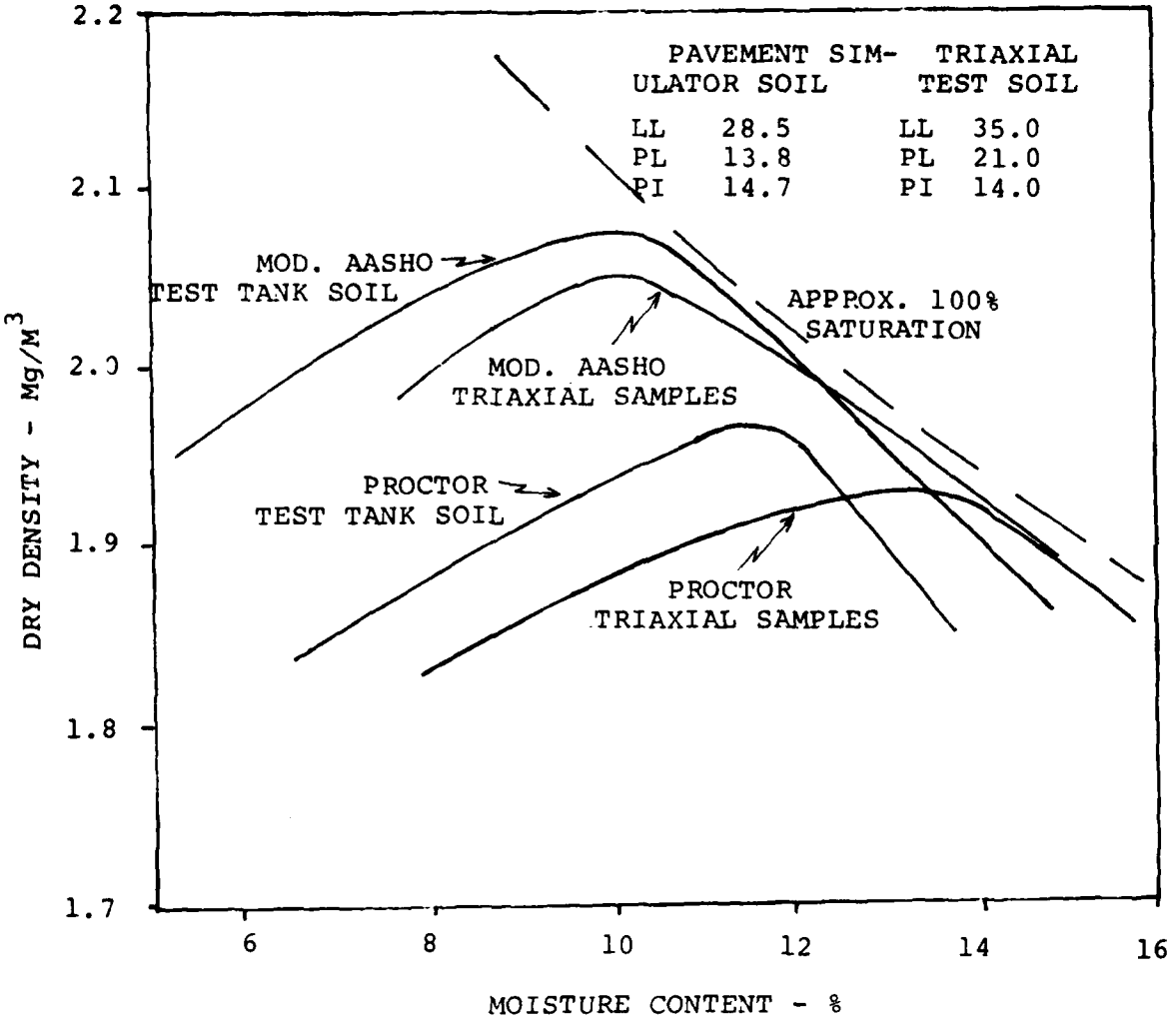

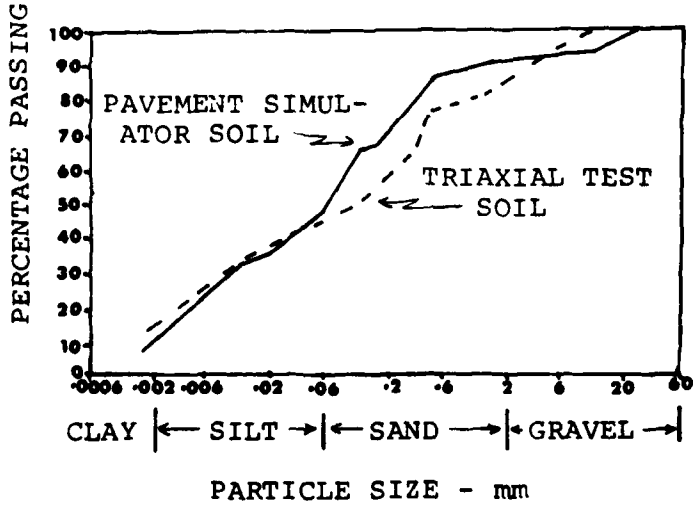

GRADINGS AND INDEX PROPERTIES FOR TEST GLACIAL TILLS

Fig. 6.1

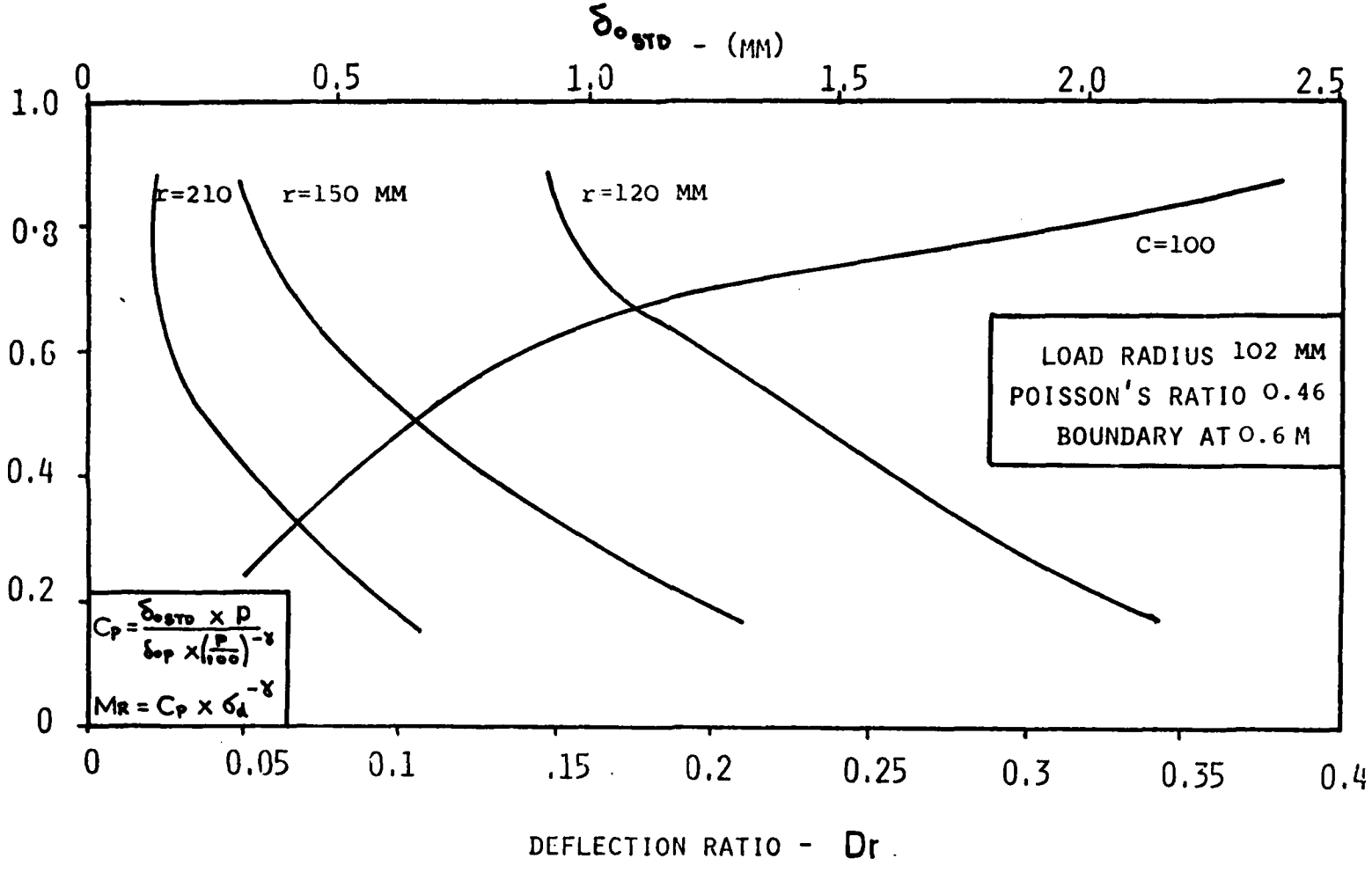

Fig.6.2

MODULUS INTERPRETATION NOMOGRAPH FOR TESTS ON WICKLOW GLACIAL TILL

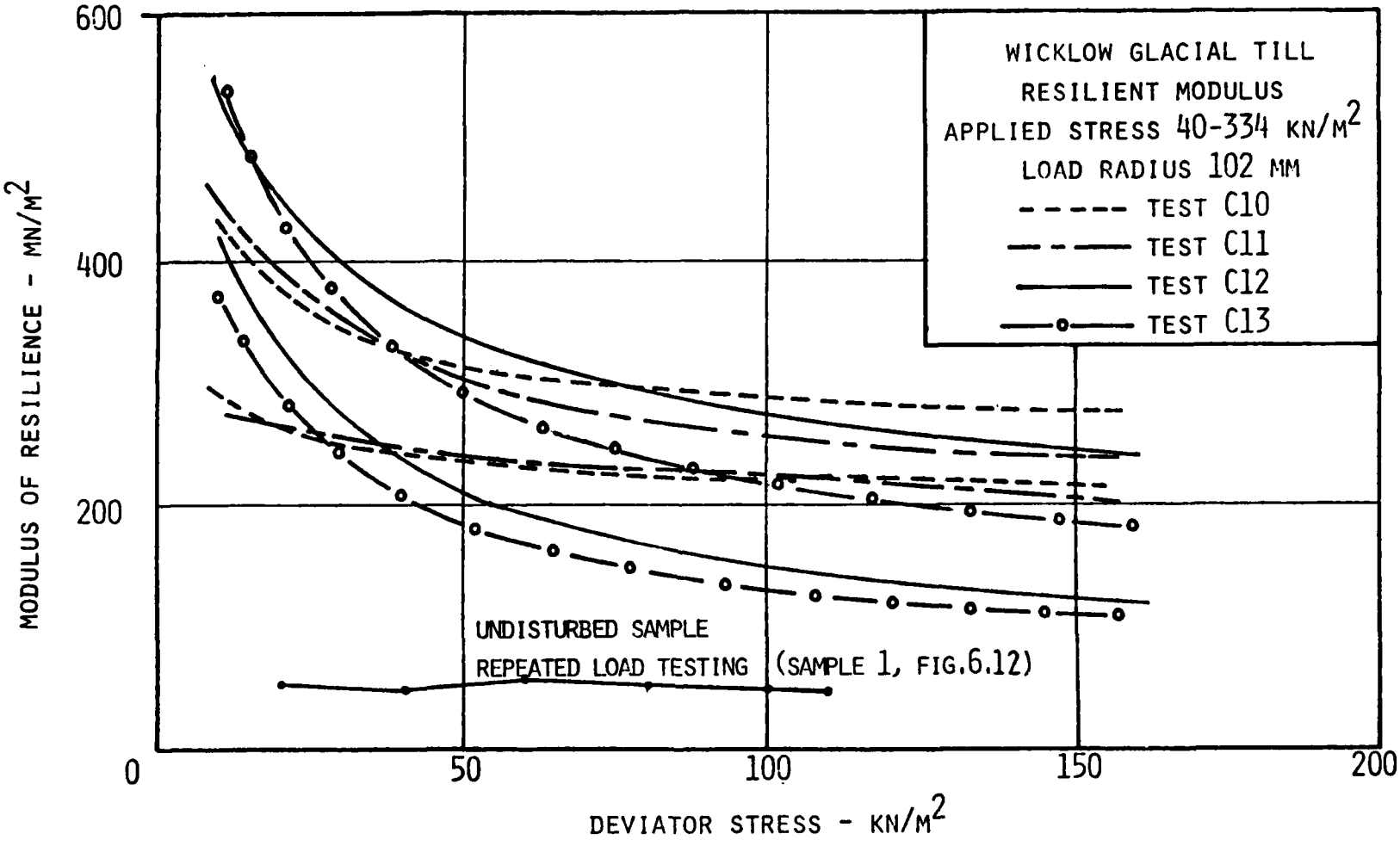

Fig. 6.3 MODULUS OF RESILIENCE RELATIONSHIPS FOR WICKLOW GLACIAL TILL

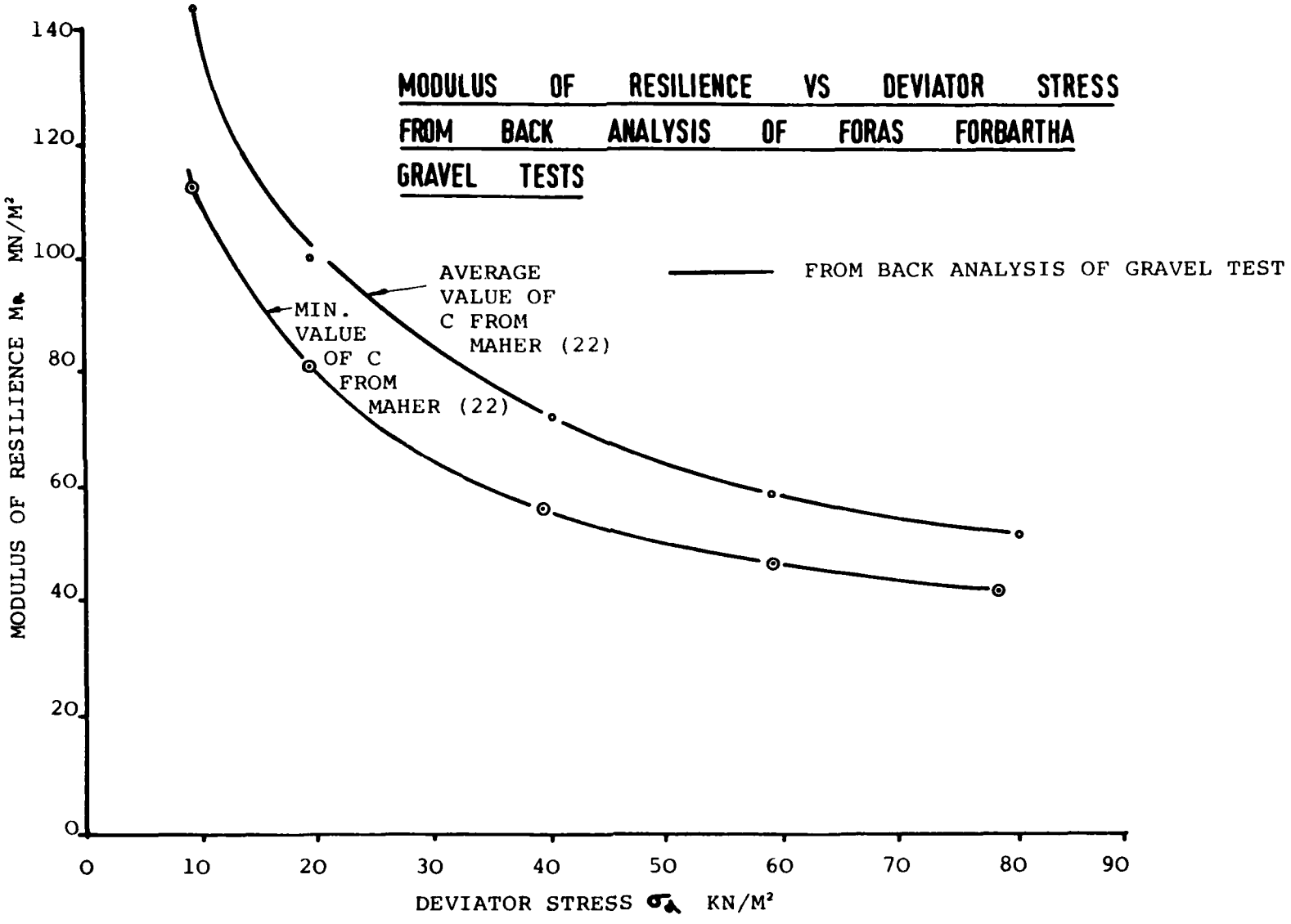
MODULUS OF RESILIENCE FROM BACK ANALYSIS OF FORAS FORBARTHA GRAVEL TESTS
FROM BACK ANALYSIS OF GRAVEL TEST
AVERAGE VALUE OF C FROM MAHER (22)
MIN. VALUE OF C FROM MAHER (22)
MODULUS OF RESILIENCE M_R MN/M²
DEVIATOR STRESS σ_d KN/M²
0
20
40
60
80
100
120
140
0
10
20
30
40
50
60
70
80
90

Fig. 6.4

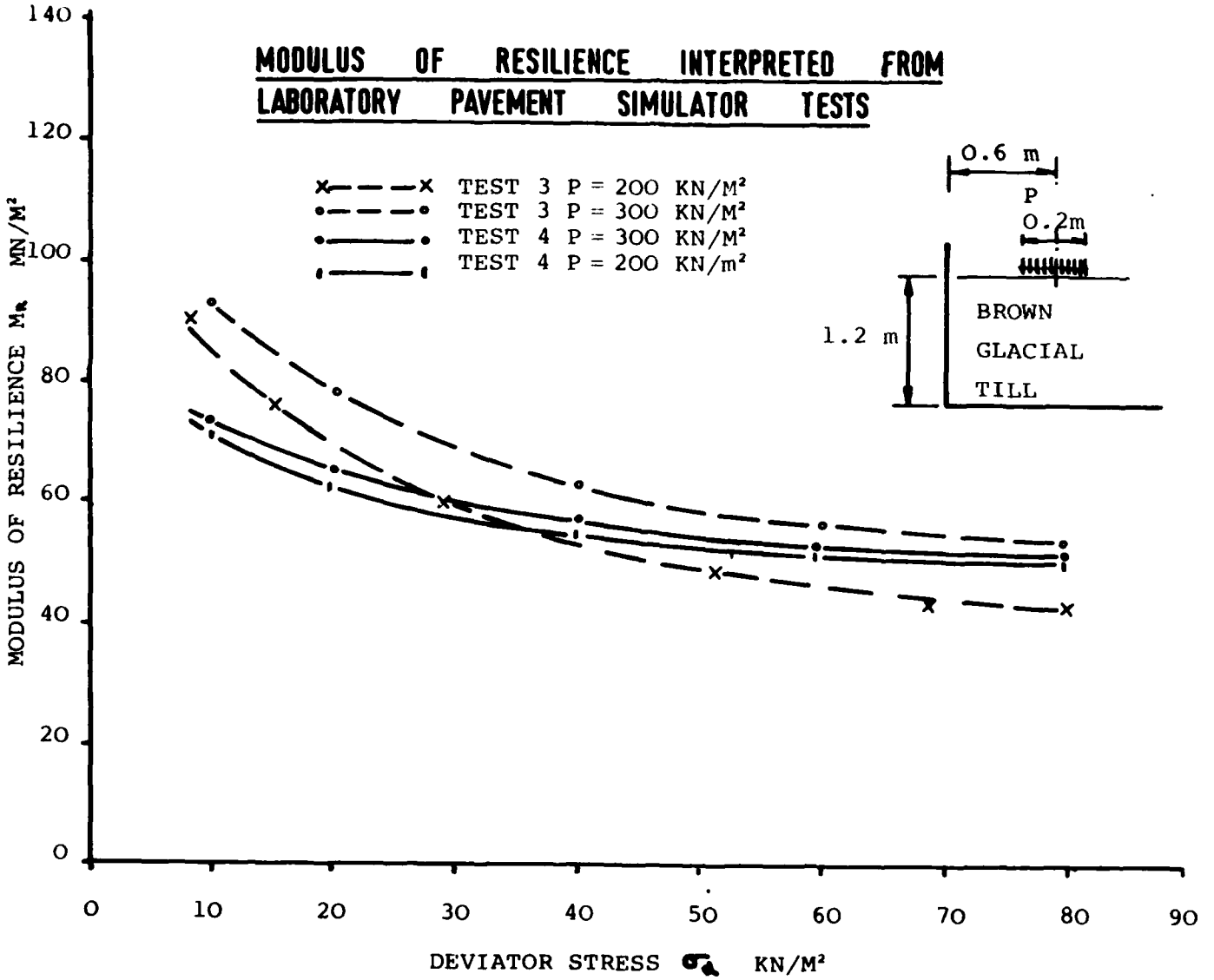
MODULUS OF RESILIENCE INTERPRETED FROM LABORATORY PAVEMENT SIMULATOR TESTS
TEST 3 P = 200 KN/M²
TEST 3 P = 300 KN/M²
TEST 4 P = 300 KN/M²
TEST 4 P = 200 KN/m²
0.6 m
P
0.2m
1.2 m
BROWN
GLACIAL
TILL
MODULUS OF RESILIENCE Mr MN/M²
DEVIATOR STRESS σd KN/M²
0
20
40
60
80
100
120
140
0
10
20
30
40
50
60
70
80
90

Fig. 6.5

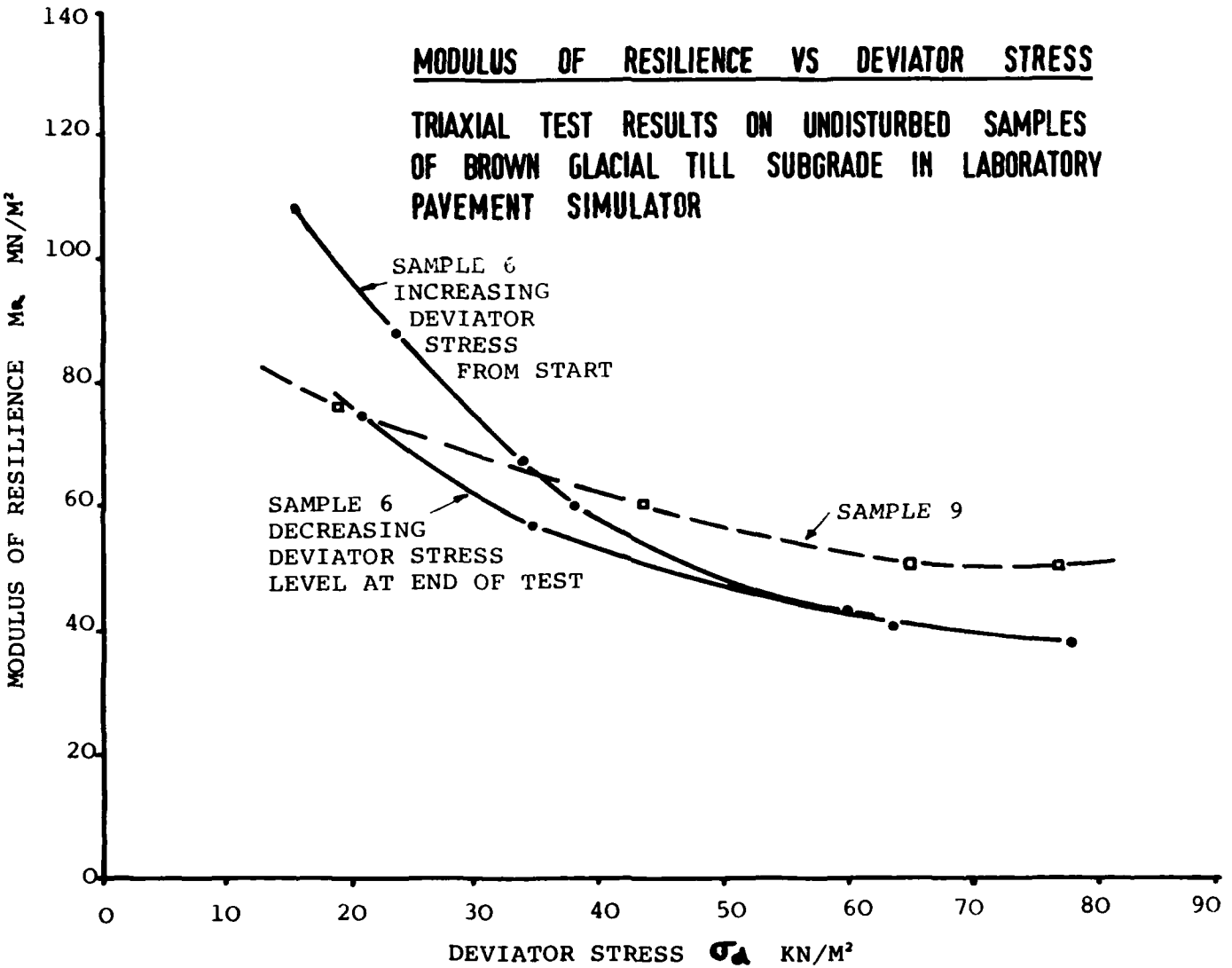
MODULUS OF RESILIENCE VS DEVIATOR STRESS
TRIAXIAL TEST RESULTS ON UNDISTURBED SAMPLES OF BROWN GLACIAL TILL SUBGRADE IN LABORATORY PAVEMENT SIMULATOR
SAMPLE 6 INCREASING DEVIATOR STRESS FROM START
SAMPLE 6 DECREASING DEVIATOR STRESS LEVEL AT END OF TEST
SAMPLE 9
MODULUS OF RESILIENCE Mr MN/M²
DEVIATOR STRESS σd KN/M²
140
120
100
80
60
40
20
0
0
10
20
30
40
50
60
70
80
90

Fig. 6.6

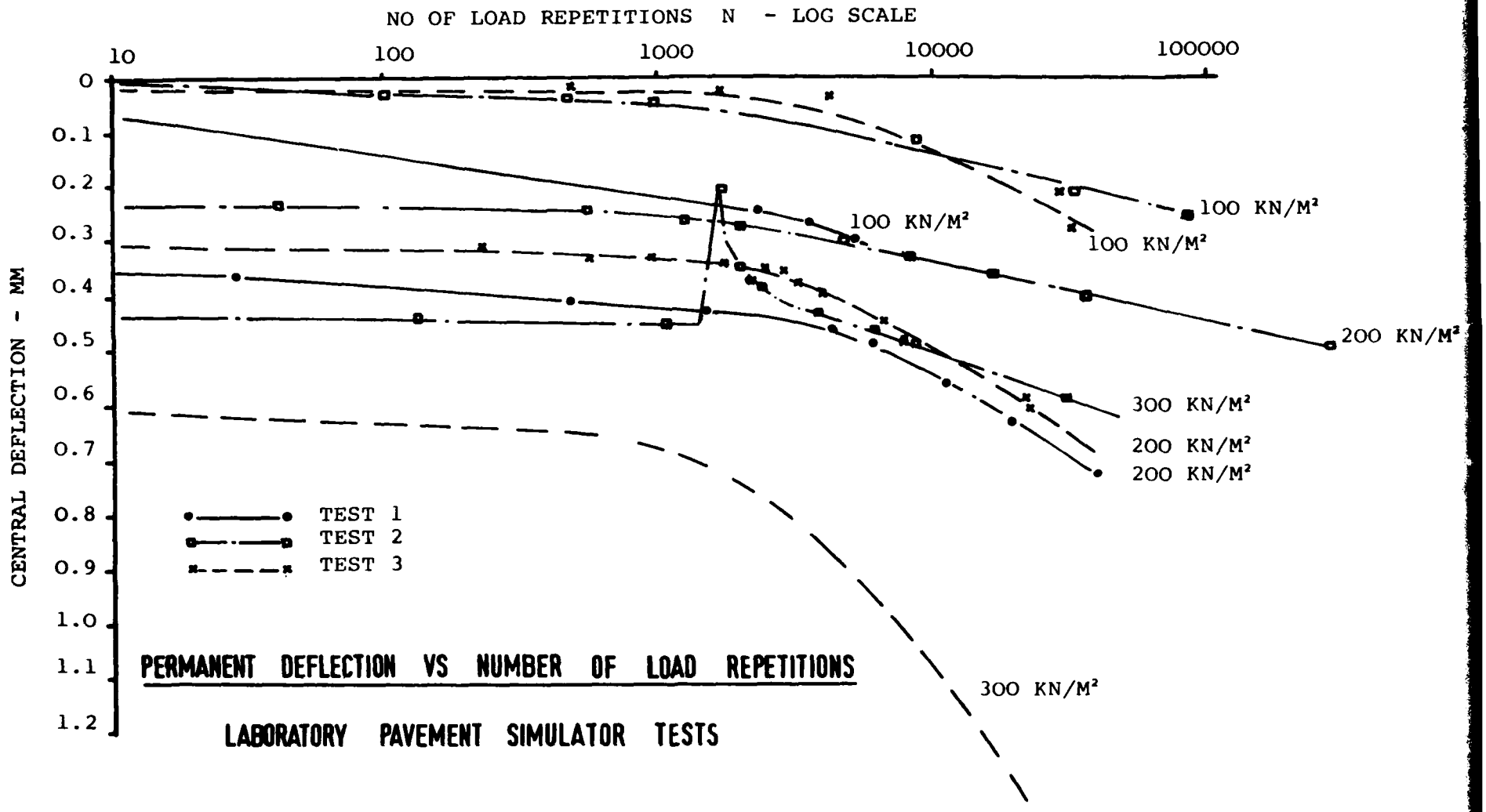
NO OF LOAD REPETITIONS N - LOG SCALE
10
100
1000
10000
100000
CENTRAL DEFLECTION - MM
0
0.1
0.2
0.3
0.4
0.5
0.6
0.7
0.8
0.9
1.0
1.1
1.2
100 KN/M²
100 KN/M²
100 KN/M²
200 KN/M²
300 KN/M²
200 KN/M²
200 KN/M²
300 KN/M²
TEST 1
TEST 2
TEST 3
PERMANENT DEFLECTION VS NUMBER OF LOAD REPETITIONS
LABORATORY PAVEMENT SIMULATOR TESTS

Fig. 6.7

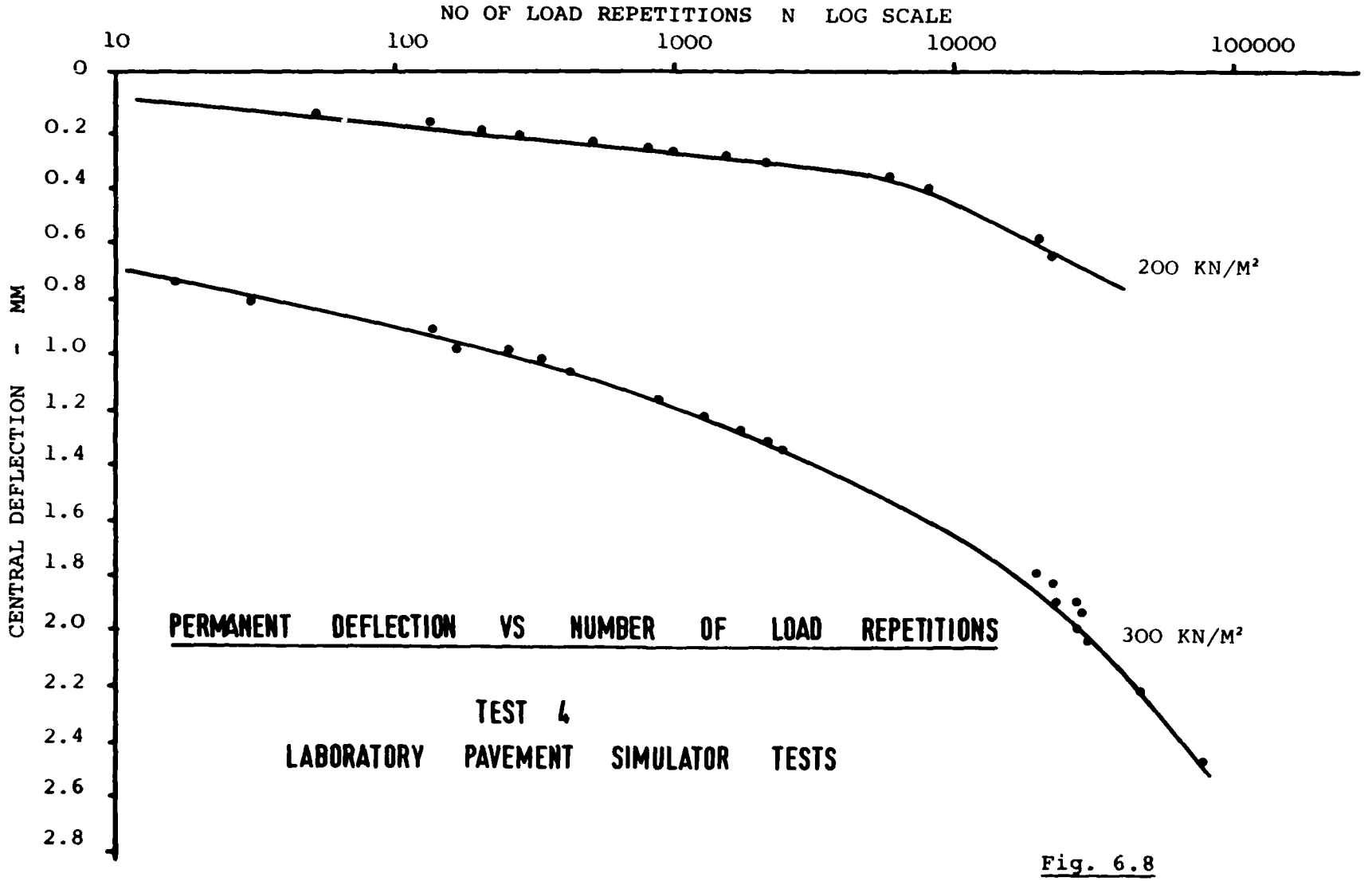
NO OF LOAD REPETITIONS N LOG SCALE
10
100
1000
10000
100000
0
0.2
0.4
0.6
0.8
1.0
1.2
1.4
1.6
1.8
2.0
2.2
2.4
2.6
2.8
CENTRAL DEFLECTION - MM
200 KN/M²
300 KN/M²
PERMANENT DEFLECTION VS NUMBER OF LOAD REPETITIONS
TEST 4
LABORATORY PAVEMENT SIMULATOR TESTS

Fig. 6.8

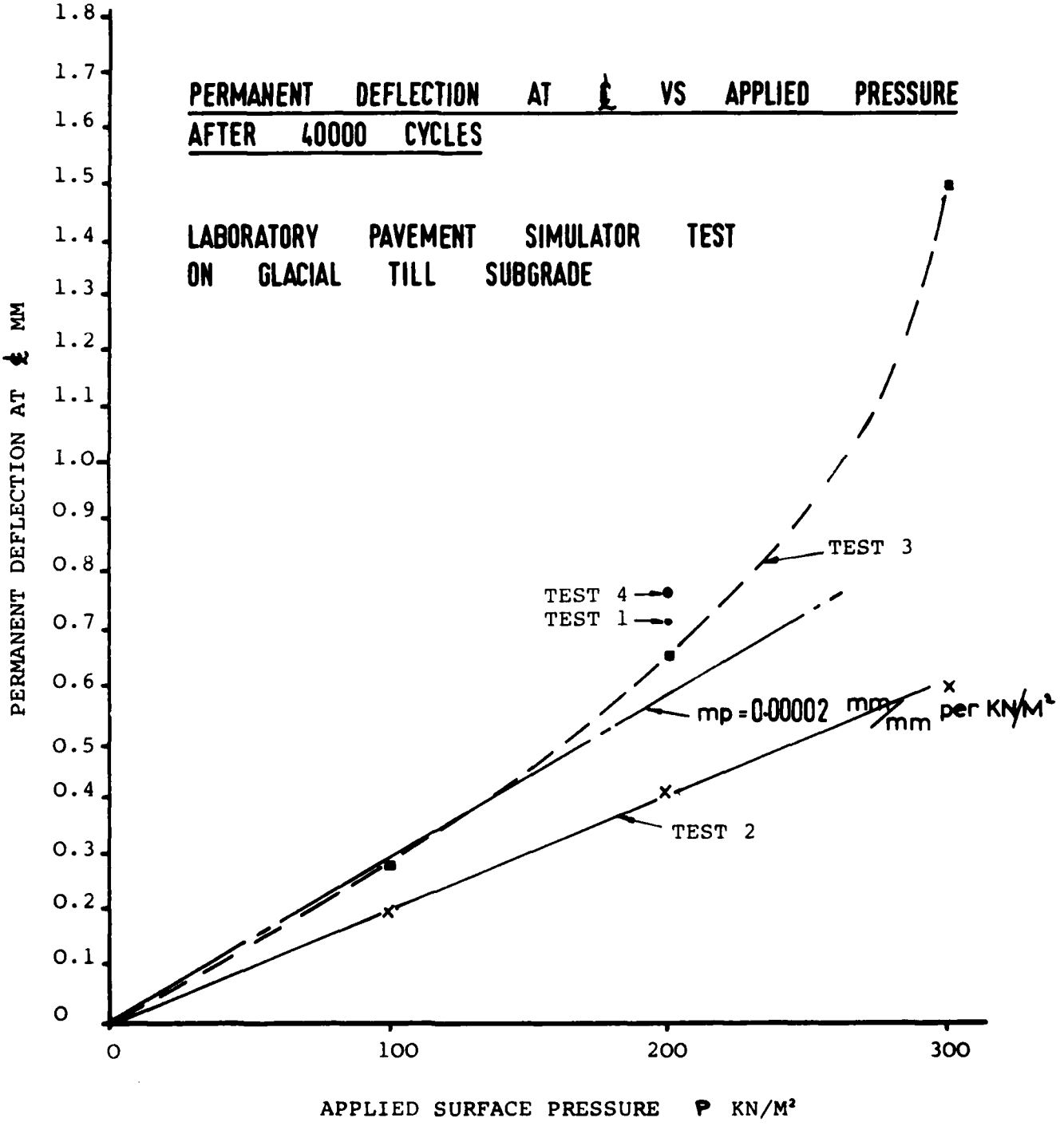
PERMANENT DEFLECTION AT ℄ VS APPLIED PRESSURE
AFTER 40000 CYCLES
LABORATORY PAVEMENT SIMULATOR TEST
ON GLACIAL TILL SUBGRADE
PERMANENT DEFLECTION AT ℄ MM
1.8
1.7
1.6
1.5
1.4
1.3
1.2
1.1
1.0
0.9
0.8
0.7
0.6
0.5
0.4
0.3
0.2
0.1
0
TEST 3
TEST 4
TEST 1
mp = 0·00002 mm/mm per KN/M²
TEST 2
0
100
200
300
APPLIED SURFACE PRESSURE P KN/M²

Fig. 6.9

CHAPTER 7

ANISOTROPIC VERSION OF DEFPAV

Several investigators have reported different moduli of resilience for samples taken vertically to those taken horizontally from road pavement layers (Shackel (27)). This is not surprising considering that the method of construction involves compaction in layers using a roller. It is therefore important that methods of analysis are available to study the effect of the layered anisotropy on the road response and performance. Such methods may also allow more satisfactory modelling of fabric layers than those which use transition layers with isotropic properties. The Trinity College, Dublin finite element program DEFPAV has been modified to include horizontally layered anisotropic elastic material properties.

The formulation of the finite element program DEFPAV for isotropic material properties has been described by Kirwan and Glynn (28). Modification to layered anisotropic behaviour involves altering the [D] matrix which relates stresses in individual elements to strains

$$\{\sigma\} = [D]\ \{\varepsilon\}$$

This modification of stress-strain relationship effects the element stiffness matrix

$$[\bar{k}] = \int [B]^t\ [D]\ [B]\ dv$$

where [B] relates strains to nodal displacements in local co-ordinates.

The stresses are computed from the relationship

$$\{\sigma\} = [D]\ [B]\ [A]^{-1}\ \{U\}$$

where A relates nodal displacement in global co-ordinates to nodal displacement in local co-ordinates.

The derivation of the [D] matrix for layered anisotropic elastic materials assumes that the vertical direction will be the axis of symmetry for any anisotropy which may exist. This implies that the governing parameters are independent of the horizontal direction. Some aspects of the behaviour of anisotropic soils have been discussed by Pickering (1970)

DEFPAV used a rectangular annular element as shown in Fig.7.1. The strains in a section of the element shown in Fig. 7.1 are given by:

$$\varepsilon_z = \frac{\sigma_z}{E_z} - \nu_{zh}\frac{\sigma_r}{E_h} - \nu_{zh}\frac{\sigma_\theta}{E_h}$$

$$\varepsilon_r = -\nu_{hz}\frac{\sigma_z}{E_z} + \frac{\sigma_r}{E_h} - \nu_{hh}\frac{\sigma_\theta}{E_h}$$

$$\varepsilon_\theta = -\nu_{hz}\frac{\sigma_z}{E_z} - \nu_{hh}\frac{\sigma_r}{E_h} + \frac{\sigma_\theta}{E_h}$$

$$\gamma_{rz} = \frac{1}{G_2}\tau_{rz}$$

Where

σ_z , ε_z represent stress and strain in the vertical direction.

σ_z , ε_z represent stress and strain in the radial direction.

σ_θ , ε_θ represent stress and strain in the circumferential direction.

τ_{rz} , γ_{rz} represent stress and strain in shear.

ν_{zh} represents the degree of vertical strain due to horizontal strain.

ν_{hz} represents the degree of horizontal strain due to vertical strain.

ν_{hh} represents the degree of horizontal strain due to horizontal strain in the orthogonal direction.

G_2 represents the shear modulus in the vertical plane.

The input requirements of the program are similar to those of the isotropic version however they must be extended to include the terms illustrated in APPENDIX 1.

From energy considerations $\frac{\nu_{zh}}{E_h} = \frac{\nu_{hz}}{E_z}$

Let $\frac{E_h}{E_z} = \frac{G_2}{E_z} = m$ and ordering the matrix in the same way as used by Kirwan and Glynn (28), a modified [D] matrix which relates stresses to strains in a horizontally layered anisotropic material is then obtained. This [D] matrix is illustrated in Fig. 7.2.

The [B] matrix remains unaltered thus the stiffness matrix in local coordinates is given by:

$$[\bar{k}] = \iiint [B]^t [D][B] \, dz. \, dr. \, r \, d\theta$$

Fig. 7.3 shows a simplified form of this stiffness matrix where the following substitutions have been made;

M1 :- $bn(1-n\nu_{hz}) \cdot \ell n (r_j/r_i)$

M2 :- $bn(1+\nu_{hh})(r_j-r_i)$

M3 :- $bn(1+\nu_{hh})(r_j^2-r_i^2)$

M4 :- $(b^2/2)n(1-n\nu_{hz})\ell n(r_j/r_i)$

M5 :- $b^2n(1+\nu_{hh})(r_j-r_i)$

M6 :- $(b^3/3)n(1-n\nu_{hz}^2)\ell n(r_j/r_i)+bm\{(1+\nu_{hh})(1-\nu_{hh}-2n\nu_{hz}^2)(r_j^2-r_i^2)/2\}$

M7 :- $(b^2/2)n(1+\nu_{hh})(r_j-r_i)$

M8 :- $(b^2/2)n(1+\nu_{hh})(r_j^2-r_i^2)$

M9 :- $(b^3/3)n(1+\nu_{hh})(r_j-r_i)+bm\{(1+\nu_{hh})(1-\nu_{hh}-2n\nu_{hz}^2)(r_j^3-r_i^3)/3\}$

M10:- $(b^3/3)n(1+\nu_{hh})(r_j^2-r_i^2)+bm\{(1+\nu_{hh})(1-\nu_{hh}-2n\nu_{hz}^2)(r_j^4-r_i^4)/4\}$

M11:- $mb(1+\nu_{hh})(1-\nu_{hh}-2n\nu_{hz}^2)(r_j^2-r_i^2)/2$

M12:- $mb(1+\nu_{hh})(1-\nu_{hh}-2n\nu_{hz}^2)(r_j^3-r_i^3)/3$

M13:- $mb(1+\nu_{hh})(1-\nu_{hh}-2n\nu_{hz}^2)(r_j^2-r_i^2)/2$

M14:- $bn(1+\nu_{hh})(r_j-r_i)$

M15:- $bn\nu_{hz}(1+\nu_{hh})(r_j^2-r_i^2)$

M16:- $(b^2/2)n\nu_{hz}(1+\nu_{hh})(r_j-r_i)$

M17:- $b^2n\nu_{hz}(1+\nu_{hh})(r_j^2-r_i^2)/2$

M18:- $b(1-\nu_{hh}^2)(r_j^2-r_i^2)/2$

M19:- $bn\nu_{hz}(1+\nu_{hh})(r_j^2-r_i^2)/2$

M20:- $2bn\nu_{hz}(1+\nu_{hh})(r_j^3-r_i^3)/3$

M21:- $(b^2/2)n\nu_{hz}(1+\nu_{hh})(r_j^2-r_i^2)/2+m(b^2/2)\{(1+\nu_{hh})(1-\nu_{hh}-2n\nu_{hz}^2)(r_j^2-r_i^2)/2\}$

M22:- $b^2n\nu_{hz}(1+\nu_{hh})(r_j^3-r_i^3)/3+m(b^2/2)\{(1+\nu_{hh})(1-\nu_{hh}-2n\nu_{hz}^2)(r_j^3-r_i^3)/3$

M23:- $m(b^2/2)(1-\nu_{hh}-2n\nu_{hz}^2)(r_j^2-r_i^2)/2$

M24:- $b(1-\nu_{hh}^2)(r_j^3-r_i^3)/3$

M25:- $b(1-\nu_{hh})(r_j^4-r_i^4)/4+m(b^3/3)\{(1+\nu_{hh})(1-\nu_{hh}-2n\nu_{hz}^2)(r_j^2-r_i^2)/2$

The individual terms of the matrix products [D] x [B] for the anisotropic material are included in the subroutine FIN6EL in DEFPAV and are illustrated in Fig. 7.4. This matrix is somewhat different to that used in the isotropic version of DEFPAV, as a result modifications have been made to the subroutines DATAIN, FIN8EL, FIN2EL, FIN6EL and FINSTR in the program as well as other minor alterations elsewhere.

It is clear from the $[\bar{k}]$ matrix given in Fig. 7.3 that the stiffness becomes indeterminate with

$$1-\nu_{hh}-2n\nu_{hz} = 0$$

Pickering (29) has carried out an interesting study on the limiting values of elastic parameters of horizontally layered anisotropic materials. In order to keep strain energy positive the following conditions must hold:

a) E_z and E_h must be greater than zero.

b) $\{\frac{E_h}{E_z}(1-\nu_{hh}) - 2\nu_{zh}^2\}\{1+\nu_{hh}\}$ must be positive.

This is similar to

$$1-\nu_{hh}-2n\nu_{hz}^2 > 0$$

c) G_2 must be positive

d) $2(1+\nu_{hh})$ must be positive i.e. $\nu_{hh} > -1$

Condition (b) can restrict what seem to be reasonable values for the elastic parameters.

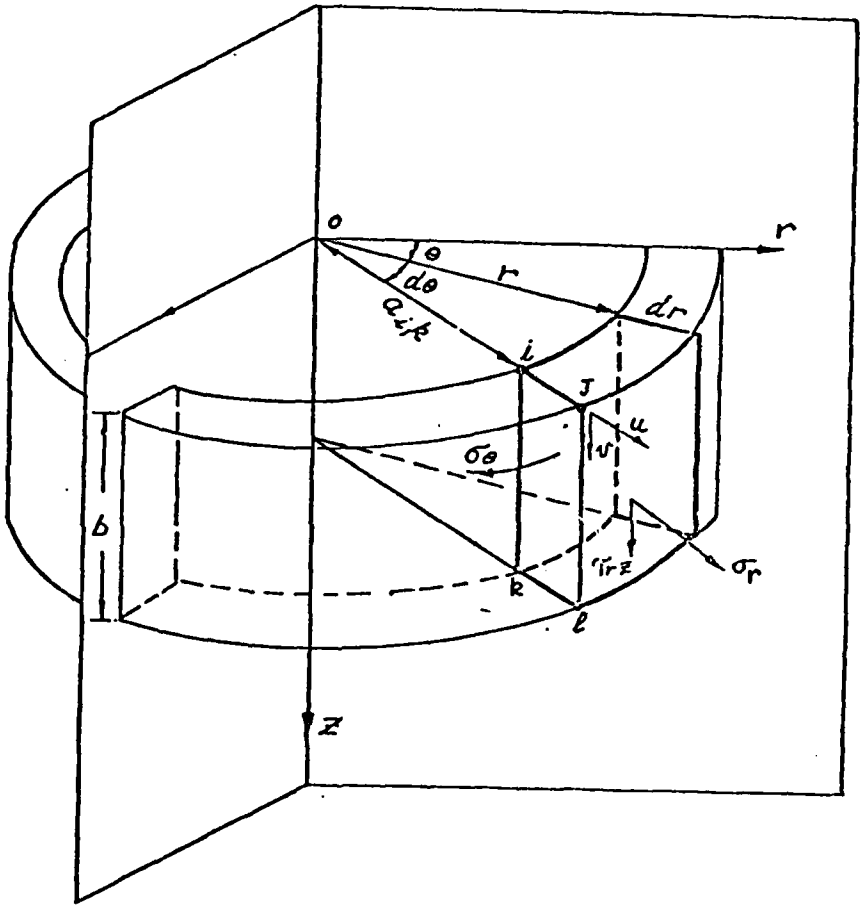

ANNULAR RECTANGULAR ELEMENT: COMPONENTS OF STRESS AND DISPLACEMENT IN CYLINDRICAL COORDINATES

Fig. 7.1

$$\begin{bmatrix} \sigma_r \\ \sigma_\theta \\ \sigma_z \\ \tau_{rz} \end{bmatrix} = \frac{E_z}{(1+\nu_{hh})(1-\nu_{hh}-2n\nu_{hz}^2)} \times \begin{bmatrix} n(1-n\nu_{hz}^2) & n(\nu_{hh}+n\nu_{hz}^2) & n\nu_{hz}(1+\nu_{hh}) & 0 \\ 0 & n(1-n\nu_{hz}^2) & n\nu_{hz}(1+\nu_{hh}) & 0 \\ 0 & 0 & (1-\nu_{hh}^2) & 0 \\ 0 & 0 & 0 & m(1+\nu_{hh})(1-\nu_{hh}-2n\nu_{hz}^2) \end{bmatrix} \begin{bmatrix} \varepsilon_r \\ \varepsilon_\theta \\ \varepsilon_z \\ \gamma_{rz} \end{bmatrix}$$

MATRIX RELATING STRESS TO STRAIN IN A HORIZONTALLY LAYERED ANISOTROPIC MATERIAL

Fig. 7.2

$$[\bar{k}] = \frac{2\pi E_z}{(1-\nu_{hh})(1-\nu_{hh}-2n\nu_{hz}^2)} \begin{bmatrix} M1 & & & & & & & \\ M2 & M3 & & & & & & \\ M4 & M5 & M6 & & & & & \\ M7 & M8 & M9 & M10 & & & & \\ 0 & 0 & 0 & 0 & 0 & & & \\ 0 & 0 & M11 & M12 & 0 & M13 & & \\ M14 & M15 & M16 & M17 & 0 & 0 & M18 & \\ M19 & M20 & M21 & M22 & 0 & M23 & M24 & M25 \end{bmatrix}$$

SIMPLIFIED ANISOTROPIC ELEMENT STIFFNESS MATRIX FOR ANNULAR RECTANGULAR ELEMENT

Fig. 7.3

$$\frac{E_z}{(1+\nu_{hh})(1-\nu_{hh}-2n\nu_{hz}^2)}$$

$$\begin{bmatrix}
\frac{n}{r}(\nu_{hh}+n\nu_{hz}^2) & n(1+\nu_{hh}) & \frac{z}{r}n(\nu_{hh}+n\nu_{hz}^2) & zn(1+\nu_{hh}) & 0 & 0 & n\nu_{hz}(1+\nu_{hh}) & rn\nu_{hz}(1+\nu_{hh}) \\
\frac{n}{r}(1-n\nu_{hz}^2) & n(1+\nu_{hh}) & \frac{z}{r}n(1-n\nu_{hz}^2) & zn(1+\nu_{hh}) & 0 & 0 & n\nu_{hz}(1+\nu_{hh}) & rn\nu_{hz}(1+\nu_{hh}) \\
\frac{n}{r}\nu_{hz}(1+\nu_{hh}) & 2n\nu_{hz}(1+\nu_{hh}) & \frac{z}{r}n\nu_{hz}(1+\nu_{hh}) & 2nz\nu_{hz}(1+\nu_{hh}) & 0 & 0 & (1-\nu_{hh}^2) & r(1+\nu_{hh}^2) \\
0 & 0 & m(1+\nu_{hh}) \times (1-\nu_{hh}-2n\nu_{hz}^2) & rm(1+\nu_{hh}) \times (1-\nu_{hh}-2n\nu_{hz}^2) & 0 & mz(1+\nu_{hh}) \times (1-\nu_{hh}-2n\nu_{hz}^2) & 0 & mz(1+\nu_{hh}) \times (1-\nu_{hh}-2n\nu_{hz}^2)
\end{bmatrix}$$

INDIVIDUAL TERMS OF THE MATRIX PRODUCTS OF [D] x [B] THAT ARE INCLUDED IN THE SUBROUTINE FIN6EL

(r and z represent radial and vertical distances respectively)

Fig. 7.4

CHAPTER 8

GRAVEL PAVEMENT TESTS

8.1 INTRODUCTION

In Ireland, it has been found that certain pit run glacial gravels behave satisfactorily as pavement base course materials while others give poor results. For gravels without excessive fines passing the 75 B S Sieve, there is often no obvious reason for poor performance. This is of particular importance in this country where surface dressed gravel often forms an initial part of the stage construction of trunk roads. (The gravel base course with only a thin surface dressing is open to traffic for periods of up to several years before application of the bituminous layers).

It has been found that grading tests on gravel do not provide an indication of future performance. Compaction tests and C.B.R. tests are similarly inadequate. An Foras Forbartha therefore decided to carry out a series of repeated load tests in our laboratory pavement simulator. A base course of pit run Kilpeddar gravel placed on a subgrade of brown glacial till from Ballybrack, Dublin has been tested to date. The laboratory construction was to simulate, as closely as possible, the conditions at the road improvement scheme at Kilpeddar, County Wicklow which is being monitored in the field. The preliminary analysis of this work is reported in "The use of gravels in road pavements in Ireland" by S.Davitt, Research Officer, An Foras Forbartha. The tests are continuing with gravels from other sources.

8.2 PAVEMENT SIMULATOR TESTS

While the problem of the behaviour of gravels is still unsolved

AD-A084 135 TRINITY COLL DUBLIN (IRELAND) SCHOOL OF ENGINEERING F/G 13/2
ENVIRONMENTAL AND OTHER CRITERIA AND METHODS FOR PAVEMENT DESIG--ETC(U)
FEB 79 R W KIRWAN, E R FARRELL, M L MAHER DA-ERO-76-G-065

UNCLASSIFIED NL

2 OF 2
AD
A084135

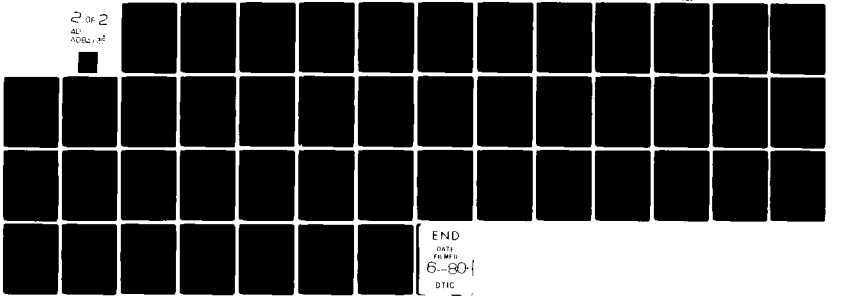

END
DATE FILMED
6-80
DTIC

at present, some interesting trends have been observed. A brief outline of the laboratory tests is as follows:

Subgrade: Brown glacial till: 1 metre thick
Series A: Water Content 11.1% Dry Density: 1.95 Mg/m^3
C.B.R. : 25-29% thin bituminous coating on surface of subgrade
Base Course Gravel: Water Content 5% - 5.5%
Thickness 250mm and 150mm
Insitu Density: 2.22Mg/m^3

Grading, compaction characteristics and C.B.R. of gravel given on Fig. 8.1.

Moisture content of gravel after test = 3%
Applied repeated load: 552 kN/m^2
Radius of load pulse: 102mm
Duration of load pulse: 0.4 sec.
Load frequency: 2 cycles / sec.

Stresses (Vertical)at gravel/subgrade interface were measured using load cells.

Tests were normally carried out up to 100,000 repetitions of load application. Surface deflections were measured on centre line and at 120mm and 210mm each side of the centre on a diametral line.

Tests were carried out:

1) On the gravel at placement water content
2) After increasing the water content of the gravel by soaking for various periods of time.
3) With ponding of water round the point of application of load, to achieve saturation of the gravel.

The following trends were observed on the behaviour of the whole pavement:

1) 'Dry': After 10,000 loading cycles, the permanent deformation of the pavement showed a very small increase with further applications of load. The total permanent deformation for 150mm thickness of gravel was less than 3mm after 100,000 cycles.

2) After soaking: an increase was observed in the resilient deflection, and also in the initial permanent deformation. Again, after 10,000 cycles, when no further moisture entered the system, very little further permanent deformation occurred.

3) Ponding of load application area: The permanent deformation as expected, increased rapidly due to the loading pad punching into the gravel. Resilient modulus also decreased as expected.

It is concluded that the unsaturated gravel base had an extremely high load carrying capacity under the vertical load applied in the Laboratory Pavement Simulator. The extent to which the confining effect of the walls influenced the results has not been ascertained.

As expected, the increase in water content towards saturation had an adverse effect which emphasised the importance of both the free draining requirements of the gravel and the need to slope the formation to ensure rapid drainage between base and subgrade. It may be advantageous to blind the surface of the basecourse to limit ingress of water in the event of surface dressing breakdown.

The subgrade has been tested insitu and in triaxial repeated load tests as part of our materials characterisation, these tests are reported and discussed in Chapter 6.

8.3 INTERPRETATION OF RESILIENT RESPONSE BY BACK ANALYSIS

A modulus interpretation system has been developed for the two layer pavements used in the L.P.S. This method is based on estimation of modulus of resilience from deflection basin measurements assuming isotropic, homogeneous materials as described in Chapter 5.

The stress dependence of the resilient modulus is therefore ignored, which is certainly incorrect for this gravel. Despite these assumptions, this method is helpful in analysing the behaviour of the materials. This analysis has enabled the behaviour of the gravel to be separated from that of the subgrade and to compare the calculated stresses with those recorded on the embedded stress cells.

Interpretation nomographs corresponding to the two pavement thicknesses are shown in Figs. 8.2 and 8.3. A curve relating the stress on the subgrade to the deflection ratio is included for comparison with the measured values.

The results of this analysis are summarised on Tables 8.1 to 8.6. The main trends which can be observed from these are:

1) Dry (ref GC1 to GC4) : The resilient modulus of the gravel layer increased considerably during the tests. That of the subgrade appears to increase slightly although this is partly due to a reduction in the subgrade stress level.

2) Soaked (ref GC5 to GC6) : The resilient modulus of the soaked gravel decreased significantly with increase in the number of cycles while that of the subgrade increased slightly, probably as a result of compaction of the subgrade. The increase in resilient deflection therefore took place in the gravel.

3) Ponded : The resilient modulus of the gravel beneath a free water surface decreased by half during the test, presumably due to pore pressure build-up. The increase in modulus of the subgrade is unexplained.

4) Reduction in thickness of gravel from 250 to 150mm: The modulus of the gravel increased during the first test and reached values slightly lower than those obtained from the thicker pavement. This is in keeping with the trend noted by Klomp and Dorman (30).

5) The average ratio, between the modulus of the gravel layer and that of the subgrade, was six for the thick layers and three for the thinner layers. These are higher ratios than those found by the Shell investigators.

6) Using the constant modulus for both subgrade and gravel, the calculated stresses at the top of the subgrade do not always compare favourably with those measured, Table 8.4. But taking a stress dependent modulus for the subgrade of the form $M = C\sigma_d^{-0.5}$, the comparison between measured and calculated values of stresses compare favourably for the two tests GC8 and GC9 which showed poor agreement using the former method.

Using this stress dependent modulus for the subgrade, a revised nomograph was prepared and the layer moduli for the tests were re-interpreted. The results of this, given in Table 8.3, show an increase in gravel moduli of 10 - 12% and a decrease in moduli of the subgrade.

While we emphasise that the gravel testing program is only in the initial stage, we feel that the results to date are useful. The series of tests would benefit from additional instrumentation.

Test No.	No. of Cycles (approx.)	δ_o (mm)	D_{120}	$\frac{Mrsg^*}{Mrgr^{**}}$	δ_o x Mrgr (mm x MN/m^2)	Mrgr (MN/m^2)	Mrsg (MN/m^2)
GC1	100	.29	.586	.125	139	479	60
	1,000	.28	.571	.147	134	479	70
	10,000	.26	.596	.120	144	552	66
	100,000	.18	.528	.232	120	664	154
GC2	100	.25	.500	.31	111	444	138
	1,000	.231	.563	.161	131	567	91
	10,000	.225	.538	.205	123	545	112
	100,000	.18	.539	.205	123	683	140
GC3	100	.254	.571	.145	134	528	76
	1,000	.246	.581	.130	138	561	73
	10,000	.25	.56	.165	130	520	86
	100,000	.18	.556	.172	129	715	123
GC4	100	.285	.526	.225	119	416	94
	1,500	.30	.533	.22	121	403	89
	10,000	.275	.509	.275	114	415	114
	100,000	.18	.569	.15	131.5	731	110

Table 8.1 Summary of Modulus Interpretation for Tests GC1 to GC4.

* M_{rsg} SUBGRADE MODULUS

** M_{rgr} GRAVEL MODULUS

Test No.	No. of Cycles (approx.)	δ_o (mm)	D_{120}	$\frac{Mrsg}{Mrgr}$	δ_o x Mrgr (mm x MN/m^2)	Mrgr (MN/m^2)	Mrsg (MN/m^2)
GC5	100	.50	.454	.531	99	199	106
	1,000	.49	.457	.575	100	204	117
	10,000	.455	.429	.70	94	207	147
	100,000	.434	.461	.485	101	233	113
GC6	100	.335	.507	.288	113	338	97
	1,000	.325	.508	.288	113	347	100
	10,000	.315	.502	.305	112	355	108
	100,000	.28	.518	.256	117	417	107
GC7	100	.30	.52	.255	117	390	99
	1,000	.30	.50	.310	111	370	115
	31,000	.565	.403	1.1	89	158	173
	40,000	.56	.393	1.26	87	155	196

Table 8.2 Summary of Modulus Interpretation for Tests GC5 to GC7.

Test No.	No. of Cycles (approx.)	δ_o (mm)	D_{120}	$\frac{C}{Mrgr}$	δ_o x Mrgr (mm x MN/m^2)	Mrgr (MN/m^2)	C	Mrsg (MN/m^2)	
								σ_d = 20kN/m^2	σ_d = 50 kN/m^2
GC8	180	.72	.410	3.6	101	140	505	113	71
	1,650	.64	.414	3.52	102	159	561	125	79
	10,000	.48	.438	2.94	108	225	662	148	94
	100,000	.28	.554	0.76	164	586	445	100	63
GC9	100	.39	.538	0.9	155	397	358	80	51
	1,000	.38	.526	1.04	149	392	408	91	58
	22,000	.35	.514	1.24	142	406	502	112	71
	100,000	.26	.529	1.0	150	577	577	129	82
GC10	100	.345	.565	0.69	170	493	340	76	48
	1,250	.345	.551	0.78	162	470	366	82	52
	11,300	.305	.574	0.63	176	577	364	81	51
	100,000	.27	.565	0.69	170	630	434	97	61

Table 8.3 Revised Modulus Interpretation for Tests GC8 to GC10.

TEST GC8			TEST GC9			TEST GC11		
No. of Cycles	Stress on Subgrade (kN/m^2)		No. of Cycles	Stress on Subgrade (kN/m^2)		No. of Cycles	Stress on Subgrade (kN/m^2)	
	Measured	Estimated		Measured	Estimated		Measured	Estimated
500	145	230	87	90	163	4,700	52	50
1,500	127	222	1,800	89	172	6,700	50	49
2,740	119	212	24,900	94	180	9,340	46	40
7,080	119	200	30,760	95	161	25,400	48	48
14,730	94	181	46,820	77	176	45,000	46	48
27,660	91	184	64,800	66	152	53,000	41	49
75,640	97	164	78,300	97	168	67,500	43	46
84,000	101	158	83,300	85	159	84,130	40	38
101,000	101	158	103,000	73	169	100,000	36	34

Table 8.4 Measured and Estimated Subgrade Stresses.

TEST GC8			TEST GC9		
No. of Cycles (approx.)	Stress on Subgrade (kN/m^2)		No. of Cycles (approx.)	Stress on Subgrade (kN/m^2)	
	Measured	Estimated		Measured	Estimated
500	145	180	87	90	88
1,500	127	178	1,800	89	82
2,740	119	156	24,900	94	112
7,080	119	146	30,760	95	89
14,730	94	113	46,820	77	98
27,660	91	114	64,800	66	71
75,640	97	90	78,300	97	84
84,000	101	82	83,300	85	85
101,000	101	82	103,000	73	93

Table 8.5 Measured and Estimated Subgrade Stresses.

(ν for subgrade = .5)

Test No.	No. of Cycles (approx.)	δ_o (mm)	D_{120}	$\frac{Mrsg}{Mrgr}$	δ_o x Mrgr (mm x MN/ m^2)	Mrgr (MN/m^2)	Mrsg (MN/m^2)
GC8	180	.72	.410	.94	91	127	119
	1,650	.64	.414	.90	92	144	130
	10,000	.48	.438	.685	100	207	142
	100,000	.28	.554	.266	146	523	139
GC9	100	.39	.538	.305	138	353	108
	1,000	.38	.526	.336	132	347	117
	22,000	.35	.514	.363	127	361	131
	100,000	.26	.529	.327	133	513	168
GC10	100	.345	.565	.24	152	441	106
	1,250	.345	.551	.275	145	419	115
	11,300	.305	.574	.220	158	516	114
	100,000	.27	.565	.24	152	563	135
GC11	100	.265	.584	.13	139	525	68
	1,000	.26	.587	.128	140	537	69
	11,700	.24	.583	131	139	577	76
	100,000	.195	.615	.092	151	774	71

Table 8.6 Summary of Modulus Interpretation for Tests GC8 to GC11.

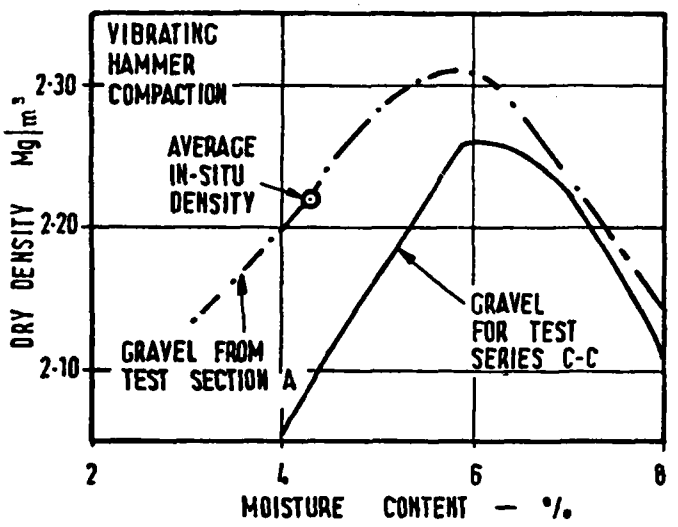

		TEST TANK	TEST SECTION
VIBRATING HAMMER COMPACTION	OPT. M/C	6%	5·7 %
	MAX. DRY DENSITY	2·265 Mg/M³	2·320 Mg/M³
	MAX. C.B.R.	180 %	250 %
LIQUID LIMIT		9 %	9%
NON PLASTIC		—	—
SPECIFIC GRAVITY		2·68	2·68
% PASSING 75 MM (200 B.S.) SIEVE		10·9	9·0
UNIFORMITY COEFFICIENT		105	100

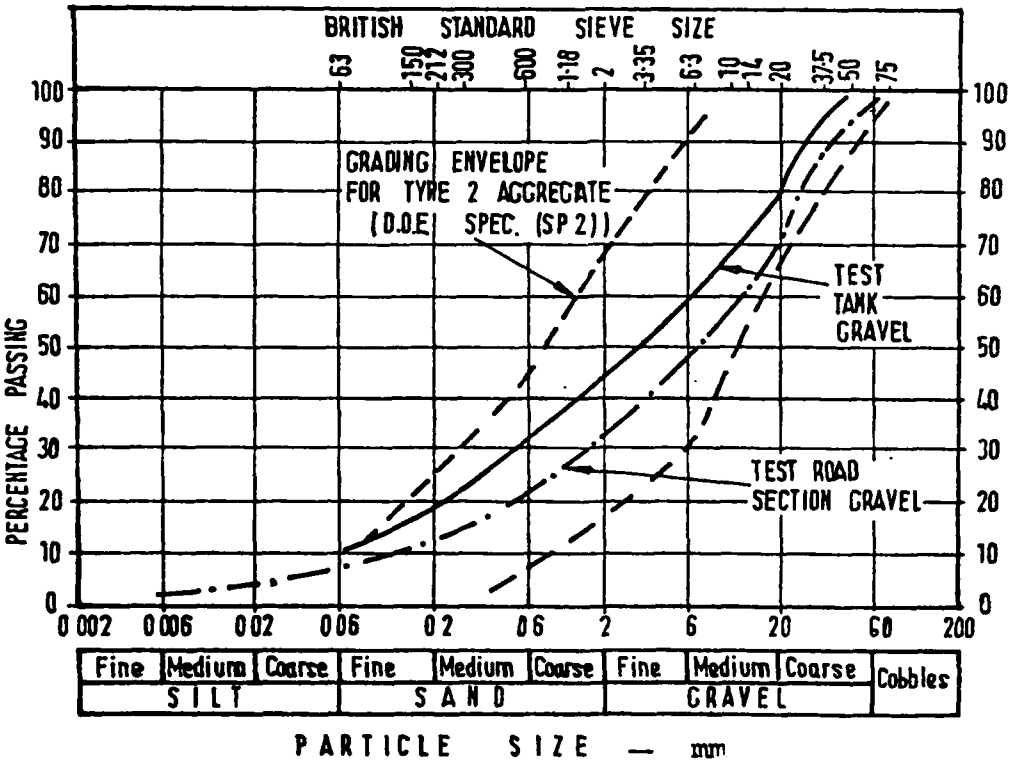

ENGINEERING PROPERTIES OF GRAVEL SUB-BASE MATERIAL (DAVITT)

Fig. 8.1

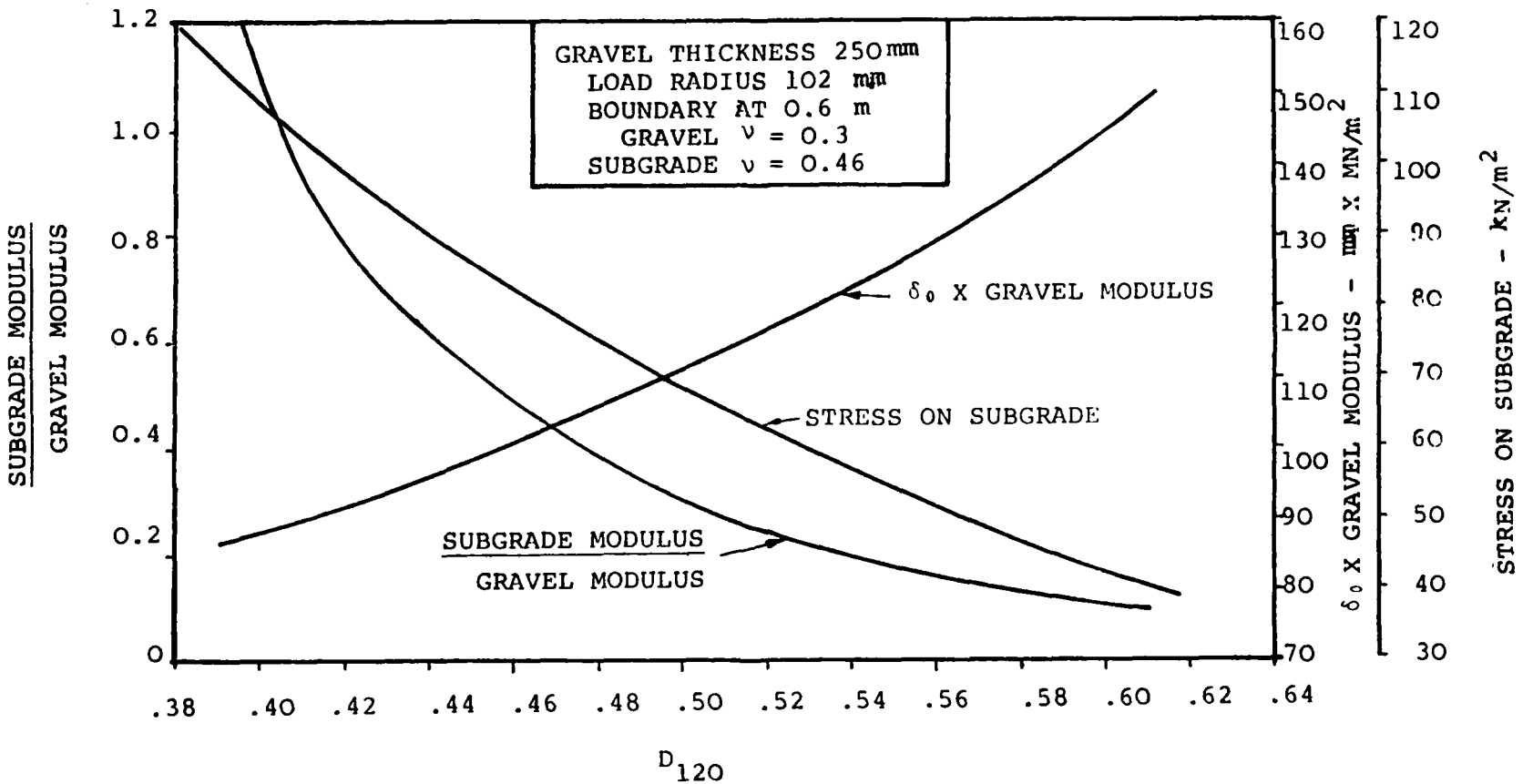

MODULUS INTERPRETATION NOMOGRAPH FOR TESTS ON KILPEDDAR GRAVEL (250 mm)

Fig. 8.2

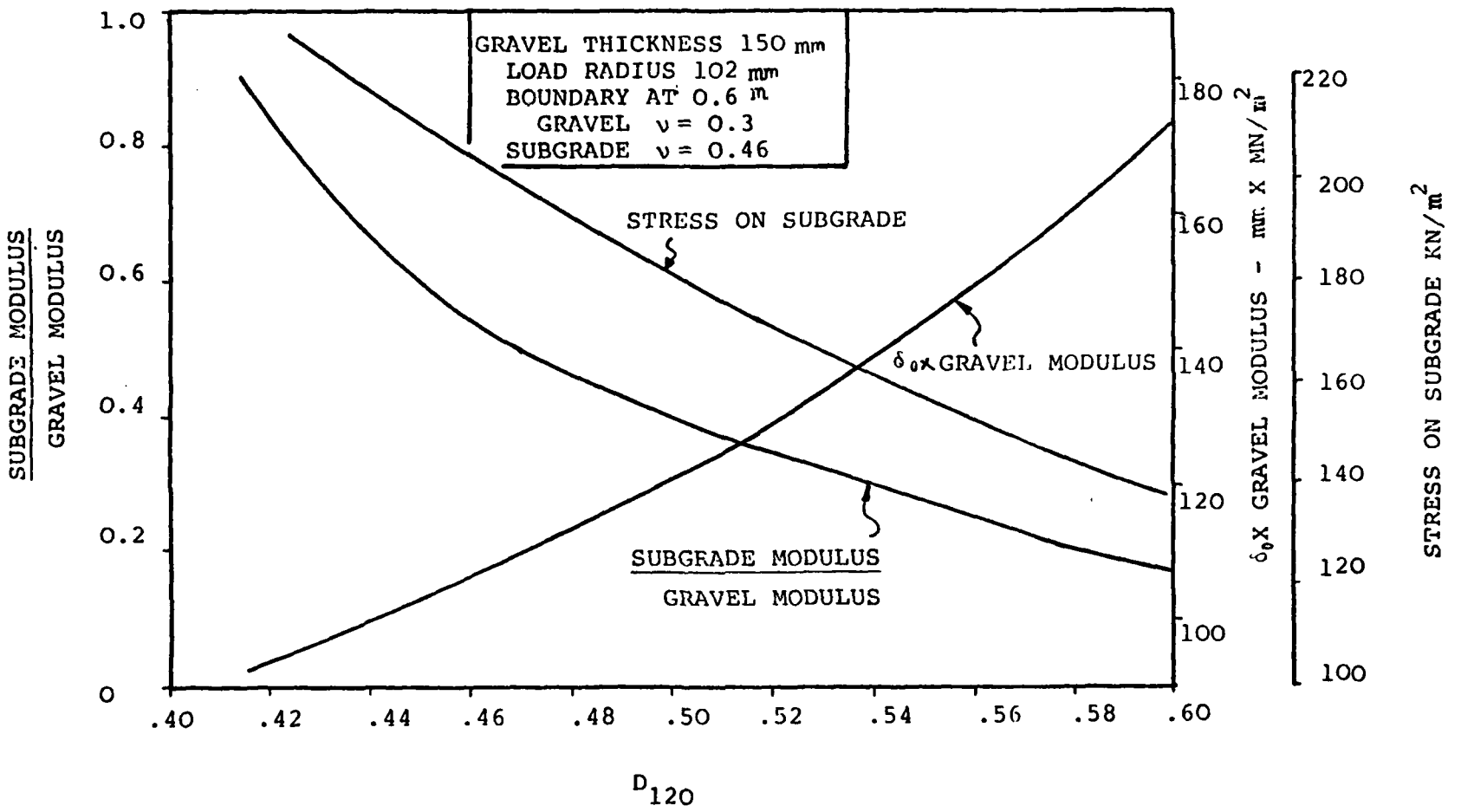

MODULUS INTERPRETATION NOMOGRAPH FOR TESTS ON KILPEDDAR GRAVEL (150 mm)

Fig. 8.3

C H A P T E R 9

OPTIMISATION IN PAVEMENT DESIGN

9.1 INTRODUCTION

Maximum economy in road design can be achieved only when information on the cost related performance of different road structures is available.

A systems analysis approach must be taken towards the problem of road design. This involves a consideration not only of the set of possible initial designs, but also the future maintenance requirements as well as the possible stage construction alternatives. Because of the complexity of this analysis and the extremely large range of alternatives to be considered, some form of computer analysis is required.

Two computer subroutines, namely SELPAV and OPTPAV have been prepared towards this end in Trinity College. The former is incorporated into the proposed design system based on the finite element program DEFPAV, (and is a modified version of that described in Kirwan and Maher (31)). The latter is intended as an independent package which considers the cost implications of a wide range of design alternatives.

9.2 ROUTINE SELPAV

A simplified flow chart for the routine is shown in Fig. 9.1. It is based on the estimation of five critical parameters. These are total construction thickness, subgrade strain, tensile strain at the base of the asphalt layers, the vertical stress on the subgrade and the surface resilient deflection.

The search routine is univariant. Only the thickness of a single layer is varied at each stage. The user specifies the range of layer thicknesses to be considered as well as the layer thickness increment. The program is written for the analysis of a four-layer system. A three-layer pavement can be considered by specifying similar properties for the two top layers.

The initial trial section is the maximun possible, i.e. that comprising the maximum thickness of each layer. This configuration is then analysed to determine whether it lies within the allowable constraints of the five specified design criteria. If the cross-section is found to provide a workable solution, it is costed and stored. The next section is then tested.

The possible configurations are obtained by first decrementing the thickness of the surface layer, until its minimum thickness is reached. Its thickness is then reset to its maximum value and the second layer is reduced in thickness by the specified decrement. The process of decrementing the surface layer is then repeated, with each trial section being tested in turn. By continuing this procedure every possible combination of layer thickness can be tested. For a four-layer pavement with each construction layer divided into ten increments, 1000 trial sections are generated.

To speed the search process, if a particular section fails, all thinner sections on that cycle are not tested. To limit storage, only the first five hundred feasible solutions are stored and sorted. Thus, if a greater number of feasible solutions are found (as specified in the output), the program should be rerun with larger layer increments.

Estimation of Design Criteria

Test 1: Minimum Pavement Thickness

In this country, a minimum thickness of 450mm of frost-resistant material is recommended over frost-susceptible

soils. This can be incorporated, omitted or altered.

Test 2: Vertical Compressive Strain in the Subgrade

The method estimating stresses and strains within the layered structure is based on the equivalent layer theory originally devised by Odemark (32). Analysis of measured subgrade deflections, carried out by Ontario Ministry of Transportation using a deflection equation based on the theory, showed it to be very accurate. It has been incorporated into overlay design procedures.

The multi-layered elastic system is converted to a homogeneous half-space with similar properties to the subgrade. Thus the required stresses and strains occurring in the original layered system, now occur in the half-space at a depth related by the layer equivalent thicknesses.

The principle behind the calculation of the equivalent thickness h_e, of a layer with thickness h_1, modulus E_1 and Poisson's Ratio ν_1, in relation to the material with modulus E_2 and Poisson's Ratio ν_2, is that the equivalent layer must have the same overall stiffness as the original layer, so as to give the same pressure distribution beneath it. The equations are based on the relationship for the modulus of rigidity of flat plates in flexure.

$$D = \frac{E\ h^3}{12\ (1-\nu^2)}$$

The basic relationship for a two-layer system takes the form:

$$h_e^3 \times \frac{E_2}{1-\nu} = n^3 \times h_1^3 \times \frac{E_1}{1-\nu}$$

where n is a correction factor and varies depending on the number of layers in the system. If Poisson's Ratio is similar for both materials, the expression reduces to:

$$h_e = 0.9Xh_1 \times \sqrt[3]{\frac{E_1}{E_2}}$$

Based on the equivalent layer theory, Ullidtz (33) has formulated simple equations for the estimation of stresses, strains and deflections in multi-layered systems which have given results comparable to those obtained using the computer program CHEVRON. The equation for subgrade strain is given by:

$$z = \frac{P\ (1+\ \nu)}{E} \left[\frac{\frac{h_e}{a}}{\left(1 + \left(\frac{h_e}{a}\right)^2\right)^{3/2}} - (1-2\nu) \left[\frac{\frac{h_e}{a}}{\left(1 + \left(\frac{h_e}{a}\right)^2\right)^{1/2}} - 1 \right] \right]$$

Where h_e is the equivalent depth to the subgrade surface, P is the applied stress, a is the load radius, E is the subgrade modulus and ν the subgrade Poisson's Ratio.

The subgrade strains for two, three and four-layer systems were estimated using this simplified approach. The results were compared with those obtained using DEFPAV. A range of values of modulus, Poisson's Ratio, layer thicknesses and applied stress were used. Fig. 9.2 illustrates the correlation. It is considered satisfactory.

Test 3: Tensile Strain at the Base of the Bound Layers

The equivalent layer theory is again used here. In this case, the subgrade is not taken into account and so the bound layers are converted to an equivalent thickness of the sub-base material.

The vertical strain at the surface of the sub-base layer is then estimated using the equation for Test 2. The vertical stress at the interface is found using Boussinesq's equation in terms of the equivalent height.

$$\sigma_{s_b} = P \left[1 - \frac{1}{\left(1 + \left(\frac{a}{h_e}\right)^2\right)^{3/2}} \right]$$

The horizontial tensile strain is estimated using the equation (given by Ullidtz (32)).

$$\varepsilon_r = \left[\frac{\frac{1 - \nu_{sb}}{2}}{E} \left(\sigma_z - E_{sb} \varepsilon_z \right) - \nu_{sb} \sigma_z \right]$$

where E_{sb} is the sub-base elastic modulus and ν_{sb}, the sub-base Poisson's Ratio.

The accuracy of the method was investigated using DEFPAV. Fig. 4.3 illustrates the correlation for the examples tested. Since the subgrade is not considered in the equations, in cases where there is a large ratio between sub-base and sub-grade moduli, larger errors occur. However, such modular ratios are not common in practice since they are limited by the inability of granular layers to take tension.

Test 4: Vertical Stress on Subgrade

The equivalent layer theory, in conjunction with the Boussinesq equation for vertical stress, is used to determine the vertical stress in the subgrade. A comparison with vertical stresses obtained with DEFPAV is shown in Fig. 9.4.

The results can be seen to be sufficiently accurate for use in the selection routine.

Test 5: Surface Deflections

A simplified deflection equation, in conjunction with the equivalent layer theory, was found to be insufficiently accurate for estimating surface deflections in a four-layer system. Therefore, another simplified approach was required. A method based on obtaining an equivalent or mean modulus for the multi-layered system was used.

The approach was suggested by Proksch (34) who used an equation of the form:

$$E_{mean} = \frac{E_1 \times h_1 + E_2 \times h_2 + \ldots\ldots\ldots}{h_1 + h_2 + \ldots\ldots\ldots\ldots}$$

for converting a multi-layered system into a two-layer system for the purposes of estimating flexural tensile stresses in a design method. This basic equation has been extended to convert a multi-layered system into a homogeneous half-space, with an equivalent modulus which affords the same centre line deflection as the original system.

However, a problem arises when dealing with a semi-infinite subgrade. It then becomes necessary to know the depth of pavement contributing to the the surface deflection. Obviously this will depend on the thickness and elastic parameters of the upper layers as well as on the magnitude of the applied stress. From preliminary investigations, this influence depth was found to be approximately the depth at which the vertical stress reached a value of 1/5 of the applied stress. It was also found that, for a system with a constant applied stress and constant material properties, the influence depth was relatively constant, irrespective of the thicknesses of the constituent layers. In cases where the influence depth falls within the upper layers, the term referring to the subgrade is omitted and the thickness of the third layer is adjusted. Thus, the equation for the equivalent modulus takes the form:

$$E_{eq} = \frac{E_1 \times h_1 + E_2 \times h_2 + E_3 \times h_3 + E_{sg} \times h_4}{INFLU}$$

where E_1, E_2 and E_3 are the successive layer moduli, E_{sg} is the subgrade modulus, and INFLU is the influence depth.

If $h_1 + h_2 + h_3 > INFLU$, $h_4 = 0$ and h_3 is made equal to

$$INFLU - (h_1 + h_2).$$

The centre-line deflection is found using Boussinesq's equation.

$$\delta_c = \frac{2 \times P \times a}{E_{eq}} (1 - \nu^2_{sg}).$$

The variation of Poisson's Ratio between the layers is ignored.

Fig.9.5 illustrates the accuracy of the results when compared with those obtained with DEFPAV.

The program estimates the appropriate influence depth given the centre-line deflection from one trial section. Therefore a trial section must first be analysed using DEFPAV. That consisting of the minimum layer thicknesses is chosen for convenience. Since SELPAV is used in conjunction with DEFPAV and although surface deflections may not be required, this procedure is not considered to be a disadvantage.

It should be mentioned that the deflection estimated by the routine is the maximum surface deflection under the specified load. It is not therefore equivalent to the Benkelman Beam deflection which is measured between two truck tyres. However, it does permit a comparative assessment of the relative structural capacity of the trial sections.

Example of SELPAV Output

The input requirements are illustrated on the user guide reproduced in Fig.9.6. It can be seen that the user has complete control over the system to be investigated and the values of the criteria used for the final selection.

Since the analysis of a typical system only takes a matter of seconds of computer time, the routine can be re-run many times to investigate the economic viability of alternative materials and to determine which is the critical parameter governing design.

An example of the SELPAV output for a typical design problem is shown in Figs. 9.7 to 9.9. The subgrade strain and asphalt

strain limits are those recommended by Shell (35) for a road designed to take a million standard axles.

ROUTINE OPTPAV

Introduction

The main concern of a road-making authority is to provide a serviceable pavement network at the minimum longrun cost. This cost consists of the initial construction cost, maintenance costs and the expenditure on future overlays. For any given project, a large number of alternatives present themselves, not only from the point of view of choice of construction materials and layer thicknesses, but also the initial design life. In deciding on this, the following points should be considered.

1) Expenditure on excessively long design life pre-empts the use of money for more urgent present-day projects.

2) Pavements may become obsolete because of required changes in alignment etc.

3) Pavements rarely deteriorate uniformly along their length. Thus most efficient use can be made of the available budget by allowing for regular rehabilitation on the basis of actual performance.

4) The use of shorter design lives allows greater flexibility of the road management system, since terminal serviceability standards can be revised to reflect variations in available resources or the relative importance of individual roads.

Hence, planned stage construction should offer the most economical solution to providing a serviceable road network. An investigation at the T.R.R.L. concluded that two-stage construction offered considerable advantages over initial design periods of greater than twenty years.

An optimization procedure has been devised which incorporates the philosophy of stage construction with maintenance.

Basic Assumptions

Certain assumptions and simplifications must be made. In order to estimate overlay requirements, the assumption is made that the elastic properties of the paving materials remain constant through the pavement life and that the effect of cumulative damage can be taken into account simply by its effect on the fatigue life of the bitum n-bound layers.

From the literature, this assumption seems acceptable, provided that overlaying takes place before failure of any of the pavement components has occurred.

Burt (36), in a review of progress in pavement design, concluded that the properties of a pavement as a whole do not change much during its life. From an analysis of the Alconbury Hill experiment (37), it was found that the curve of permanent deformation against cumulative standard axles, after an initial sharp fall, remained approximately linear. While the rate of deformation varied between summer and winter and between a good and bad year for weather, the average rate over several years was approximately constant, indicating that the material properties were remaining constant.

Measured transient vertical deflections on the same test road (38) showed little change with time and traffic until after critical conditions developed. This effect is also evident from an examination of overlay design curves based on deflection (39).

The road management strategy, based on the assumption of constant material properties, requires that strengthening is undertaken before the onset of marked visible signs of deterioration. This condition is the prerequisite of any economic design approach. The design philosophy embodied in the program OPTPAV is an attempt to fulfil these requirements.

A simplified flow chart for the procedure is given in Fig.9.10. The input requirements for the program are summarised in the user guide shown in Fig.9.11.

Design of Surface-Dressed Granular Road

The program initially considers a surface-dressed granular road to provide a pavement for the minimum life specified. The cross-section is analysed using the equivalent layer theory, described previously and the subgrade strain estimated.

The two relationships which relate allowable subgrade strain to pavement life in terms of standard axles used in the program are those of Shell (35) and Brown et al (9). First, using growth rate predictions, the number of standard axles is estimated for the trial gravel section. The subgrade strain is then checked for the initial gravel section; if the strain is too large, the thickness is incremented until the subgrade strain criterion is satisfied. The subgrade stress may also be specified as a design criterion.

When an adequate granular road has been found, the cost of construction, including that of surface dressing, is estimated. It is also necessary to estimate the maintenance costs incurred prior to the first overlay. This proves to be a complex commodity to estimate as shown by studies carried out by the Road Research Laboratory (40). It includes such items as surface treatment to restore skid resistance, renewal of road markings, resurfacing the hard shoulder, raising kerbs and gulleys and local patching. Traffic delay costs, as a result of maintenance works, should also be considered.

To combine this information in the form of a maintenance function would form a major study in itself particularly in view of the lack of documented material on maintenance costs on Irish roads. As an interim solution, a simple linear function increasing with time is assumed. There is some evidence

available (41) to indicate that this is a reasonable approximation.

In order to make valid economic comparisons between alternative strategies, all future expenditure is discounted to present-day cost using the equation:

$$\text{present-day cost} = \text{future cost} \times \left(1 + \frac{\text{DRATE}}{100}\right)^{\text{YEAR}}$$

where DRATE is the discount rate and YEAR is the number of years from present.

Using this relationship, each yearly maintenance expenditure, as well as overlay costs, are discounted and summed to determine total outlay.

Design of Asphalt Overlays

When the initial granular road has been designed, the first asphalt overlay is considered. This is designed on the basis of the allowable tensile strain in the asphalt layer, the allowable vertical subgrade strain if desired and the vertical stress on the subgrade, using the equivalent layer theory as described previously.

Then, using the appropriate fatigue equation (four standard equations at present included in OPTPAV), the allowable number of standard axles are found. Miner's Law for cumulative damage is assumed to apply for fatigue failure. For the purpose of the design method in OPTPAV, the pavement must undergo successive overlays (up to a maximum of four in the present version) without reaching a failure condition. Thus the concept of a percentage of the remaining fatigue life to be used for each overlay, is introduced.

If this percentage is denoted by F (in the form of a fraction i.e. $F < 1$), then if the first overlay has a fatigue life of Nf_1 repetitions, it is overlaid after reaching $F \times Nf_1$ repetitions. The overlaid pavement then has a remaining life of $(1 - F) \times Nf_2$.

This in turn is overlaid when F x (1 - F) x Nf_2 repetitions have been reached and continued for the remaining overlays. The value chosen for F is decided by the user. A range of values can be tried to determine the one yielding the most economic result.

It is possible that this theory of cumulative fatigue damage may produce too conservative a design for future overlays. In some existing design procedures, providing the facility of stage construction, this damage theory is not taken into account. Since, in this country, fatigue is not the predominant failure mode and also, since fatigue laws, by being based on back analysis of successful pavement designs, have a built-in factor of safety, ignoring the cumulative fatigue damage might be a legitimate assumption. Again, the option of doing this is left to the user.

When the first overlay has been found, it is costed on the basis of construction and maintenance costs to the end of the design period. A maintenance function in the same form as that for the granular road is used. All costs are reduced to present-day costs. The second, third and fourth overlay (if required) are then designed on a similar basis, until the total design life specified in the input has been reached. Its construction and cost are then stored.

Maintaining the initial granular road constant, the first overlay thickness is increased from that found in the previous solution and again the successive overlay requirements estimated and costed. The process is continued until the total design life can be reached by the application of one asphalt overlay. Then the initial granular road life is incremented and the range of possible overlays determined as before.

When either the initial granular road life or its thickness reach the maximum values, its thickness is reduced to the minimum. This then forms the sub-base layer for the initial three-layer design in which the surface layer consists of the minimum asphalt thickness. The range of possible overlay

strategies are investigated as before. Eventually, the sub-base thickness is incremented and the process continued.

In this way every possible combination of initial road construction and life and all possible overlay alternatives, within the limits specified by the user, are found and costed.

On completion of the search routine, the feasible solutions are sorted on order of lowest overall cost. The first twenty solutions are printed out.

Figures 9.12 to 9.14 illustrate the input printout for a typical design problem along with a specimen output.

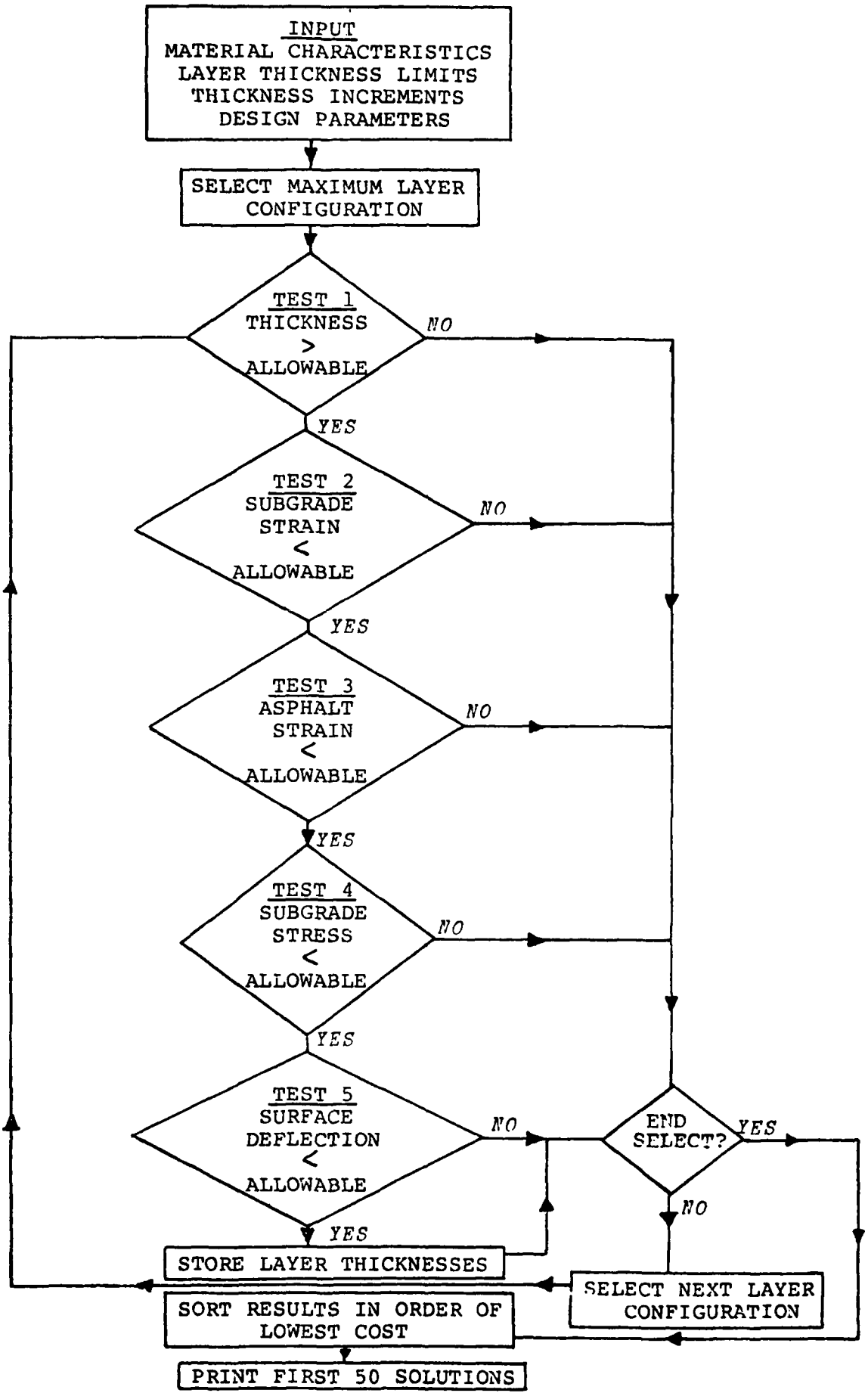

FLOW DIAGRAM FOR ROUTINE SELPAV

Fig. 9.1

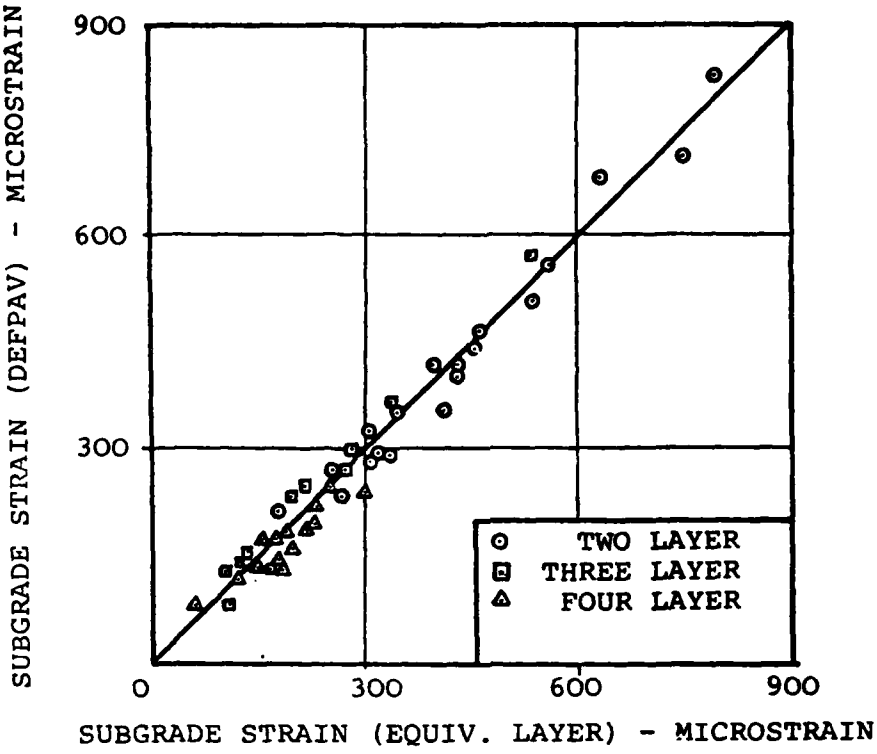

ABILITY OF EQUIVALENT LAYER THEORY TO ESTIMATE SUBGRADE STRAINS

Fig. 9.2

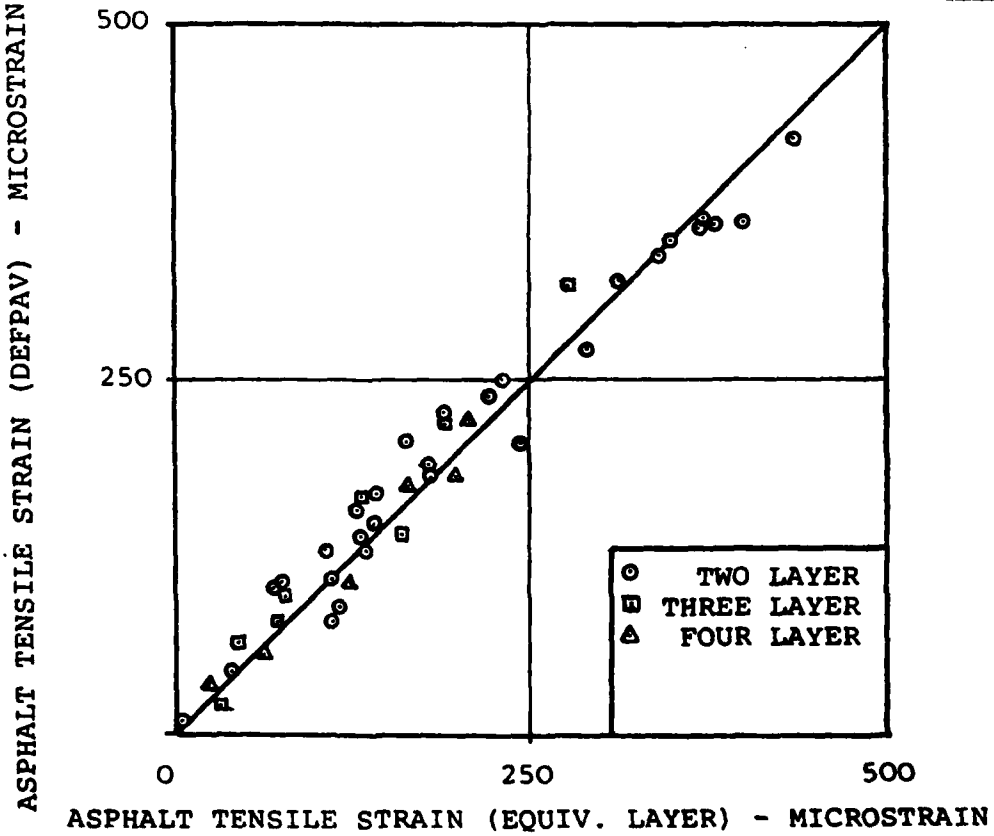

ABILITY OF EQUIVALENT LAYER THEORY TO ESTIMATE TENSILE STRAINS

Fig. 9.3

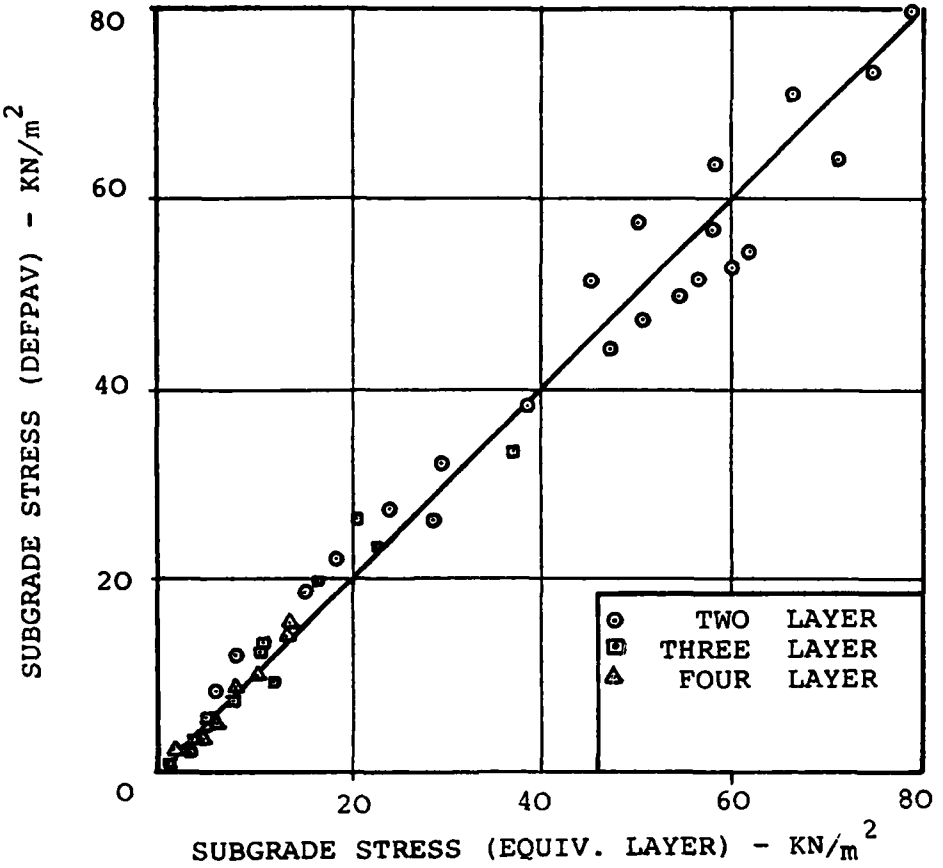

ABILITY OF EQUIVALENT LAYER THEORY TO ESTIMATE SUBGRADE STRESS

Fig. 9.4

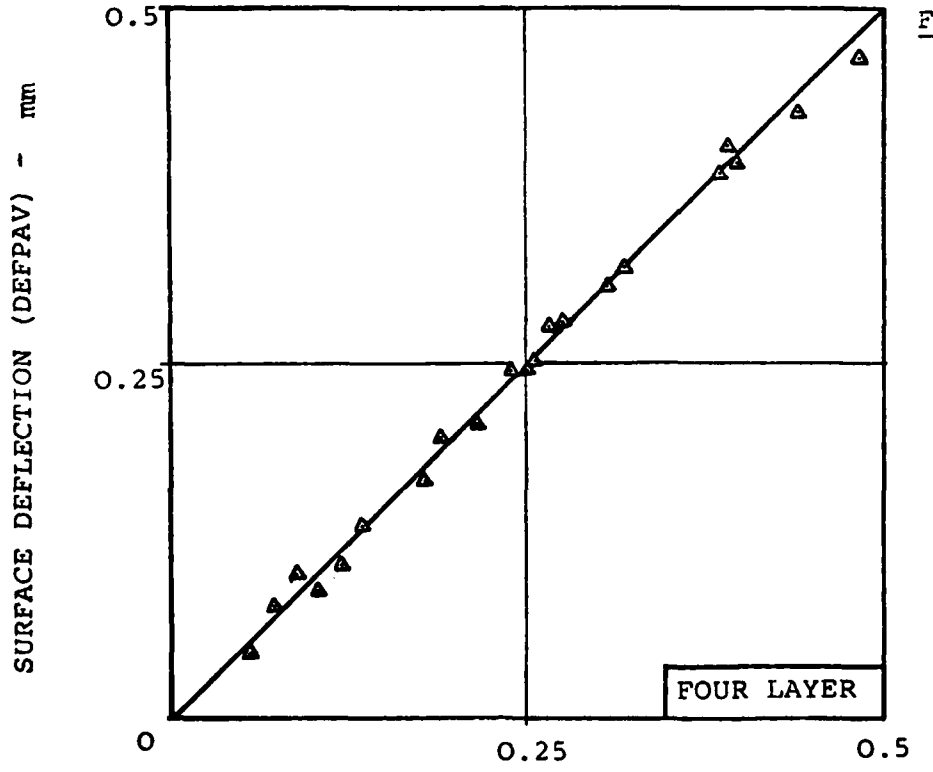

ABILITY OF EQUIVALENT MODULUS THEORY TO ESTIMATE SURFACE DEFLECTIONS

Fig. 9.5

Applied Stress + Radius

P	a

Material Parameters

E_1	E_2	E_3	E_{sg}	ν_1	ν_2	ν_3	ν_{sg}

Layer Thickness Limits

H_1 min	H_2 min	H_3 min	H_1 max	H_2 max	H_3 max

Material Costs

C_1	C_2	C_3

Allowable Design Criteria

Tic min	ϵ_r	ϵ_z	σ_z	δ_o

Layer Increments + DEFPAV Deflection

INC_1	INC_2	INC_3	F P

Notes:
Stress and Moduli in MN/M^2.

Linear Dimensions in mm.

Cost per KM length per mm thick per unit width of carriageway.

FORM OF INPUT FOR ROUTINE SELPAV

Fig. 9.9

LOADING CHARACTERISTICS:
==========

APPLIED LOAD:- 0.498 MN/SQ. m

LOADED RADIUS:- 150.0 mm

DESIGN CRITERIA:
==========

MINIMUM PAVEMENT THICKNESS:- 350 mm

MAXIMUM TENSILE STRAIN IN BASE OF ASPHALT:- .000150

MAXIMUM VERTICAL STRAIN IN SUBGRADE:- .000650

MAXIMUM SUBGRADE STRESS:- .0080 MN/SQ.m

MAXIMUM RESILIENT DEFORMATION:- 0.40 mm

LOADING AND DESIGN INPUT FOR ROUTINE SELPAV

Fig. 9.7

LAYER MATERIAL CHARACTERISTICS:
==========

LAYER 1:

MINIMUM THICKNESS:- 25 MM
MAXIMUM THICKNESS:- 150 MM
YOUNG'S MODULUS:- 4000.0 MN/SQ.M
POISSON'S RATIO:- .40
COST PER KM PER MM THICK:- £ 470.00
LAYER THICKNESS INCREMENT:- 25 MM

LAYER 2:

MINIMUM THICKNESS:- 75 MM
MAXIMUM THICKNESS:- 300 MM
YOUNG'S MODULUS:- 3000.0 MN/SQ.M
POISSON'S RATIO:- .40
COST PER KM PER MM THICK:- £ 382.80
LAYER THICKNESS INCREMENT:- 40 MM

LAYER 3:

MINIMUM THICKNESS:- 100 MM
MAXIMUM THICKNESS:- 700 MM
YOUNG'S MODULUS:- 700.0 MN/SQ.M
POISSON'S RATIO:- .35
COST PER KM PER MM THICK:- £ 30.00
LAYER THICKNESS INCREMENT:- 100 MM

SUBGRADE:

AVERAGE YOUNG'S MODULUS:- 30.0 MN/SQ.M
POISSON'S RATIO:- .42
INFLUENCE DEPTH FOR DEFLECTION ANALYSIS:- 1907 MM

INPUT MATERIAL CHARACTERISTICS FOR ROUTINE SELPAV

Fig. 9.8

LAYER 1 THICKNESS (MM)	LAYER 2 THICKNESS (MM)	LAYER 3 THICKNESS (MM)	COST PER KM (£)	TOTAL THICKNESS (MM)	ASPHALT TENSILE STRAIN	SUBGRADE COMPRESSIVE STRAIN	SUBGRADE STRESS (MN/SQ.M)	RESILIENT DEFLECTION (MM)	EQUIVALENT HEIGHT (M)
50.0	100.0	300.0	70780.	450.0	.00015	.00023	.0069	.31	1.553
50.0	100.0	400.0	73780.	550.0	.00015	.00017	.0050	.29	1.833
50.0	100.0	500.0	76780.	650.0	.00015	.00013	.0037	.26	2.112
50.0	100.0	600.0	79780.	750.0	.00015	.00010	.0029	.25	2.392
75.0	100.0	300.0	82530.	475.0	.00012	.00020	.0059	.28	1.680
50.0	100.0	700.0	82780.	850.0	.00015	.00008	.0024	.23	2.671
50.0	140.0	200.0	83092.	390.0	.00011	.00027	.0078	.29	1.458
75.0	100.0	400.0	85530.	575.0	.00012	.00015	.0043	.26	1.960
50.0	140.0	300.0	86092.	490.0	.00011	.00019	.0055	.27	1.738
75.0	100.0	500.0	88530.	675.0	.00012	.00011	.0033	.24	2.239
50.0	140.0	400.0	89092.	590.0	.00011	.00014	.0041	.25	2.017
100.0	100.0	200.0	91280.	400.0	.00009	.00024	.0071	.27	1.527
75.0	100.0	600.0	91530.	775.0	.00012	.00009	.0026	.22	2.519
50.0	140.0	500.0	92092.	690.0	.00011	.00011	.0032	.23	2.297
100.0	100.0	300.0	94280.	500.0	.00009	.00017	.0051	.25	1.807
75.0	100.0	700.0	94530.	875.0	.00012	.00007	.0021	.21	2.798
75.0	140.0	200.0	94842.	415.0	.00009	.00023	.0066	.26	1.585
50.0	140.0	600.0	95092.	790.0	.00011	.00009	.0025	.22	2.576
100.0	100.0	400.0	97280.	600.0	.00009	.00013	.0038	.23	2.086
75.0	140.0	300.0	97842.	515.0	.00009	.00016	.0048	.24	1.865
50.0	140.0	700.0	98092.	890.0	.00011	.00007	.0021	.21	2.856
50.0	180.0	200.0	98404.	430.0	.00008	.00021	.0062	.25	1.643

Fig. 9.9

SAMPLE OUTPUT FROM ROUTINE SELPAV

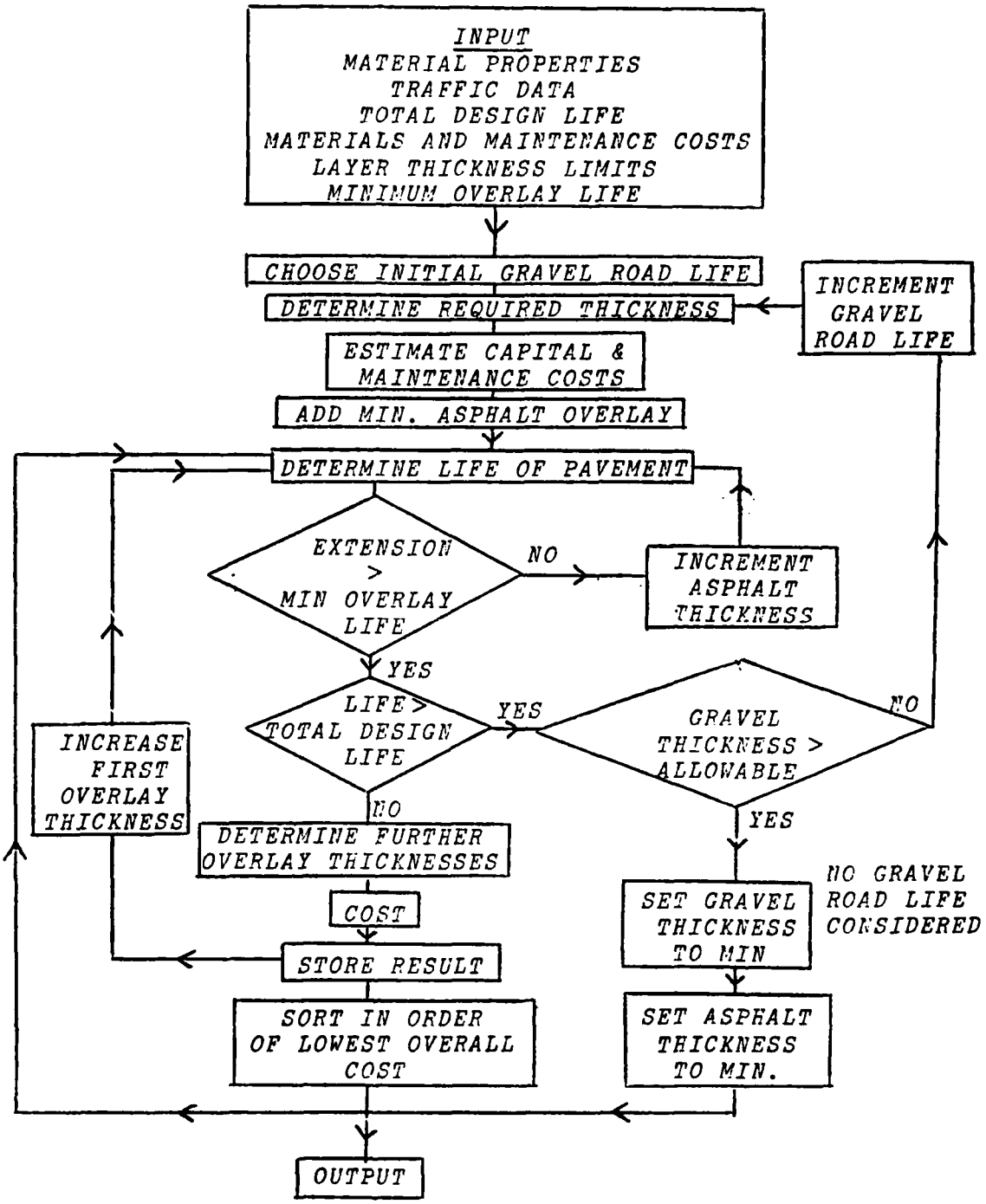

FLOW DIAGRAM FOR OPTPAV

Fig. 9.10

SM	SP	Stress	JSC

SM: subgrade modulus
SP: subgrade Poisson's Ratio
Stress: allowable subgrade stress
JSC: subgrade strain code 1. Shell 2. Nottingham
Default: 1.

GM	GP	GC	GD	Q	R	Gmin	Gmax	Ginc	GRL	LMG	LIFINC

GM: granular modulus
GP: granular Poisson's Ratio
GC: cost per km length per mm thick as layed
GD: cost of surface dressing per km length
Q,R: maintenance function, Q + R (AGE)
G min: minimum granular thickness Default: 150 mm
G max: maximum granular thickness Default: 3000 mm
G inc: granular layer increment Default: 150 mm
GRL: minimum granular road life Default: 1 year
LMG: maximum granular road life Default: 15 years
LIFINC: granular road life increment Default: 1 year

AM	AP	AC	W	X	ASmin	ASmax	ASinc	MINLIF	KFC

AM: asphalt modulus
AP: asphalt Poisson's Ratio
AC: cost per km length per mm thick as layed
W,X: maintenance function, W + X (AGE)
AS min: minimum overlay thickness Default: 50 mm
AS max: maximum total asphalt thickness Default: 1000 mm
AS inc: asphalt overlay increment Default: 25 mm
MINLIF: minimum life for asphalt overlay Default: 5 years
KFC: fatigue law code 1. Shell 2. HRA
3. DBM (100 pen) 4. DBM (200 pen)

NSD	Grate	TDL	FP	DF	Drate

NSD: number of standard axles per day
GRATE: percentage traffic growth rate
TDL: total design life
FP: fatigue life percentage Default: no cumulative fatigue
DF: minimum thickness to prevent frost damage damage considered.
DRATE: discount rate

INPUT USER GUIDE FOR PROGRAM OPTPAV

Fig. 9.11

SUBGRADE CHARACTERISTICS
==========

RESILIENT MODULUS:- 70.0 MN/SQ.M

POISSON'S RATIO:- .42

MAXIMUM ALLOWABLE SUBGRADE STRESS:- .010 MN/SQ.M

NOTTINGHAM CRITERION FOR ALLOWABLE SUBGRADE STRAIN

GRANULAR LAYER CHARACTERISTICS
==========

RESILIENT MODULUS:- 400.0 MN/SQ.M

POISSON'S RATIO:- .35

COST PER KM LENGTH PER MM THICK AS LAYED:- £ 30.00

COST OF SURFACE DRESSING PER KM LENGTH:- £ 600.00

MAINTENANCE FUNCTION:- £ 75.0 + 40.00 (AGE)

GRANULAR LAYER VARIES FROM 120.0 MM TO 1200.0 MM IN INCREMENTS OF 50.0 MM

SURFACE DRESSED GRANULAR ROAD LIFE VARIES FROM 3 YEARS TO 8 YEARS IN INCREMENTS OF 1 YEAR(S)

SUBGRADE AND GRANULAR INPUT CHARACTERISTICS FOR PROGRAM OPTPAV

Fig. 9.12

ASPHALT LAYER CHARACTERISTICS
==========

RESILIENT MODULUS:- 3500.0 MN/SQ.M
POISSON'S RATIO:- .40
COST PER KM LENGTH PER MM THICK AS LAYED:- £ 800.00
MAINTENANCE FUNCTION:- £ 60.0 + 30.00 (AGE)
MINIMUM ASPHALT OVERLAY THICKNESS:- 50.0 MM
MAXIMUM ASPHALT THICKNESS:- 300.0 MM
ASPHALT OVERLAY INCREMENT:- 25.0 MM
MINIMUM LIFE FOR ASPHALT OVERLAY:- 4 YEARS
FATIGUE LIFE FOR HOT ROLLED ASPHALT (NOTTINGHAM)

DESIGN INFORMATION
==========

INITIAL NUMBER OF STANDARD AXLES PER DAY:- 600
TRAFFIC GROWTH RATE:- 2. %
TOTAL DESIGN LIFE:- 30. YEARS
FATIGUE LIFE PERCENTAGE:- 0. %
MINIMUM DEPTH TO PREVENT FROST DAMAGE:- 350. MM
DISCOUNT RATE:- 10.0 %

*** NOTES ***

STRESS AND MODULI IN MN/SQ.M
MAINTENANCE ONLY ESTIMATED TO END OF DESIGN PERIOD
ALL COSTS DISCOUNTED TO PRESENT DAY COSTS
COSTS ARE ESTIMATED PER KM OF CARRIAGEWAY 10 M WIDE

ASPHALT CHARACTERISTICS AND DESIGN INFORMATION FOR INPUT TO PROGRAM OPTPAV

Fig. 9.13

GRANULAR LAYER

THICKNESS(MM)	1120.	1120.	1020.	1070.	970.	870.	970.	870.	820.
LIFE(YEARS)	6.	3.	0.	0.	0.	0.	0.	0.	0.
CAPITAL COST(£)	34200.	34200.	30600.	32100.	29100.	26100.	29700.	26700.	25200.
MAINTENANCE COST(£)	885.	378.	0.	0.	0.	0.	0.	0.	0.

ASPHALT OVERLAY 1

THICKNESS(MM)	50.	50.	50.	50.	50.	50.	75.	75.	75.
LIFE(YEARS)	45.	48.	33.	41.	26.	14.	29.	17.	12.
CAPITAL COST(£)	22579.	30053.	40000.	40000.	40000.	40000.	60000.	60000.	60000.
MAINTENANCE COST(£)	1552.	2228.	3145.	3145.	2834.	1758.	3090.	1997.	1502.

ASPHALT OVERLAY 2

THICKNESS(MM)	0.	0.	0.	0.	200.	50.	175.	150.	125.
LIFE(YEARS)	0.	0.	0.	0.	14.	5.	10.	11.	8.
CAPITAL COST(£)	0.	0.	0.	0.	13698.	10209.	8549.	24242.	31439.
MAINTENANCE COST(£)	0.	0.	0.	0.	34.	137.	4.	273.	254.

ASPHALT OVERLAY 3

THICKNESS(MM)	0.	0.	0.	0.	0.	125.	0.	25.	25.
LIFE(YEARS)	0.	0.	0.	0.	0.	8.	0.	12.	8.
CAPITAL COST(£)	0.	0.	0.	0.	0.	15578.	0.	1399.	3053.
MAINTENANCE COST(£)	0.	0.	0.	0.	0.	146.	0.	11.	143.

ASPHALT OVERLAY 4

THICKNESS(MM)	0.	0.	0.	0.	0.	25.	0.	0.	25.
LIFE(YEARS)	0.	0.	0.	0.	0.	12.	0.	0.	5.
CAPITAL COST(£)	0.	0.	0.	0.	0.	1399.	0.	0.	1399.
MAINTENANCE COST(£)	0.	0.	0.	0.	0.	11.	0.	0.	11.

FINAL TOTALS

TOTAL LIFE(YEARS)	51.	51.	33.	41.	40.	40.	40.	40.	33.
TOTAL MAINT. COST(£)	2437.	2606.	3145.	3145.	2868.	2052.	3094.	2281.	1910.
TOTAL OV'LAY COST(£)	22579.	30053.	40000.	40000.	53698.	67187.	68549.	85641.	95891.
OVERALL COST(£)	60101.	67237.	73745.	75245.	85666.	95339.	101343.	114622.	123001.

Fig. 9.14

SAMPLE OUTPUT FROM PROGRAM OPTPAV

REFERENCES

1. GLYNN,T.E.
"Deformation characteristics of boulder clay subjected to repeated stress applications", Ph.D. Thesis, University of Dublin, 1968.

2. BARKSDALE,R.D.
"Compressive stress pulse times in flexible pavements for use in dynamic testing." Highway Research Board No. 345, Washington D.C., 1971.

3. EL-RUWAYIL,A.A.
"Design manufacture and performance of a lateral strain device" Geotechnique, Vol. XXVI, No.1 March 1976 pp 215-216.

4. KIRWAY,R.W. and SNAITH,M.S.
"A simple chart for the prediction of resilient modulus". Geotechnique, Vol. XXVI, No.1 1976, pp 212-215.

5. SNAITH,M.S.
"Repeated load testing of boulder clay subgrades". M.Sc., Thesis University of Dublin, 1968.

6. CASEY,T.L.
"A Laboratory pavement simulator and an investigation to relate dynamic and ordinary soil properties", M.Sc. Thesis, University of Dublin, 1973.

7. SEED,H.B., CHAN,C.K., and LEE,C.E.
"Resilient characteristics of subgrade soils and their relation to fatigue failures in asphalt pavements" Int. Conf. Structural Design of Asphalt Pavements, pp 611-636, 1962.

8. MAJIDZADEH,K. and GUIRGUIS,H.R.
"Fundamentals of soil compaction and performance". Highway Research Board H.R.R. No.438, 1973 pp 1-15.

9. BROWN,S.F., PELL,P.S., and STOCK,A.F.
"The application of simplified, fundamental design procedures for flexible pavements". 4th Int. Conf. Struct. Design of Asphalt Pavements pp 327-341, Ann Arbor, 1977.

10. KIRWAN,R.W., SNAITH,M.S.
"Further investigations towards a rational method of Design for Flexible Pavements" Part II, Final Technical Report, E.R.O. April, 1975.

11. BARKER,W.R., BRABSTON,W.N. and CHOU,Y.T.
"A general system for the structural design of flexible pavements". Fourth Int. Conf. Structural Design of Asphalt Pavements pp 209-248, Ann Arbor, 1977.

11a. BARKER,W.R.
"The relationship between resilient and permanent strain in the design of asphalt pavements". Symposium on Rutting in Asphalt Concrete Pavements.

12. MONISMITH,C.L., OGAWA,N. and GREENE,C.R.
"Permanent Deformation characteristics of subgrade soils due to repeated loading". Transportation Record 537, 1975.

13. SKEMPTON,A.W.
"The pore-pressure coefficients A and B". Geotechnique 4, 143-47, 1954.

14. BISHOP,A.W. and HENKEL,D.J.
"The measurement of soil properties in the Triaxial Test". 2nd Ed. 1962

15. CALLADINE,C.R.
"Overconsolidated Clay: a microstructural view" Symposium on Plasticity and Soil Mechanics, Cambridge, 1973.

15a. ALLEN,J.J. and THOMSON,M.R.
"Resilient response of granular materials subjected to time-dependent lateral stresses". T.R.R. 510, 1974, p 1-13.

16. LEGER,P.
"Le Deflectographe Lacroix, evaluation due material et procedes d'exploitation" Revue Generale des Routes et des Aerodromes, June 1969.

17. GRANT,M.C. and WALKER,R.N.
"The development of overlay design procedures based on the application of elastic theory" Proc. 3rd Int. Conf. Structural Design of Asphalt Pavement, London 1972, pp 1155-1166.

18. VALKERING,C.P.
"Pavement Evaluation by measuring deflection and shape of deflection bowl". Proc. 3rd Int. Conf. Structural Design of Asphalt Pavements, Vol. 2 London, 1972 pp 353-356.

19. DORMON,G.M. and METCALF,C.T.
"Design curves for flexible pavements based on layered system theory". Highway Research Board, Vol. 17 No. 71, pp 69-84.

20. CLAESSEN,A.I.M. and DITMARSH,R.
"Pavement evaluation and overlay design". Proc. 4th Int. Conf. Structural Design of Asphalt Pavements, Ann Arbor, 1977, pp 649-662.

21. ULLIDTZ,P.
"Overlay and stage by stage design". Proc. 4th Int. Conf. Structural Design of Asphalt Pavements, Ann Arbor 1977, pp 722-735.

22. MAHER,M.L.
"Optimisation and in-situ materials characterisation in the rational structural design of Flexible Pavements" Thesis to be submitted to the University of Dublin for the Degree of Doctor of Philosophy.

23. ULLIDTZ,P.
"Laboratory testing of a full scale pavement"
Report No. 19, The Technical University of
Denmark 1978.

24. SPARROW,R.W. and TORY,A.C.
"Behaviour of a soil mass under dynamic loading".
Journal of the Soil Mechanics and Foundation
Division., Proc. A.S.C.E. 4825, No. SM3,
pp 59-83, May 1966.

25. BROWN,S.F. and PELL,P.S.
"An experimental investigation of the stresses,
strains and deflections in a layered pavement
structure subjected to dynamic loads". Proc. 2nd
Int. Conf. Structural Design of Asphalt Pavements,
Ann Arbor, 1967 pp 487-504.

26. KIRWAN,R.W. and GLYNN,T.E. and BONNER,G.A.
"The significance of material properties in flexible
pavement analysis". Final Tech. Report E.R.O.,
U.S. Army, University of Dublin, April 1973.

27. SHACKEL,B.
"Repeated loading of soils - a review".
Australian Road Research Vol. 5, No.3,
October 1973.

28. KIRWAN,R.W. and GLYNN,T.E.
"Experimental and theoretical investigation of
pavement deflections". Final Technical Report
E.R.O. DAJA37-68-C-1490, 1969.

29. PICKERING,D.J.
"Anisotropic Elastic Parameters for Soil"
Geotechnique 20, pp 271-276, 1970.

30. KLOMP,A.G.J. and DORMON,G.M.
"Stress distribution and dynamic testing in
relation to road design". Proc. Australian
Road Research Board, Vol.2, Part 2, 1964.

31. KIRWAN,R.W. and MAHER,M.L.
"Further investigations towards a rational method of design for flexible pavements".
Final Technical Report E.R.O. DA-ERO-591-73-60017, 1976.

32. ODEMARK,N.
"Investigations as to the elastic properties of soils and design of pavements according to the theory of elasticity".
Statens Vaginstitut, Maddelande, 77, 1949.

33. ULLIDTZ,P.
"The use of dynamic plate loading tests in design of overlays". Res. Report No. 22, Tech., University of Denmark, 1973.

34. PROKSCH,H.
"Thickness design methods for asphalt roads in the USSR, GDR, Poland and the CSSR Bitumen, 34, No.6, 1972.

35. DORMON,G.M. and METCALF,C.T.
"Design curves for flexible pavements based on layered system theory".
Highway Research Record, Vol. 17, No. 71, pp 69-84, 1965.

36. BURT,M.E.
"Progress in pavement design".
T.R.R.L. Report LR 508,
1972.

37. THOMPSON,P.D., CRONEY,D. and CURRER,E.N.H.
"The Alconbury Hill experiment and its relation to flexible pavement design".
Proc. 3rd Int. Conf. on the Structural Design of Asphalt Pavements, Vol. 1. pp 920-937.
London, 1972.

38. LISTER,N.W.
"Deflection criteria for flexible pavements".
T.R.R.L. Report LR 375, 1972.

39. NORMAN,P.J., SNOWDON,R.A. and JACOBS,J.C.
"Pavement deflection measurements and their application to structural maintenance and overlay design". T.R.R.L. Laboratory Report 571, 1973.

40. ROAD RESEARCH LABORATORY
The cost of constructing and maintaining flexible and concrete pavements over 50 years .
Road Research Laboratory, Report LR 256, 1969.

41. DONOVAN,T.J. and DAVITT,S.
Performance of gravel in road pavements .
Paper presented at Symposium on "Road Improvement in Ireland", Dublin. March 1978.

ACKNOWLEDGEMENTS

The research work described in the Report has been carried out with the financial support of

1. European Research Office of the United States Army.
2. An Foras Forbartha - The National Institute for Physical Planning and Construction Research in Ireland.
3. National Board for Science and Technology, Ireland.

We are very grateful for the support of these three organisations.

We wish to show our appreciation for the encouragement and help given to us by Mr. R. G. Alvin (U.S. Army Waterways Experiment Station), Dr. H. Lemons (Chief Scientist, European Research Office U.S. Army) and Mr. P. O'Keefe (An Foras Forbartha).

We would like to thank Mr. S. Davitt, Mr. D. Hartford, Dr. T. Orr and Mr. L. Prendergast for their assistance with certain facets of this report.

A P P E N D I X

APPENDIX 1

ADDITIONAL INPUT PARAMETERS FOR ANISOTROPIC VERSION OF DEFPAV

E_z : Vertical Resilient Modulus

n : The ratio of the Horizontal Resilient Modulus to the Vertical Resilient Modulus, $(\frac{E_h}{E_z})$

ν_{hz} : The ratio of horizontal strains resulting from vertical strains

ν_{hh} : The ratio of horizontal strains resulting from horizontal strains in the orthogonal direction

m : The ratio of Shear Modulus in the vertical plane to Vertical Resilient Modulus, $(\frac{G_2}{E_z})$